NASA Technical Memorandum 104591

Circulation and Rainfall Climatology of a 10-Year (1979 - 1988) Integration With the Goddard Laboratory for Atmospheres General Circulation Model

J.-H. Kim
Applied Research Corporation
Landover, Maryland

Y. C. Sud Goddard Space Flight Center Greenbelt, Maryland



National Aeronautics and Space Administration

Scientific and Technical Information Branch

PREFACE

The 10-year simulation analyzed in this report was produced under Atmospheric Model Intercomparison Project (AMIP) by Dr. W. K.-M. Lau and his colleagues. The EOS-DIS funding by NASA Headquarters for studies of global hydrological process and climate enabled the participation of the primary author, JK, to carry out the analysis.

TABLE OF CONTENTS

PAGE

I. Introduction
II. Description of the AMIP Run
III. List of Quantities
IV. Discussion
V. Reference
VI. The First Momentum Fields
A. Seasonal Averages21
a. December, January, February
b. March, April, May32
c. June, July, August41
d. September, October, November50
B. Annual Averages59
C. Seasonal Cycle71
D. Zonal Mean Anomalies
VII. Hydrology83
A. Precipitation83
a. Seasonal and annual mean84
Simulated84
Observed
Simulated – Observed
b. Monthly mean90
Simulated90

PRECEDING PAGE BLANK NOT FILMED

Observed94
c. Seasonal and annual anomalies94
Simulated
Observed
d. Time Series of the Zonal Mean
B. Evaporation
a. Seasonal and annual mean142
b. Monthly mean
c. Seasonal and annual anomalies148
d. Time Series of the Zonal Mean
C. Time Series of the Zonal Mean P-E171
D. Soil Moisture
a. Seasonal and annual mean
b. Seasonal and annual anomalies
E. Time Series of P, E, and Soil Moisture in 12 Biomes 203
VIII. Radiation
A. Net Short Wave Radiation
B. Outgoing Long Wave Radiation

I. Introduction

The Climate and Radiation Branch of Goddard Laboratory for Atmospheres (GLA) participated in the Atmospheric Model Intercomparison Project (AMIP) sponsored by the Department of Energy. Under this project, we produced a 10-year (1979 - 1988) integration with the GLA General Circulation Model (GCM). We present the first momentum fields (time mean averages) of major circulation variables and also hydrological variables including precipitation, evaporation, and soil moisture. A comparison of the model simulated radiative flux with those of the Earth Radiation Budget Experiment (ERBE) observation for the period 1985 to 1988 is also included.

The aim of this technical memorandum is to document the key features of the GCM simulations and to compare them whenever possible with the observed (or analyzed) atmosphere. Our goals are i) to produce a benchmark documentation of the GLA GCM for the AMIP intercomparison and future model improvements, ii) to examine systematic errors between the simulated and the observed circulation, precipitation, and hydrologic cycle, iii) to examine the interannual variability of the simulated atmosphere and compare it with observation, and iv) to examine the ability of the model to capture the major climate anomalies in response to an event such as El Niño.

II. Description of the AMIP Run

The current version of GLA GCM has evolved from the earlier 9-layer Goddard Laboratory for Atmospheric Sciences (GLAS) GCM (Kalnay et al., 1983). Although we have made several changes in the GCM, we continue to use the 4° latitude and 5° longitude resolution for climate studies. The fortuitous benefit of this is that the model improvements reflected in our results are not related to better horizontal resolution. Since it is difficult to describe the model in this memorandum, we give reference to the papers that discuss the various parameterizations in the model in Table 1. This version of the GLA GCM has 17 layers, together with a number of new physical parameterizations (see Table 1). The 10-year integration period is from January 1/00 UTC, 1979 to January 1/00 UTC, 1989.

Table I. Particulars of the 17-layer GCM

No.	ITEM	DESCRIPTION	REFERENCE
1.	Horizontal Resolution	4° lat. x 5° long.	Kalnay <u>et al.</u> , (1983)
2.	Vertical Resolution	17 σ-Layers	Fox-Rabinovitz et al., (1991)
3.	Longwave Radiation	Modified HV Radiation Package	Harshvardhan <u>et al.</u> , (1987)
a)	Water-vapor & CO ₂ absorption	An adaptation of Chou & Chou et al.	Chou (1984) Chou et al., (1983)
b)	Ozone absorption	Modified Rodgers	Rodger (1968) and Rosenfield <u>et al</u> ., (1987)
4.	Shortwave Radiation	Slightly Modified HV Radiation Package	Harshvardhan <u>et al</u> ., (1987)
a)	Ozone absorption, Water-vapor absorption, Rayleigh Scattering	Slightly Modified Lacis and Hansen	Lacis and Hansen (1974)
b)	Aerosol absorption and Scattering	Sud and Walker using Pinker and Laszlo (1992)	Formulated by Harshvardhan* in 1991
5.	Turbulence and PBL	Mellor-Yamada 2.5	Helfand and Labraga, (1988)
6.	Biosphere	SiB (Simple Biosphere)	Sellers <u>et al.</u> , (1986) and Sud <u>et al.</u> , (1990) Xue <u>et al.</u> , (1991)
7.	Non-Precipitating	Relative Humidity Dependent Fractional Clouds	Sud and Walker (1992) Slingo (1987) adaptation
8.	Cumulus Clouds	Detraining Anvils	Sud and Walker (1992)
9.	Moist-Convection	An adaptation of Arakawa-Schubert	Sud <u>et al.</u> , (1991) with Tokioka <u>et al.</u> , (1988)
10.	Large-scale Precip.	Fractional Cover	Sud and Walker (1992)
11.	Conv. & Large-scale Rain-evaporation	Kessler (1969) with Ruprecht and Gray (19 76) Cloud Fractions.	Sud-Molod (1988)

12.	Soil Temperature Parameterization	Force Restore; 2-layers: diurnal and seasonal	Deardorff's (1987)
13.	Soil Moisture Initialization & Parameterization	3-soil layers initialization with off-line SiB, Liston and Sud (1992)	Sellers <u>et al</u> ., (1986)
14.	Vegetation Properties Roughness and Biome	Surface Albedo Analysis of veg. data characteristics data	Dorman and Sellers (1989) ERBE data over Bare-land
15.	General Modification	Several Improvements in the physics package	Sud and Walker (1992) (for a detailed discussion)

^{*} Personal Communication

^{**}HV = Harshvardhan

III. List of Quantities

This section describes the analyzed quantities and units used. The first momentum fields in Section VI mainly follow those of Schubert et al. (1990) except for the following differences. The global maps for the 10-year averages primarily include the 850 and 200 mb fields. But the streamfunction field and its eddy part (deviation from the zonal mean) are shown only at the 200 mb level. The geopotential height and the vertical p-velocity fields are shown at the 500 mb level. The specific humidity fields are shown at the 850 mb level. The vertical cross sections are based on the zonal averages on the pressure levels 1000, 925, 850, 700, 500, 400, 300, 250, 200, 150, and 100 mb. The following table shows the fields whose seasonal and annual means have been plotted. The fields are shown in the sequence of the plots. Negative values are shaded for the fields marked with *.

Seasonal and Annual Mean First Momentum Fields

Global Map

		
Title	Field	Contours
U850	850 mb zonal wind	$3 m s^{-1}*$
U200	200 mb zonal wind	$5 m s^{-1}*$
V850	850 mb meridional wind	$2~m~s^{-1}$ *
V200	200 mb meridional wind	$2~m~s^{-1}$ *
T850	850 mb temperature	$5~^{\circ}K$
T200	200 mb temperature	$2~^{\circ}K$
SLP	sea level pressure	$4\ mb*$
Z500	500 mb geopotential height	20 m*
q850	850 mb specific humidity	$1 \ g \ kg^{-1}$
$\omega 500$	500 mb vertical p-velocity	$3 \times 10^{-2} Pa \ s^{-1} *$
Full	200 mb streamfunction	$10 \times 10^6 m^2 \ s^{-1} *$
EDDY	200 mb eddy streamfunction	$5 \times 10^6 m^2 \ s^{-1} *$
$\chi 850$	850 mb velocity potential	$1 \times 10^6 m^2 \ s^{-1} *$
$\chi 200$	200 mb velocity potential	$1 \times 10^6 m^2 \ s^{-1} *$

Longitude-Height Cross Section

Title	Field	Contours
U	zonal wind	$5 m s^{-1}*$
V	meridional wind	$0.5 \ m \ s^{-1}*$
ω	vertical p-velocity	$0.5 \times 10^{-2} Pa\ s^{-1}*$
${ m T}$	temperature	10 °K
q	specific humidity	$1 \ g \ kg^{-1}$

Seasonal Cycle

The seasonal cycle of the following quantities is based on the 10-year monthly averages of zonal mean of each field.

Title	Field	Contours
U200	200 mb zonal wind	$5 m s^{-1}*$
V200	200 mb meridional wind	$3 m s^{-1}*$
T200	200 mb temperature	$3~^{\circ}K$
U850	850 mb zonal wind	$3 m s^{-1}*$
V850	850 mb meridional wind	$2 m s^{-1}*$
T850	850 mb temperature	$5~^{\circ}K$
$\mathbf{Q}850$	950 mb specific humidity	$1 \ g \ kg^{-1}$
$\omega 500$	500 mb vertical p-velocity	$2 \times 10^{-2} Pa\ s^{-1}$
E-P	evaporation - precipitation	$1\ mm\ day^{-1}$

Zonal Mean Anomalies

The zonal averages of the monthly mean deviation from the seasonal cycle is shown from 1979 to 1988.

Title	Field	Contours
U200	200 mb zonal wind	$2~m~s^{-1}*$
V200	200 mb meridional wind	$0.5 \ m \ s^{-1}*$
T200	200 mb temperature	$0.5~^{\circ}K*$
T850	850 mb temperature	$0.5~^{\circ}K*$
Q850	850 mb specific humidity	$0.3 \ g \ kg^{-1}*$
$\omega 500$	500 mb vertical p-velocity	$1 \times 10^{-2} Pa \ s^{-1} *$

Hydrology

Precipitation

The model-simulated total precipitation P, as well as the observed precipitation, are shown for the seasonal and annual averages of 10 year mean fields. The observed precipitation is a combination of raingauge measurement over land and Microwave Sounding Unit (MSU) analysis over the ocean (Spencer, 1993). The precipitation anomalies for the simulated and the observed are shown as deviations from their seasonal cycles. The annual anomalies are yearly deviations from the 10-year mean fields. The time series of the zonal mean precipitation for the simulated and observation is shown for the total, anomaly with seasonal cycle (10-year climatology subtracted), and anomaly with seasonal cycle removed (10-year seasonal mean subtracted). These maps have contours with 1 mm day⁻¹ interval.

Evaporation

The 10-year mean seasonal and annual averages of simulated evaporation E (and also monthly averages) are shown using 1 mm day⁻¹ contour interval. The seasonal and annual evaporation anomaly are shown with thick (thin) contours of interval 1 (0.5) mm day⁻¹. The time series of the zonal mean evaporation is shown for the total, as well as anomaly with seasonal cycle (contour interval 0.5 mm day⁻¹), and the anomaly without seasonal cycle (0.2 mm day⁻¹). The time series of the zonal mean P-E (precipitation minus evaporation) is shown for the total, anomaly with seasonal cycle, and anomaly without seasonal cycle with contour intervals of 1 mm day⁻¹.

Soil Moisture

The 10-year mean seasonal and annual mean soil moisture at the SiB model layer-2 is shown with shading for regions having soil moisture fraction from 0.3 to 0.8. The seasonal and annual anomaly soil moisture are shown with contours at \pm 0.05, 0.1, 0.2, and 0.3.

Time Series of P, E, and Soil Moisture in 12 SiB Vegetation Region

These are the averaged quantities over the area of 12 different Simple Biosphere (SiB) Model vegetation types (also called biomes). All curves with open circle or rectangle are from AMIP run, and the curves with closed circle are either from observation or from estimation. The upper two curves in the left panel are the soil moisture at the SiB layer 2 (root zone) with scale on the left ordinate (fraction from 0 to 0.75). The estimated soil moisture in closed circle is taken from the Liston et al. (1993a, b), where off-line SiB model is run, with the gridded raingauge precipitation produced by J. Schemm (personal communication), following Mintz and Walker (1993) procedure. The lower two curves in the left panel are the evapotranspiration with scale on the ordinate in the right panel from 0 to 10 mm day⁻¹. The curves in the right panel are the AMIP (open circle) and observed (closed circle) precipitation, and they follow the scale from 0 to 10 mm day⁻¹.

Monthly Mean Radiative Flux

The monthly mean net shortwave radiation into the earth-atmosphere system and outgoing longwave radiation (OLR) out of the atmosphere are plotted for the simulated radiative flux (AMIP, top panel), and for the ERBE observations (ERBE, middle panel). The simulated radiative flux minus observed/analyzed radiative flux (DIFF, bottom panel) are also shown. The contour interval for these fields is $20 \ W \ m^{-2}$.

IV. <u>Discussion</u>

A. First Momentum Fields

a. Zonal Winds

The 850 mb zonal winds show a realistic meridional structure, i.e., easterlies in the tropics, westerlies in the midlatitudes, and easterlies again in the polar regions. The winds also show a decent annual cycle. For example, in the summer season, the easterlies change to westerlies over tropical Africa and India. As expected, they are stronger in the local winters and weaker in local summers. As compared to the

European Center for Medium Range Weather Forecast (ECMWF) analysis (hereafter analysis/observations), the simulated winds are much stronger. Particularly at the polar latitudes, the simulated winds become quite unrealistic and large, which suggests model deficiency. Also, wintertime north Atlantic storm track winds are stronger than the observed. At the 200 mb level, the zonal winds, although somewhat stronger than the observed, better agree with the analysis except for the polar regions. Some notable deficiencies are: the simulated easterlies in the tropics are not as widely spread as those in the observationa; moreover, winds in the polar regions are too strong. These effects can also be identified in the seasonal and annual mean fields.

b. Meridional Winds

The 850 mb meridional winds have a reasonable distribution except for the excessive magnitudes in the polar regions. Over North America, the winds are equatorwards while over the north Pacific and Atlantic regions, they are polewards; this agrees well with observations. The wind magnitudes over South America, Northern and Southern Africa and Eurasia are large in the seasonal means but appear quite reasonable in the annual mean. The meridional winds at the 200 mb level are somewhat stronger than observed, but better agree with the analysis than they do at the 850 mb level except for the polar regions. Some notable deficiencies are in the European regions, Highland regions of India, and China while both polar regions have much stronger winds, which may well be related to inaccurate solutions of the primitive equations in the viscinity of orography.

c. Temperature

As compared to observation, the 850 mb temperature distribution seems much better than that of 200 mb level. In the latter case, particularly during winter and spring, the temperature gradients in the meridional direction are much stronger than observed, with the highest gradients in the polar regions. This is accompanied by excessive cooling in the entire troposphere, which is strong in the polar regions. The 200 mb temperature over the south (north) polar region is about 20 (10) K too

low, and this seems to be consistent throughout all the seasons, except that south polar regions at upper levels are warm enough to be close to the observed during summer and autumn. This is a model deficiency that needs to be addressed.

d. SLP and 500 mb Height

The SLP and the zonal departure of 500 mb height fields show some strong gradients in the poleward direction. They appear quite reasonable in the southern high latitude regions in both seasonal, as well as annual, variations, but the gradients are much too strong in the northern high latitudes. Often SLP gradients translate into the geopotential height gradients for which only the eddy part has been shown. Lower SLPs, simulated over the western Antarctic, produce convergence, as opposed to divergence, in the region leading to spurious precipitation. This weakness did not exist in the 9-layer model and needs further investigation.

e. Specific Humidity at 850 mb and 500 mb ω

The 850 mb specific humidities are well simulated. The model is somewhat drier in the tropics because the 850 mb level is above the cloud base level where sinking dries it. A new downdraft scheme (Sud and Walker, 1993) is implemented into the model, which is likely to improve this condition. The 500 mb ω (vertical p-velocity) fields appear to be quite reasonable. Strong values in the vicinity of orographic gradients are related to rising/sinking components of the strong motion fields. The large-scale vertical p-velocity structure appears quite reasonable as compared to ECMWF analysis. However, rising motion over the western and central tropical Pacific is up to four times stronger than the analysis.

f. Streamfunction at 200 mb

The 200 mb streamfunction depicts the rotational part of wind structure of the model. The simulated winds correspond well with the ECMWF analysis. Strong gradients over the south pole region point to the pole problems. The analyzed winds in the region have a smooth zonal pattern. The winds over the midlatitudes seem quite reasonable and agree well with the analysis, except that they are a bit too

strong, particularly in their seasonal depictions.

g. Velocity Potentials at 200 and 850 mb

The 200 and 850 mb velocity potentials depict the planetary scale divergent motion fields. The convergence towards the center of the maximum velocity potential and divergence away from the minimum value agree well with the ECMWF analysis. The velocity potential gradients at 850 mb are stronger than those in the ECMWF analysis, which is consistent with stronger simulated winds at the 850 mb level. Otherwise, the location of the centers of convergence and divergence appear reasonable.

h. Zonal Mean U, V, and ω

The zonal mean U-winds are somewhat weaker in the tropics. Although the variation of the annual cycle is well simulated (with the strongest winds in the summer), the middle tropospheric winds do not become easterly in the tropics. The subtropical jets seem to have resonable strength: a closed (open) jet of annual mean strength of 25 (35) m s⁻¹ at the 200 mb level in the northern (southern) latitudes is quite reasonable as compared to ECMWF analysis. The V-wind simulation also appears quite reasonable; whereas, the vertical motion fields, ω 's, are somewhat stronger. In the seasonal depictions, the intra-annual variation of these fields seems to be quite reasonable. The extreme vertical motion over Antarctica is again the manifestation of the orographic influence on the strong simulated wind. Another point to be noted is that in the midlatitude, the upward motion is not strong enough to be comparable to the observation.

i. Zonal Mean Temperature and Humidity

The temperature fields show upper level cooling everywhere and some significant cooling at the high latitudes. This problem has already been pointed out earlier. In fact, the problem of cooling at the poles has been plaguing the GLA GCM for quite some time, and it has still to be solved. The humidity fields cannot be compared because the analyses are model dependant; therefore, we reckon that

they cannot be verified and are shown here for completeness.

j. Zonal Mean Annual Cycle for U, V, and T at 200 and 850 mb

The seasonal cycle of U and V at 200 mb level agrees well with the observations. The T-field shows closed highs at 30° N – 60° N latitudes. This is not seen in the ECMWF analysis. Since it is the middle of summer for the northern latitudes, we believe that such a depiction is not unreasonable. At the 850 mb level, we get stronger winds and stronger wind gradients. This is reflected in the seasonal structure of U-winds; for example, the strong subtropical westerlies from May to October are not seen in the observation. The pole problems reflect severely in the V-wind errors at high latitudes. The annual cycle of wind structure simulated by the model is much stronger than that in the ECMWF analysis. However, the improvement in the analysis in the later years (1984 - 1987) helps to close the large gap between our simulations and the analysis.

k. Annual Cycle for Zonal-Mean Humidity-850 mb, ω -500 mb, and E-P

The simulated humidities appear reasonable. In this case, too, the recent improvement in the ECMWF analysis brings the analyzed fields closer to our simulations. This suggests that the discrepancies between the simulated and analyzed fields are not entirely caused by simulation errors. The large-scale seasonal variation of the vertical winds at 500 mb is quite reasonable, even if the strong upward motion from May to October is not seen in the observation. The 500 mb vertical winds and moisture divergence correspond well to each other. Rising motion is consistent with increased precipitation.

l. Fluctuations in U, V, T-200 mb and T-850 mb, Q-850 mb and ω -500 mb

At high latitudes, 200 mb winds have higher magnitude and lower frequencies, as compared to the tropics. The period appears to be about 90 days at midhigh latitudes, with only an annual fluctuation. Correspondingly, T-200 mb has much stronger fluctuations, as compared to T-850 mb. As expected, the strongest fluctuations occur in the polar regions. The humidities over the southern polar caps

are naturally quite low, while over the southern oceans, they are quite uniform; therefore, the fluctuations appear over the northern high latitude regions only. In the tropics, low (high) humidities can be seen in 1987 (1988).

B. <u>Hydrology</u>

a. Total Precipitation Climatology

The seasonal vis-a-vis observed precipitation climatologies show that the model does a good job of simulating the rainfall patterns. The fields are much more realistic over the oceans, as compared to land; however, the simulation is poor, particularly in the vicinity of orography. High rainfall over Colombia in South America is spurious; the Indian monsoon is also somewhat displaced because of sharp Himalayan orography; the precipitation over the South Pole, which the 9layer model did not have, has appeared as a result of strong convergence and is a source of some concern. It is related to the polar problems where extremely strong vertical winds dominate over Antartica. In the observations, some mismatch between the land and ocean rainfall is the result of blending satellite inferred rainfall over the oceans with raingauge observations. The differences show that the modelsimulated precipitation are systematically less, as compared to satellite data in the Intertropical Convergence Zone (ITCZ) and South Pacific Convergence Zone (SPCZ) regions, whereas, they are better correlated with observations over land. Systematic errors over the Sahara region may be related to 4% – 8% lower albedo of deserts, as compared to ERBE products. Model tends to rain more over coastal North America but less over coastal West Africa. High simulated rainfall over the tropics in Columbia seems to be a problem. The monthly precipitation climatology in the next four figures can be compared with the observations given in the following figures. Problems with precipitation structure over Amazonia, monsoonal northern India, North America, and Africa can be noted. Strong precipitation from May through December over Greenland deserves attention.

b. Simulated and Observed Precipitation Anomalies

The seasonal and annual rainfall anomalies show that the model has some

large systematic errors, but it capture salient features of Sahelian droughts for 1982 and 1983; influence of El Niño sea surface temperature (SST) anomaly on the tropical Pacific for 1983 and its reversal in 1984, which is accompanied by increased rainfall over western tropical Africa; the reduced (increased) rainfall over the tropical Pacific, in 1985 (1986) is also well captured. By 1987 another El Niño began to affect tropical Pacific and the model simulates it reasonably. It is associated with droughts over India and North Africa and Amazonia, and the model captures it. However, the skill in the midlatitudes is not good enough, as can be inferred from the simulated and the observed fields. We believe that this is related to the unrealistically strong winds, which affect the orientation of stationary waves in the midlatitudes. As we have seen before, the zonal winds in the 850 mb are comparable to the observed values, while the vertical winds are weaker than the observation. We assume that this is related to insufficient baroclinic activity in the storm track. The coarse resolution of our model could also yield weakerthan-observed transient activity over storm track region. In turn, the midlatitude baroclinic system itself might not be efficient enough to create sufficient meridional and vertical energy transfer, and the unrealistically strong upper layer winds could be a part of this deficient dynamic system.

Some large-scale features of the rainfall anomaly are well captured by the simulation. By 1988 the warm El Niño SST event was replaced by the cold La Niña event. The rainfall over the tropical Pacific was reduced significantly. There were also changes in India, Indonesia, Tropical North Africa and North and South America.

c. Zonal-Mean Simulated Vis-a-Vis Observed Precipitation

The zonal mean precipitation shows north-south excursions in association with the change of solar declination. The tropical rainfall appears a little too strong; whereas, high latitude rainfall is weak; see, for example, the rainfall in the region of roaring 40° S – 60° S. The zonal mean rainfall anomaly with seasonal cycle has a stronger structure in the model, as compared to observation. The observed precipitation anomaly has strong interannual variability between 30° N to 60° N,

but it is not apparent in the model. In the tropics, however, the simulated seasonal cycle is stronger than the observed for the entire period. The reduced rainfall in 1987 is not picked up by the model, even though the resemblence of patterns or lack of it in the zonal mean precipitation may be fortutious. The rainfall anomaly patterns in the Southern Hemisphere do not convey much, except for some correlation at a few places. The patterns with 10-year monthly mean subtracted do not show much resemblence with observations, but in 1983 and 1986 the northward propagation of the negative anomalies in the tropics shows some correspondence to the observation.

d. Surface Evaporation Climatology

The simulated seasonal vis-a-vis observed seasonal and annual evaporation climatologies that are consistent with the precipitation fields are included for completeness. There are no observations or analysis of observations for this field. A correspondence between evaporation and SST anomalies can be expected over the oceanic regions. This is evident for the tropical Pacific El Niño/La Niña years: 1982/1983 and 1987/1988. The zonal mean evaporation shows a stronger seasonal signal at higher latitudes when we examine the patterns after subtracting the 10-year mean, which is to be expected. The summer and winter patterns in the Northern Hemisphere show how an evaporation anomaly seasaw pattern develops between mid and high latitudes. In the annual cycle, higher (lower) evaporation in winter over the oceans (land) in midlatitudes and higher (lower) evaporation over land (ocean) occurs in summer in the high latitudes. The pattern results from land ocean distribution in the northern latitudes.

e. Annual Cycle for Zonal-Mean P-E

The patterns appear quite reasonable. The net drying can only occur over the oceans, because precipitation has to exceed evaporation over land to compensate for the runoff. The plots are included for completeness, because currently there is no data to compare. We hope future observations/analysis of observations can help us verify these.

f. Soil-Moisture Fraction

The simulated soil-moisture fractions climatology produced by the model for the root zone region appears to be reasonable. Although deserts are dry and precipitating regions are moist, there are some differences between the estimated and model simulated soil moistures. Some of these differences, such as the soil-moisture patterns over northern India, Amazonia, tropical Africa, and north Africa, can be related to the simulated rainfall deficiencies. The model produces soil moistures with an assumption that all snow melt gets into the soil, which produces the discrepancy over Greenland, but that is really inconsequential. In the evolving soil-moisture anomaly, one notices drying and moistening in response to initial adjustment that lasts up to 2-years. After a couple of years, the soil-moisture adjustment is reduced to simple interannual variability, as well as response to prescribed boundary forcings. The 10-year cycle for soil moisture and evaporation with the raingauge rainfall verification for different SiB biome regions shows the biospheric component of the model's performance. The soil moisture over the tropical forest is always below the estimated value and shows stronger seasonal variation. Also, there is some persistent decrease of the soil moisture over the years in the biome type-4 region (needleleaf evergreen trees). Other differences can be found in biome type-5 (needleleaf deciduous trees), biome type-6 (Savannah), and biome type-8 and 9 (broadleaf deciduous shrubs).

g. Radiation

The monthly mean net shortwave radiation entering the earth-atmosphere system (incoming solar radiation minus reflected solar radiation by the surface and atmosphere), as well as monthly mean OLR averaged from 1985 to 1988, is compared with the data generated by ERBE observation. The ERBE data is read from the CD-ROM made by NASA Climate Data System Staff (Olsen and Warnock, 1992). In general, the net shortwave radiation shows good agreement with ERBE data. There are, however, some systematic errors over oceans off the coast of Chile in South America, the west coast of the United States, and the west coast of Southern Africa. These areas are believed to have low level stratus clouds, which are

not well simulated by the model. These clouds reflect a significant amount of the solar radiation. We also notice that the magnitude of errors becomes larger in the Summer Hemisphere when the incoming solar radiation is stronger. The maximum error in these areas does reach up to $100~W~m^{-2}$. Errors can also be noted over the high orographic regions, especially Himalayas. There are significant errors near the snow boundary regions over Antarctica and the North Pole. OLR simulated by the model is also in good agreement with the ERBE data, except over a few regions such as Indonesia and Himalaya. Over the Sahara region, the simulated OLR is less than that of the ERBE data. These differences are being analyzed to help us improve our cloud and land-surface albedo parameterizations.

V. References

- Arakawa, A., and W. H. Schubert, 1974: Interaction of cumulus cloud ensemble with the large-scale environment, Part I. J. Atmos. Sci., 31, 674-701.
- Chou, M.-D, L. Peng, A. Arking, 1983: A parameterization of absorption in the 15 mm CO₂ spectral region with application to climate sensitivity studies, *J. Atmos. Sci.*, 40, 2183–2192.
- Chou, M.-D., 1984: Broadband watervapor transmission function for IR flux commutations, J. Atmos. Sci., 41, 1775-1778.
- Deardorff, J. W., 1987: Efficient prediction of ground surface temperature and moisture with inclusion of a layer of vegetation, J. Geophy. Res., 83, 1889–1903.
- Dorman, J. L., and P. J. Sellers, 1989: A global climatology of albedo, roughness length, and stomatal resistance for atmospheric general circulation models as represented by simple biosphere model (SiB), J. Appl. Metor., 28 (9), 833-855.
- Fox-Rabinovitz, M., H. M. Helfand, A. Hou, L. L. Tackas and A. Molod, 1991: Numerical experiments on forecasting climate simulation and data assimilation with the new 17 layer GLA GCM. Ninth Numerical Weather Prediction Conference, 21-25 October 1991, Denver, Colorado, 506-509
- Harshvardhan, R. Davis, D. A. Randall and T. G. Corsetti, 1987: A fast radiation parameterization for general circulation models, J. Geophy. Res., 92, 1009– 1016.
- Helfand, H. M., and J. C. Lebraga, 1988: Design of a non-singular level 2.5 second order closure model for prediction of atmospheric turbulence, J. Atmos. Sci., 45, 113-132.
- Kalnay, E., R. Balgovind, W. Chao, D. Edelmann, J. Pfaendtner, L. Takacs and K. Takano, 1983: Documentation of the GLAS fourth order general circulation model. Volume I., NASA Tech. Memo. 86064, NASA Goddard Space Flight Center, Greenbelt, Maryland.

- Kessler, E., 1969: On the distribution and continuity of water substance in the atmospheric circulation. Meteorological Monographs. Amer. Meteor. Soc., 32, 1-84.
- Lacis, A. and J. E. Hansen, 1974: A parameterization for the absorption of solar radiation in the earth's atmosphere, J. Atmos. Sci., 31, 118-133.
- Liston G. E., G. K. Walker, and Y. C. Sud, 1993: An analysis scheme for deriving global soil moisture from observed precipitation, air temperature, NDVI, and simple boisphere model hydrology. J. of Clim., (submitted.)
- Liston G. E., Y. C. Sud, and G. K. Walker, 1993: Design of a global soil moisture initialization procedure for the simple biosphere model. NASA Technical Memorandum 104590.
- Mintz, Y., and Y. Serafini, 1984: Global fields of normal monthly soil moisture, as derived from observed precipitation and an estimated potential evapotranspiration. Part V, Final Scientific Report Under NASA Grant No. NAS5-26. Dept. Meteorology, University of Maryland, College Park, MD. 20742.
- Mintz, Y., and G. Walker, 1993: Global fields of soil moisture and land surface evapotranspiration, derived from observed precipitation and surface air temperature. J. Appl. Meteor., 32, 1305-1334.
- Olsen, L. M., and A. Warnock III, 1992: Greenhouse Effect Detection Experiment (GEDEX) Selected data sets, NASA Climate Data System Staff, Goddard distributed Active Archive Center, NASA Goddard space Flight Center, Greenbelt, Maryland 20771
- Rodgers. C. D., 1968: Some extension and application of new random model for molecular and band frequency. Quart. J. Roy. Met. Soc., 94, 99-102.
- Rosenfield, J. E., M. R. Schoebrel, and M. A. Geller, 1987: A computation of the stratospheric diabatic circulation using an accurate radiative transfer model. J. Atmos. Sci., 44, 859-876.
- Ruprecht, E., and W. M. Gray, 1976: Analysis of satellite-observed tropical cloud clusters II thermal, moisture and precipitation fields. *Tellus*, 28, 414-426.

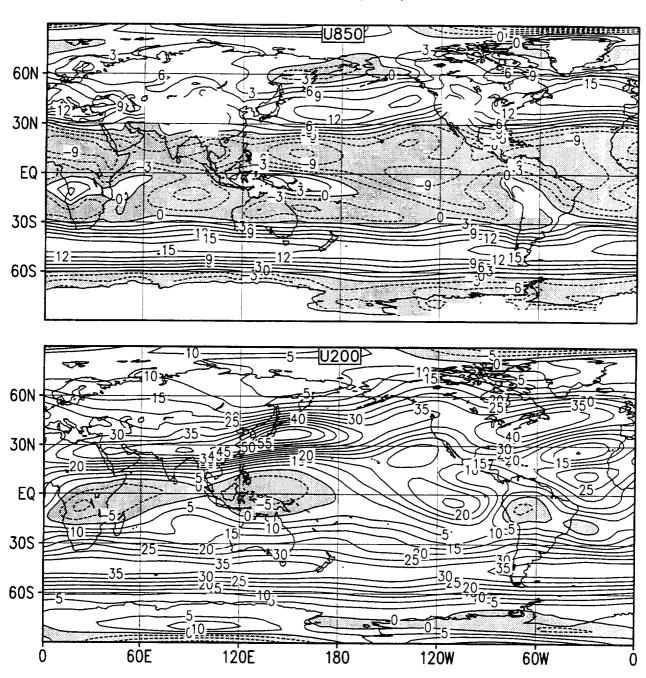
- Sellers, P. J., Y. Mintz, Y. C. Sud, A. Dalcher, 1986: A simple biosphere model (SiB) for use within general circulation models. J. Atmos. Sci., 43, 505-531.
- ——-, 1985: Canopy reflectance, photosynthesis and transpiration. In. J. Rem. Sens., 6(8), 1335-1372.
- Schubert, S., C.-K. Park, W. Higgins, S. Moorthi, and M. Suarez, 1990: An atlas of ECMWF analyses, NASA Technical Memorandum No. 100747, 258pp.
- Slingo, J. 1987: The development and verification of a cloud prediction scheme for the ECMWF model. Quart. J. Roy. Meteor. Soc., 106, 747-770.
- Spencer, R. W. 1993: Global oceanic precipitation from the MSU during 1979 91 and comparison to other climatologies, J. of Clim., 6, 1301–1326.
- Sud, Y. C., and A. Molod, 1988: The roles of dry convection, cloud-radiation feedback processes and the influence of recent improvements in the parameterization of convection in the GLA GCM. Mon. Wea. Rev., 116, 2366-2387.
- ------, P. J. Sellers, Y. Mintz, M. D. Chou, G. K. Walker, and W. E. Smith, 1990: Influence of the Biosphere on the global circulation and the Hydrologic cycle
 a GCM simulation experiment. Forest Meteorology. AGMET, 52: 1-2, 133-179.
- ——, W. C. Chao and G. K. Walker, 1991: Contributions to the implementation of Arakawa-Schubert cumulus parameterization in the GLA GCM. J. Atmos. Sci., 48, 1573–1586.
- ------, and G. K. Walker, 1990: A review of recent research on improvement of physical parameterizations in the GLA GCM. Physical Processes in Atmospheric Models, (Ed D.R. Sikka and S. S. Singh). Wiley Eastern Ltd. 4654/21 Daryaganj, New Delhi 110002.
- ----, and ----, 1993: A rain-evaporation and downdraft parameterization to complement a cumulus-updraft scheme and its evaluation using GATE data. *Mon. Wea. Rev.*, (Accepted.)
- Tokioka, T., K. Yamazaki, A. Kitoh, and O. T. Ose, 1988: The Equatorial 30-60 day and the Arakawa-Schubert Cumulus Parameterization. J. Meteor. Soc.,

- Japan, 66, 883-900.
- WCP-55, 1983: World climate research report of the experts meeting on Aerosols and their climatic effects. Ed. A. Deepak and H. E. Gerber, World Climate Research Report of WMO, 107pp.
- Xue, Y. K., P. J. Sellers, J. L. Kinter III, and J. Shukla, 1991: A simplified Biosphere model for global climate studies, J. of Climate, 4, 345–364.

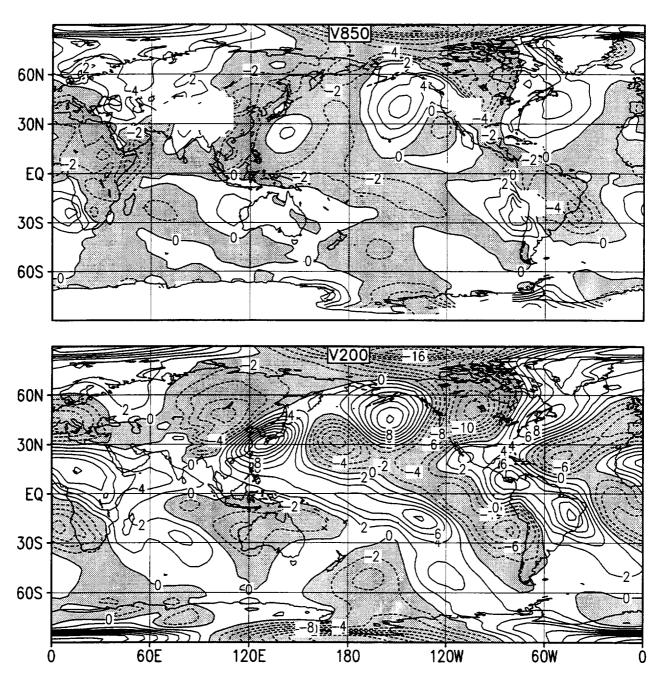
VI. THE FIRST MOMENTUM FIELDS

A. SEASONAL AVERAGES

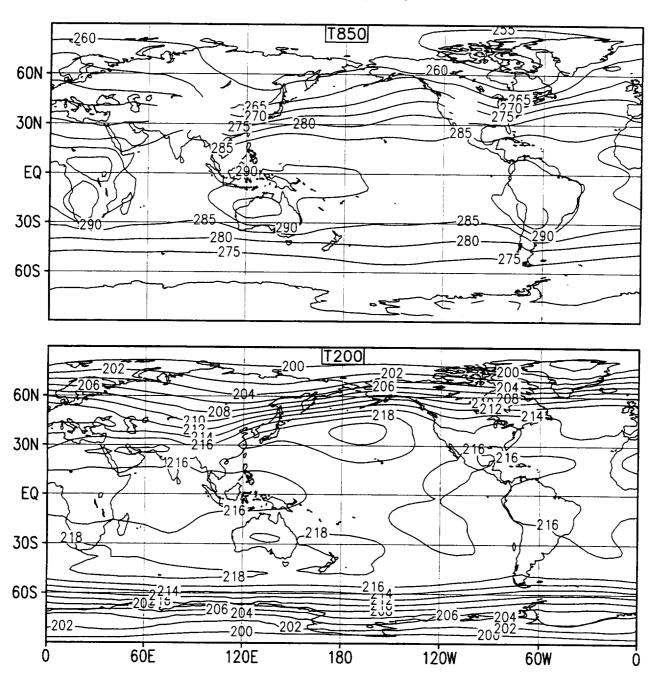
Zonal Wind (m/s)
10 Year Mean (1979-88)
Winter (DJF)



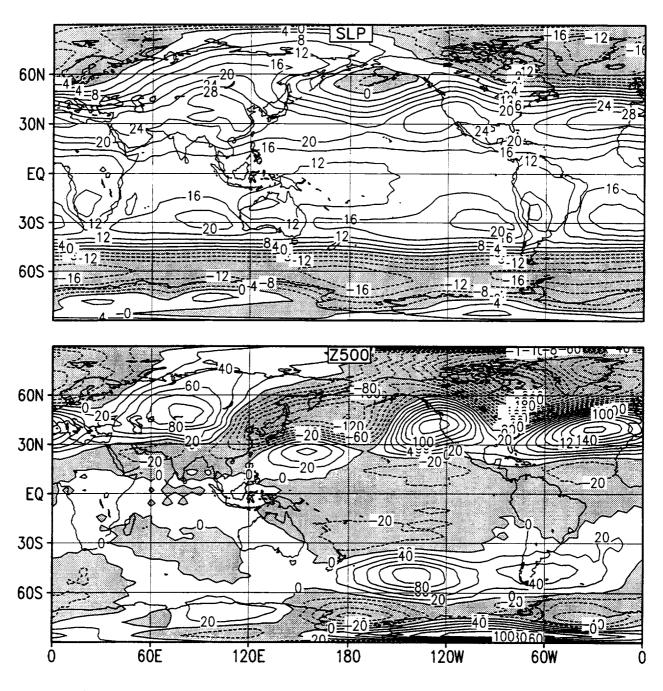
Meridional Wind (m/s)
10 Year Mean (1979-88)
Winter (DJF)



Temperature (K)
10 Year Mean (1979-88)
Winter (DJF)

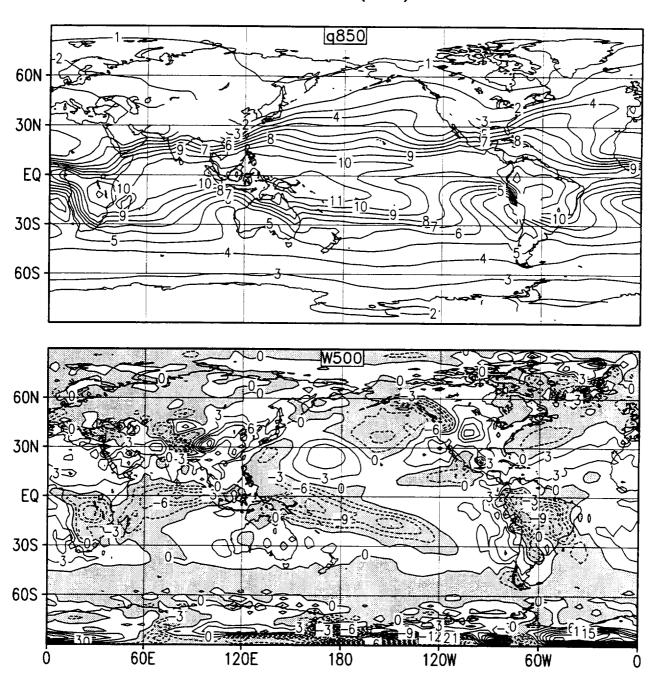


SLP-1000 (mb) and 500 mb eddy Z (m)
10 Year Mean (1979-88)
Winter (DJF)

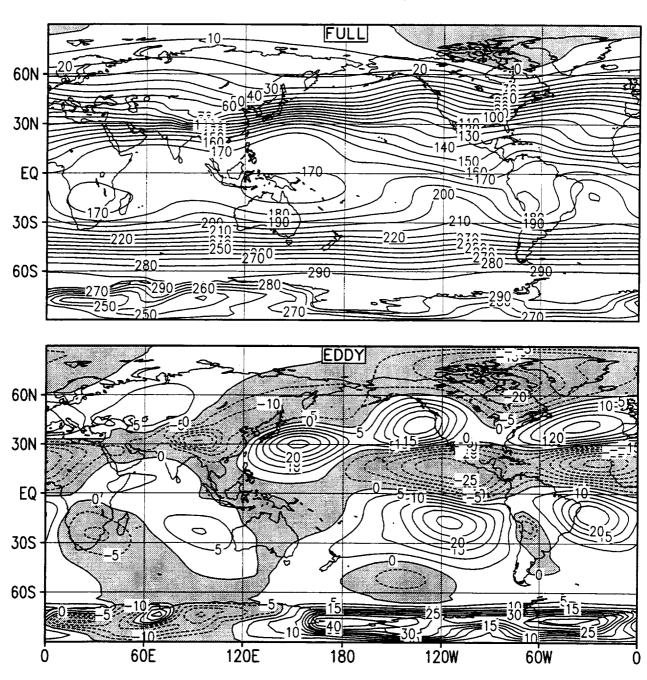


850 mb q (g/kg) and 500 mb W (Pa/s) 10 Year Mean (1979-88)

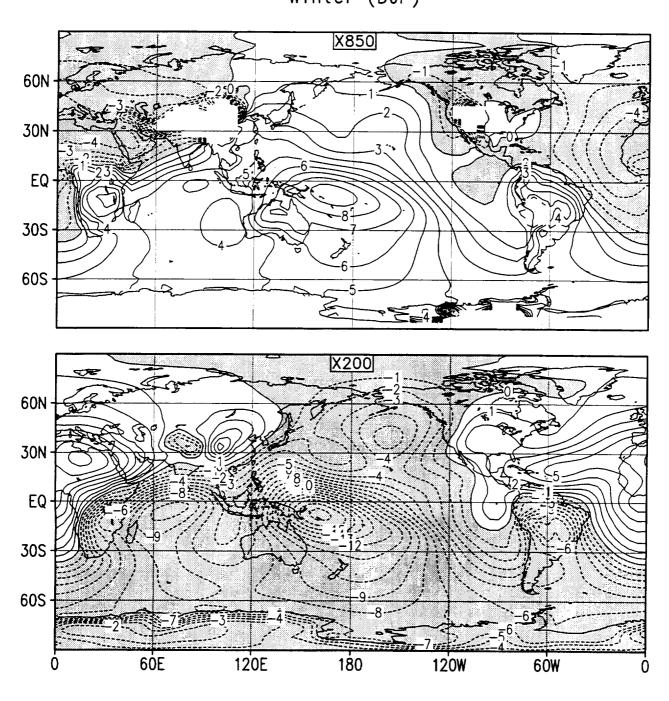
Winter (DJF)

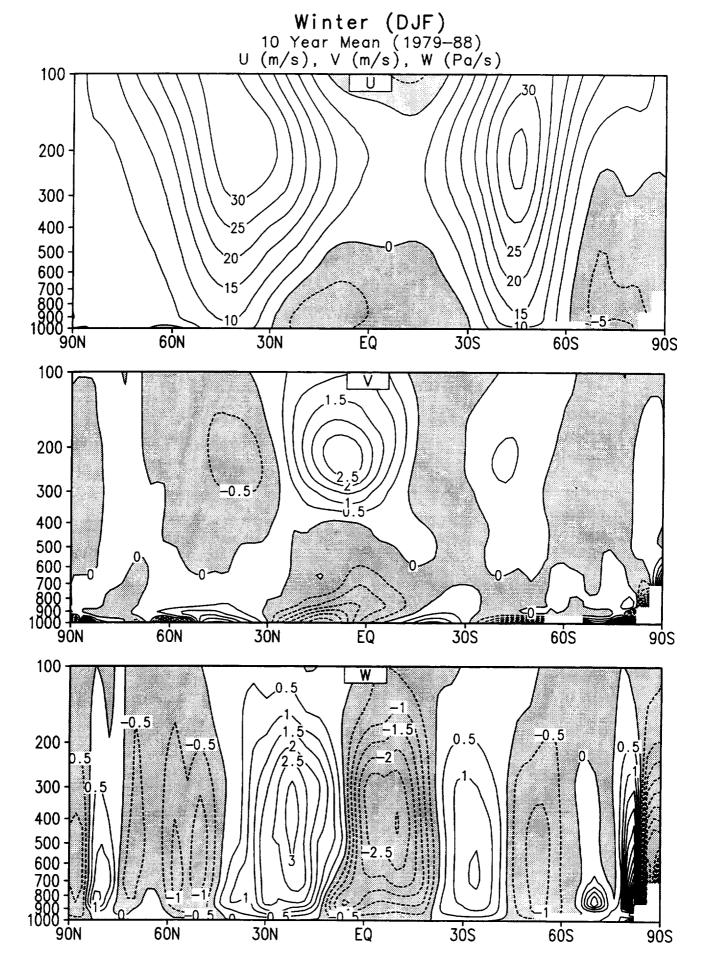


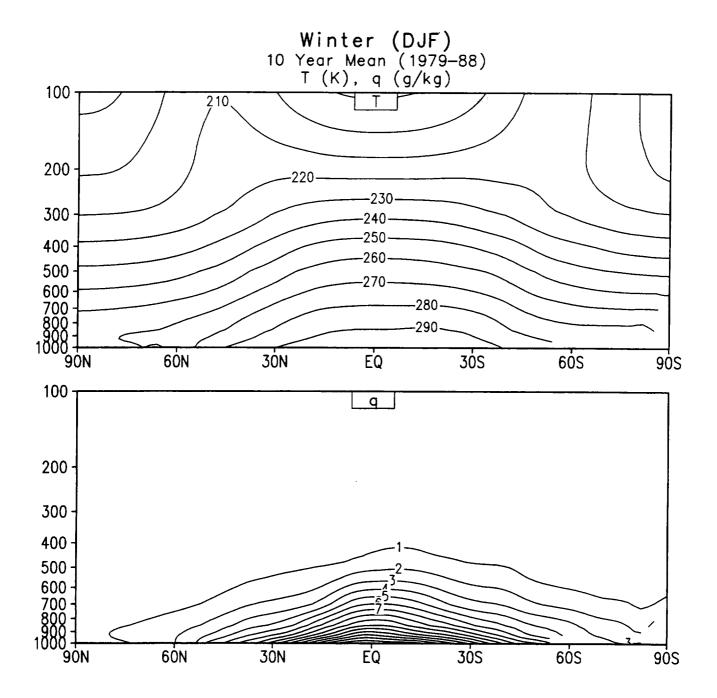
200 mb Stream Function (10E6 m**2/s) 10 Year Mean (1979-88) Winter (DJF)



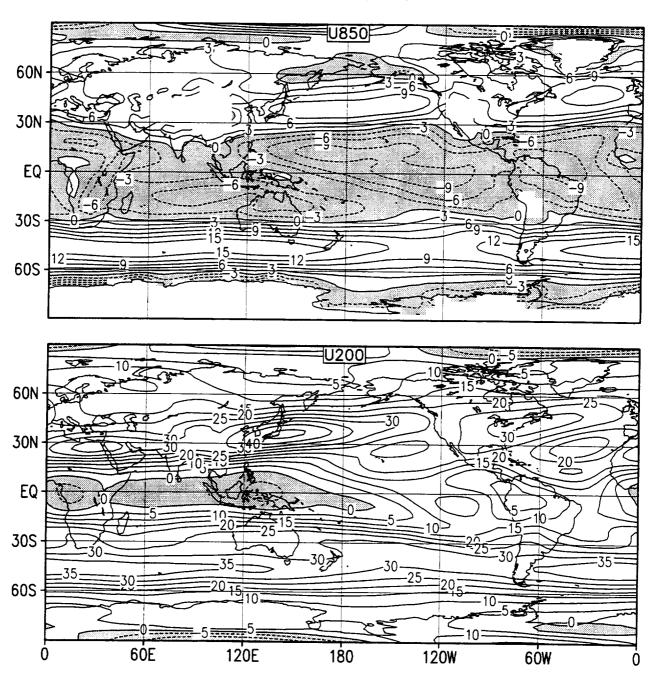
Velocity Potential (10E6 m**2/s) 10 Year Mean (1979-88) Winter (DJF)



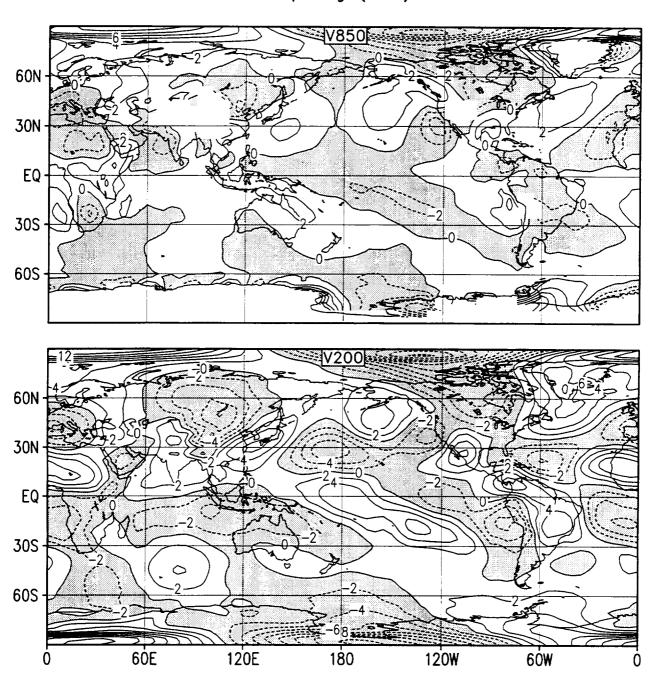




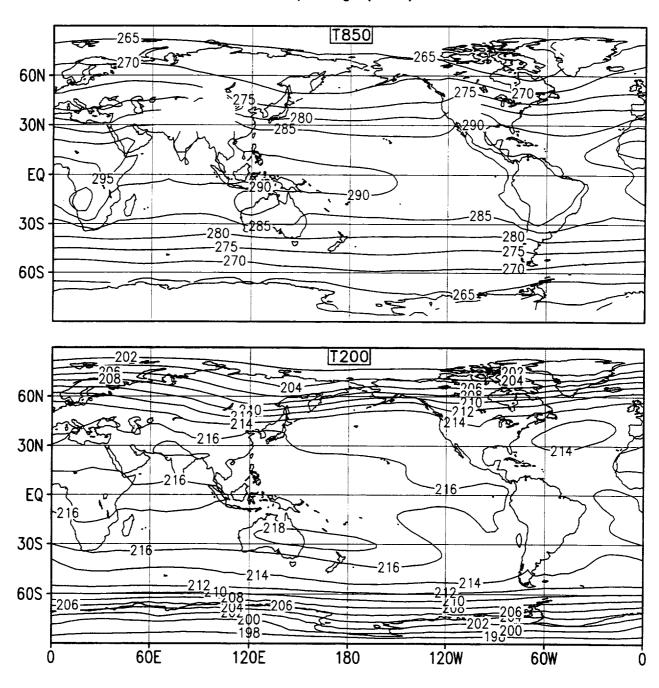
Zonal Wind (m/s)
10 Year Mean (1979-88)
Spring (MAM)



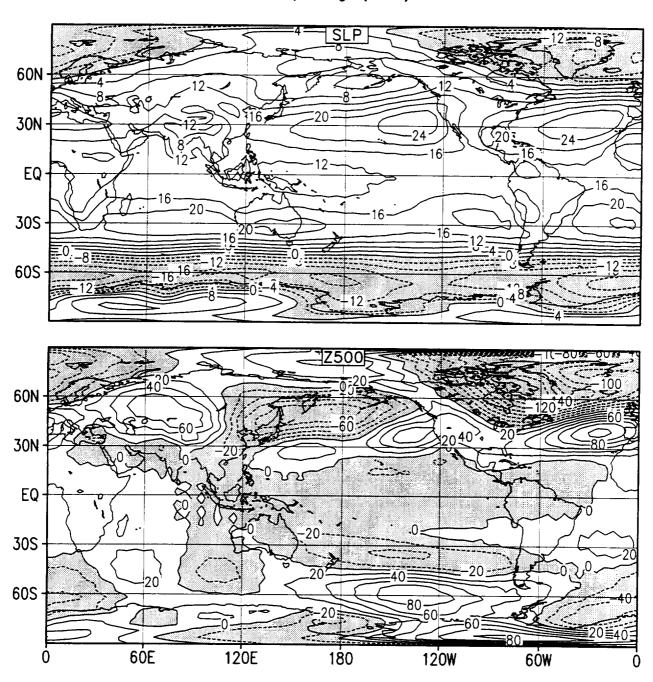
Meridional Wind (m/s)
10 Year Mean (1979-88)
Spring (MAM)



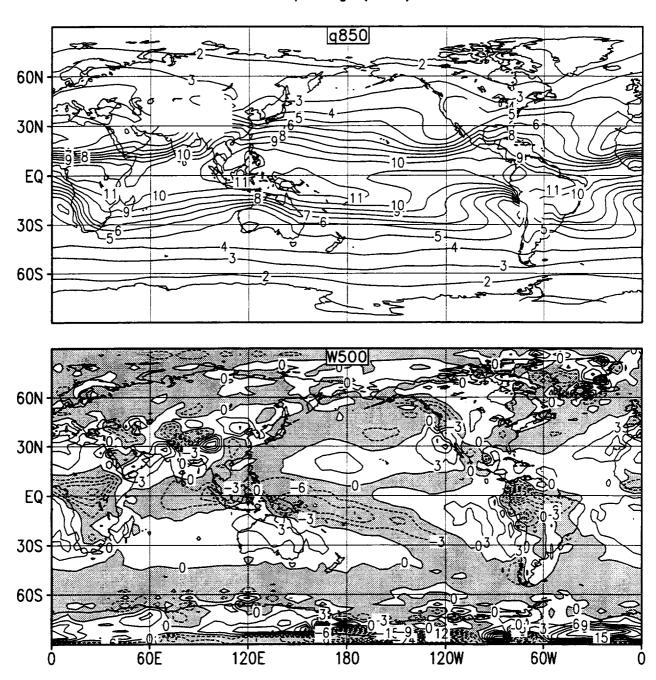
Temperature (K)
10 Year Mean (1979-88)
Spring (MAM)



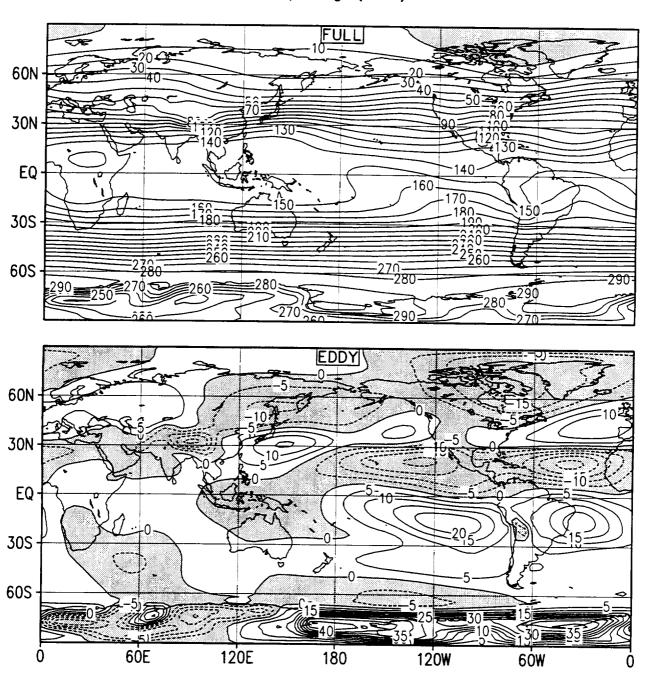
SLP-1000 (mb) and 500 mb eddy Z (m)
10 Year Mean (1979-88)
Spring (MAM)



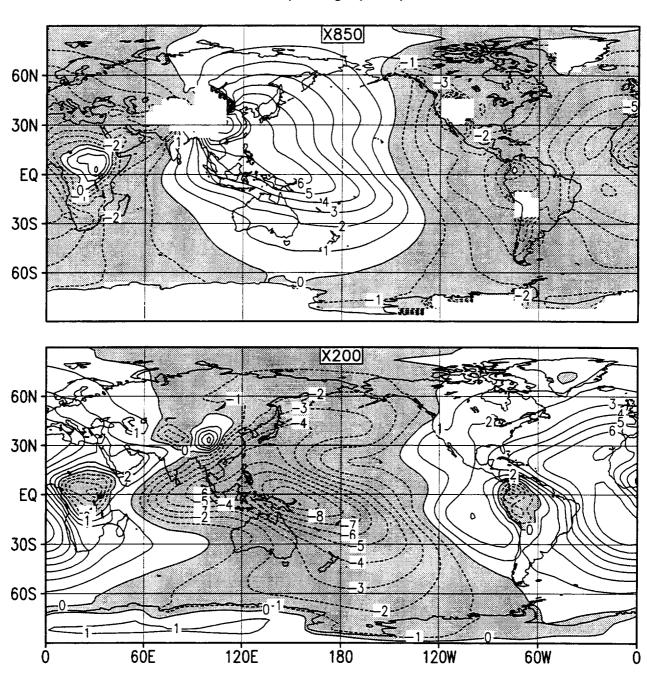
850 mb q (g/kg) and 500 mb W (Pa/s)
10 Year Mean (1979-88)
Spring (MAM)

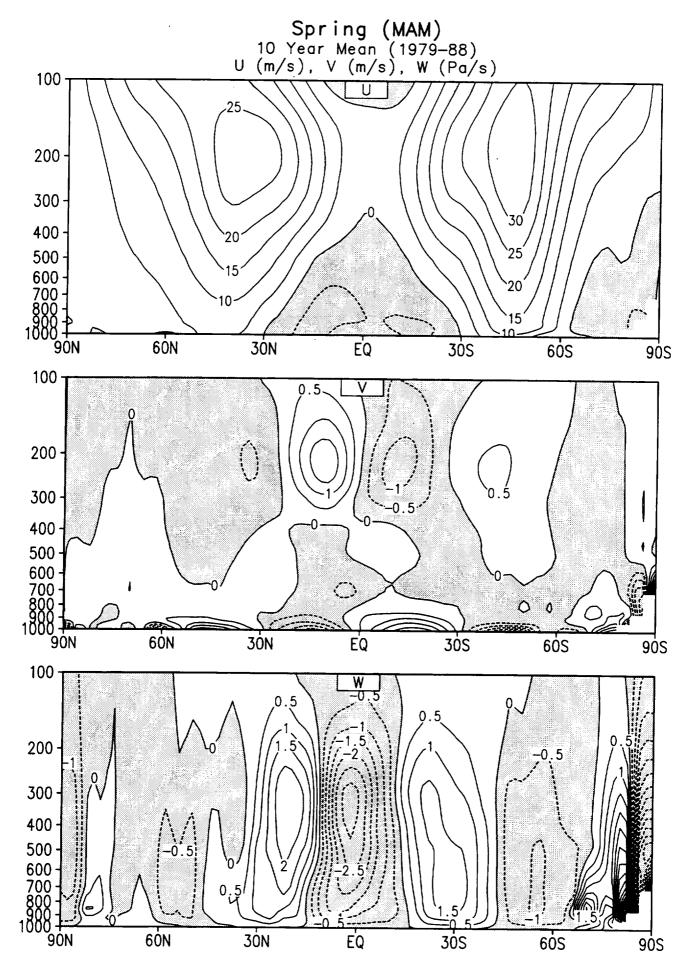


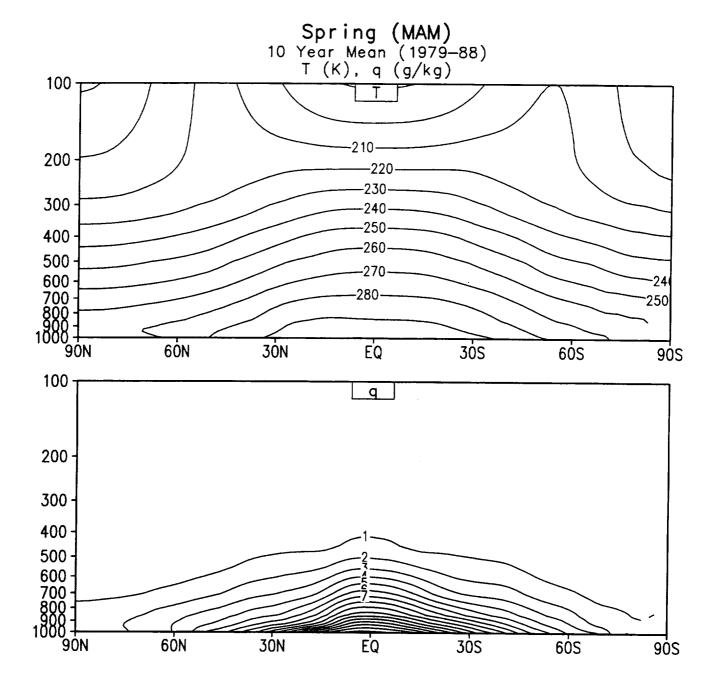
200 mb Stream Function (10E6 m**2/s) 10 Year Mean (1979-88) Spring (MAM)



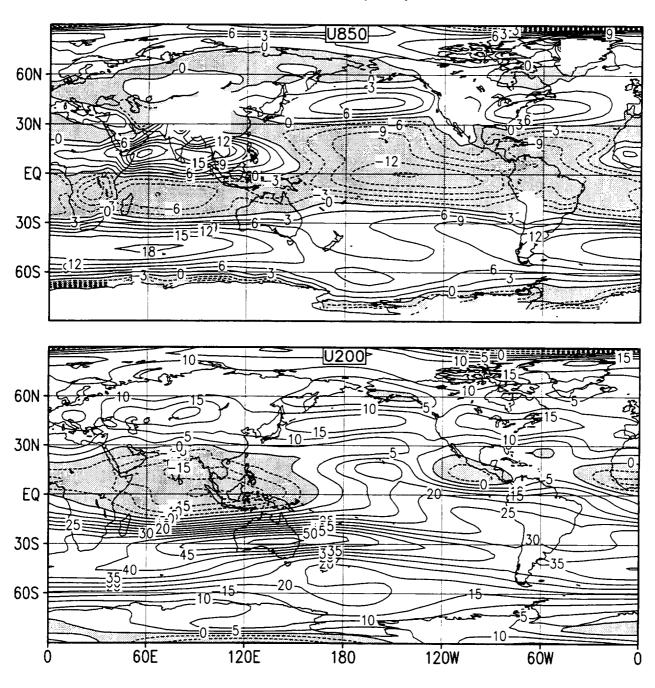
Velocity Potential (10E6 m**2/s) 10 Year Mean (1979-88) Spring (MAM)



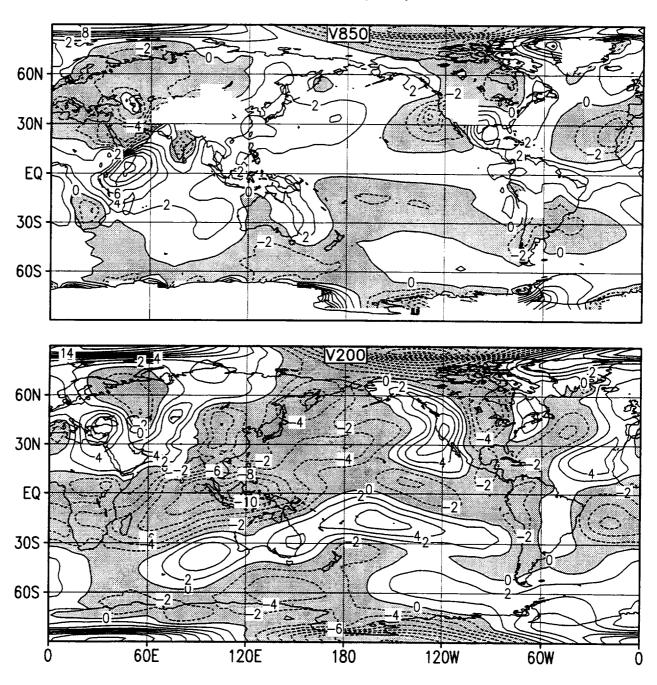




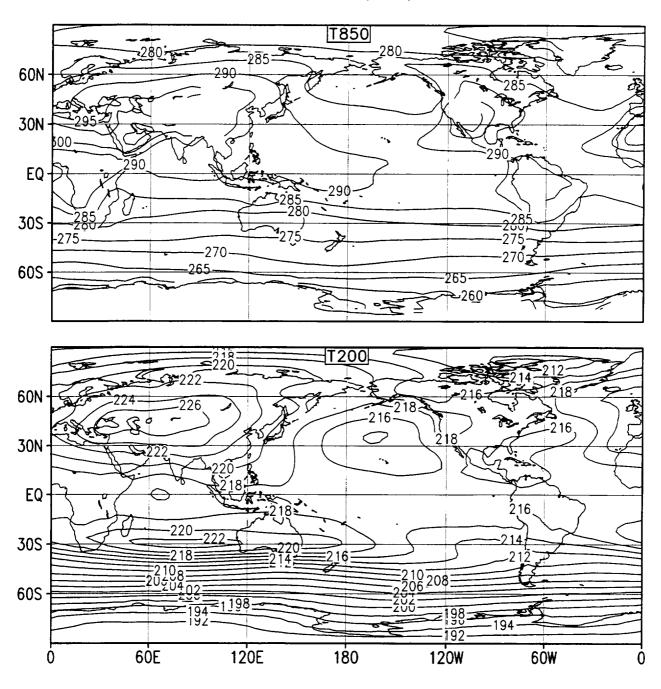
Zonal Wind (m/s)
10 Year Mean (1979-88)
Summer (JJA)



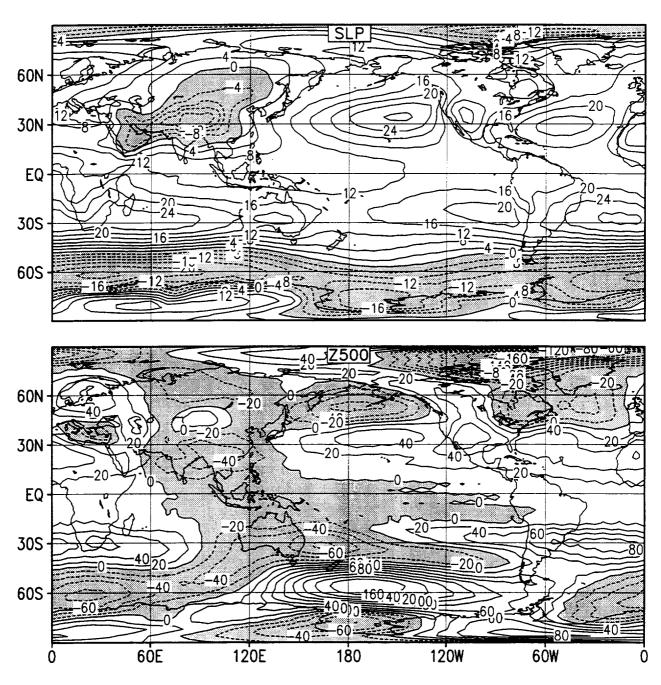
Meridional Wind (m/s) 10 Year Mean (1979-88) Summer (JJA)



Temperature (K)
10 Year Mean (1979-88)
Summer (JJA)

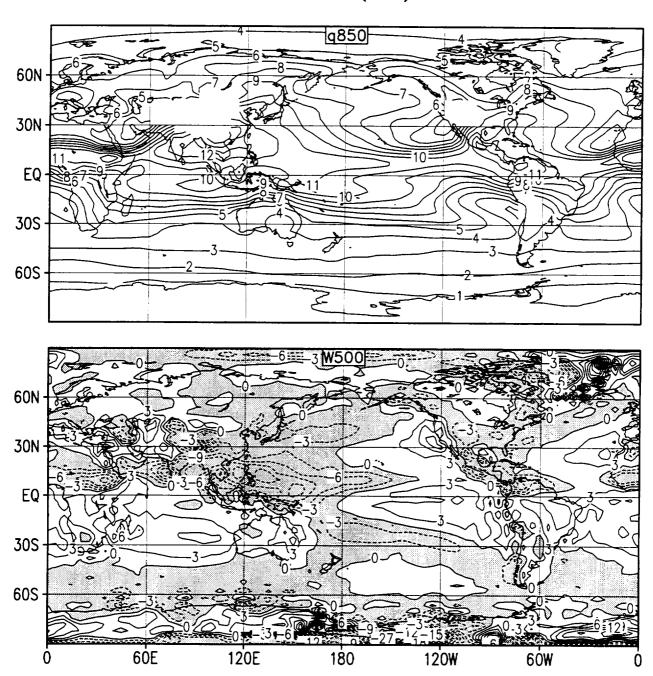


SLP-1000 (mb) and 500 mb eddy Z (m) 10 Year Mean (1979-88) Summer (JJA)

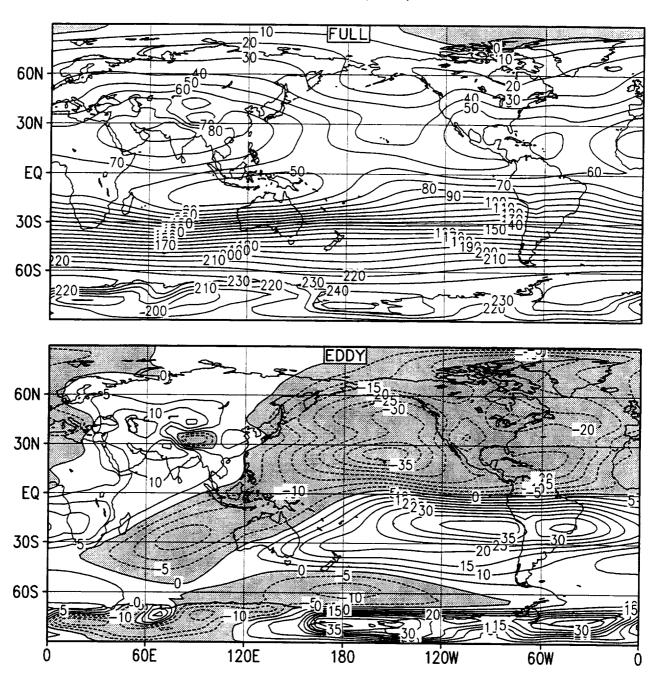


850 mb q (g/kg) and 500 mb W (Pa/s) 10 Year Mean (1979-88)

Summer (JJA)

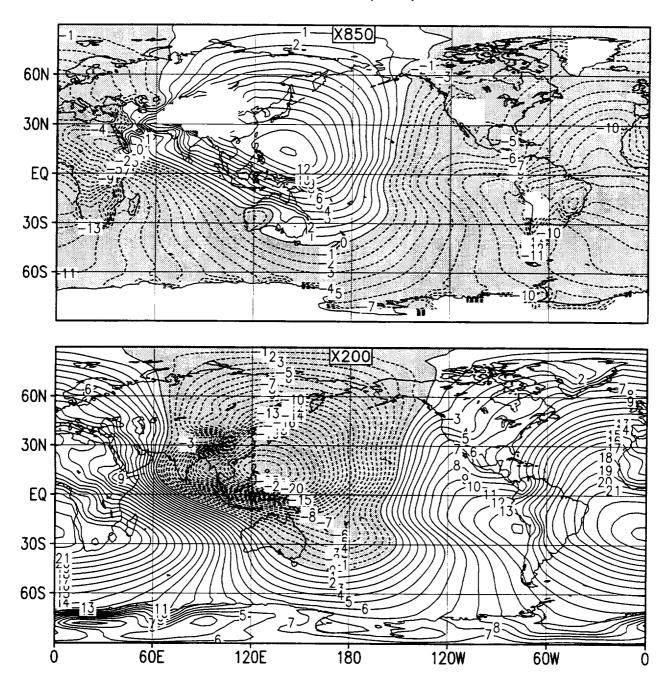


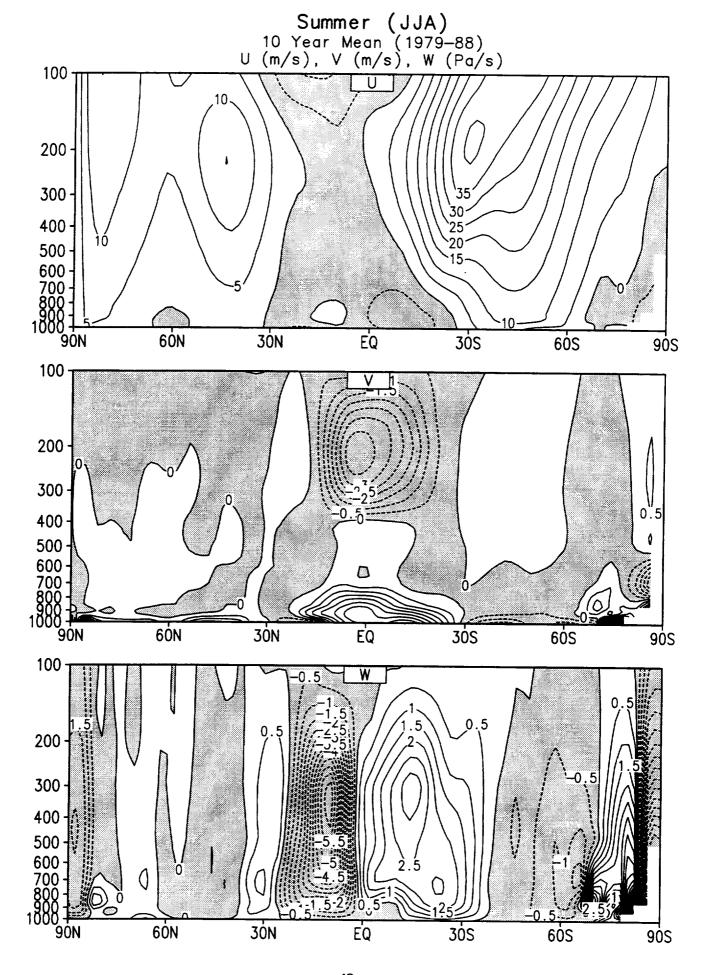
200 mb Stream Function (10E6 m**2/s)
10 Year Mean (1979-88)
Summer (JJA)

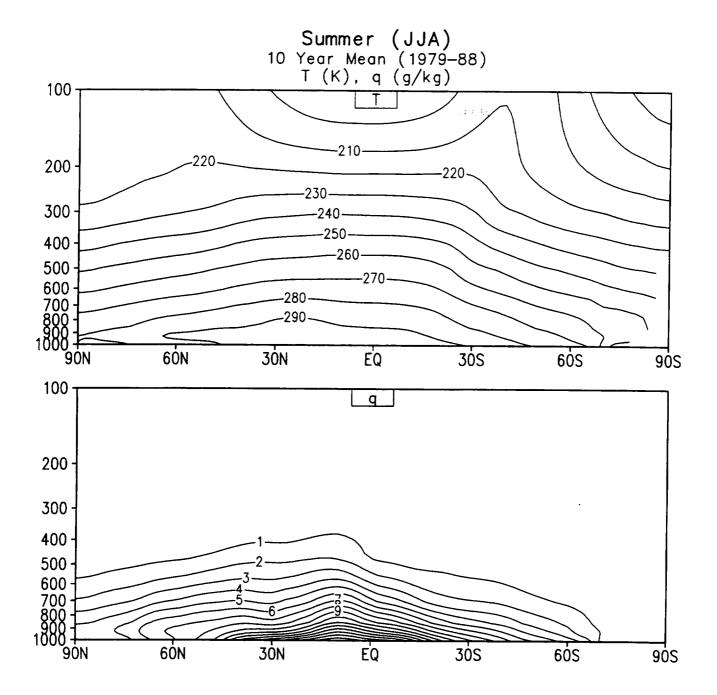


Velocity Potential (10E6 m**2/s) 10 Year Mean (1979-88)

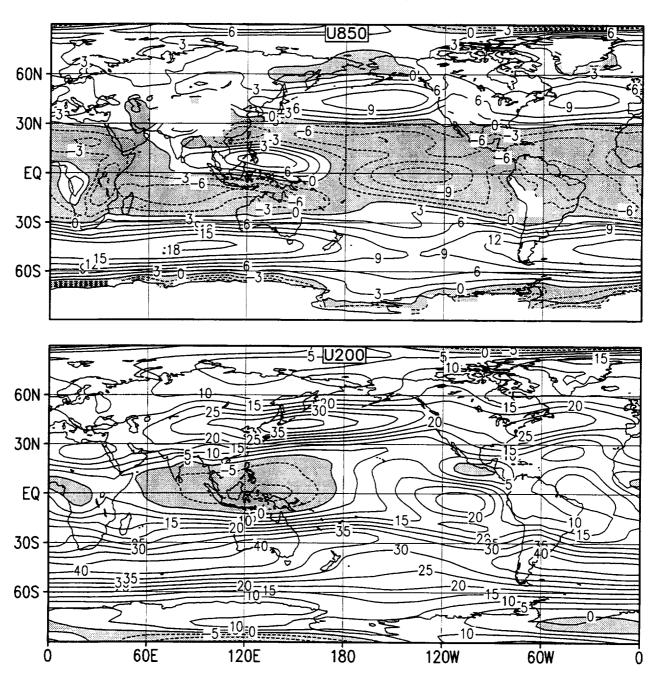
Summer (JJA)



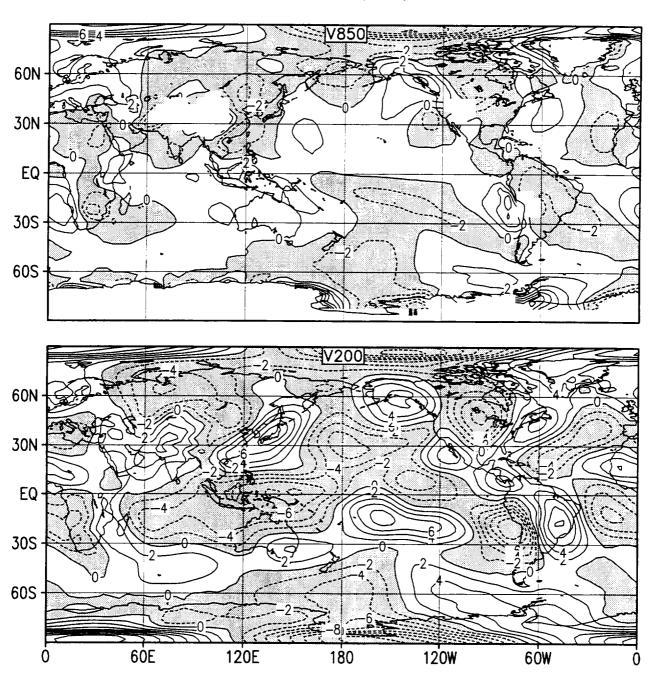




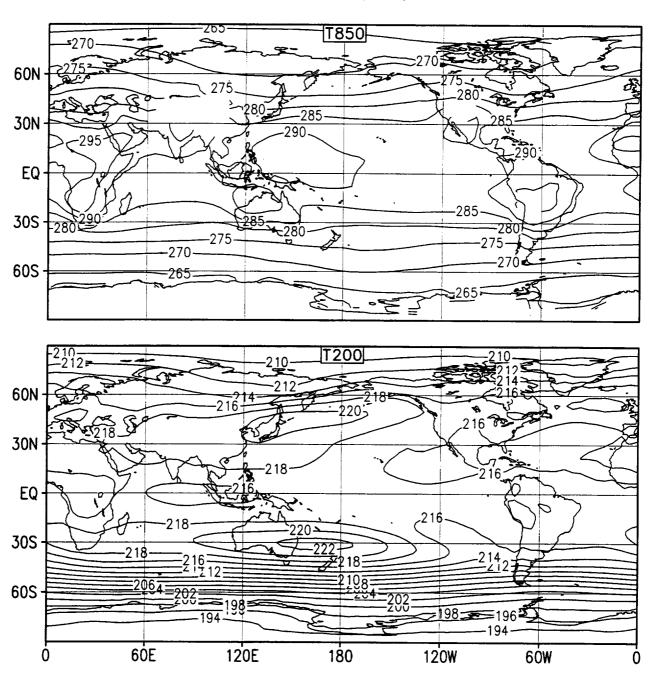
Zonal Wind (m/s)
10 Year Mean (1979-88)
Autumn (SON)



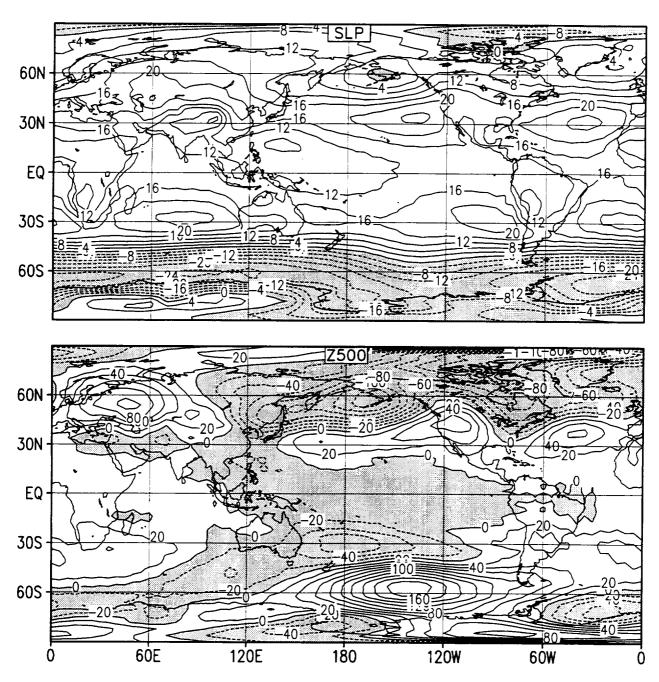
Meridional Wind (m/s)
10 Year Mean (1979-88)
Autumn (SON)



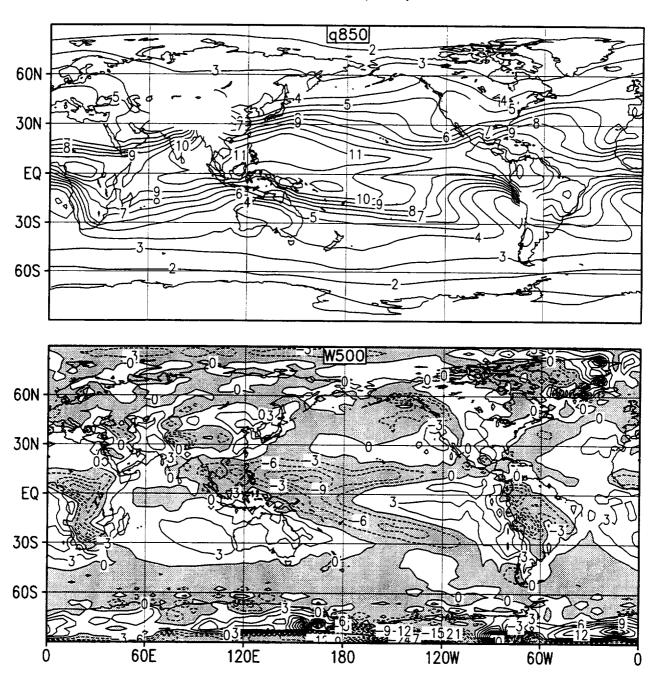
Temperature (K)
10 Year Mean (1979-88)
Autumn (SON)



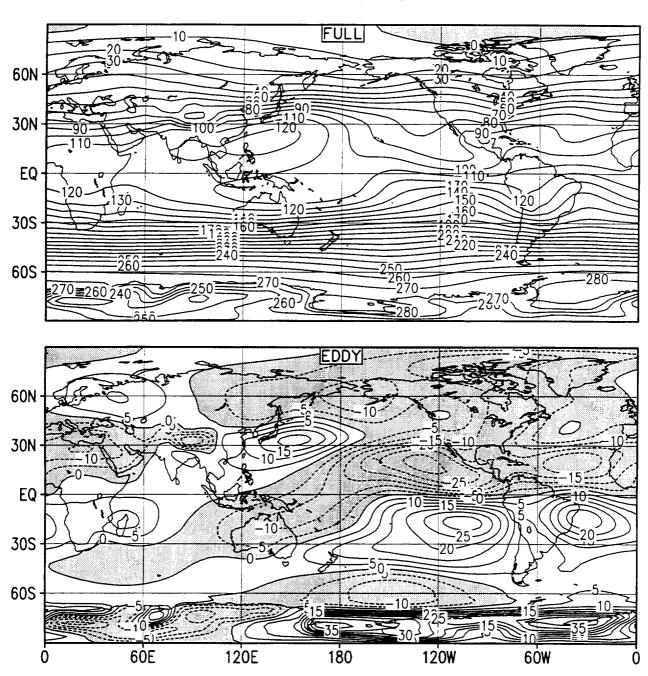
SLP-1000 (mb) and 500 mb eddy Z (m) 10 Year Mean (1979-88) Autumn (SON)



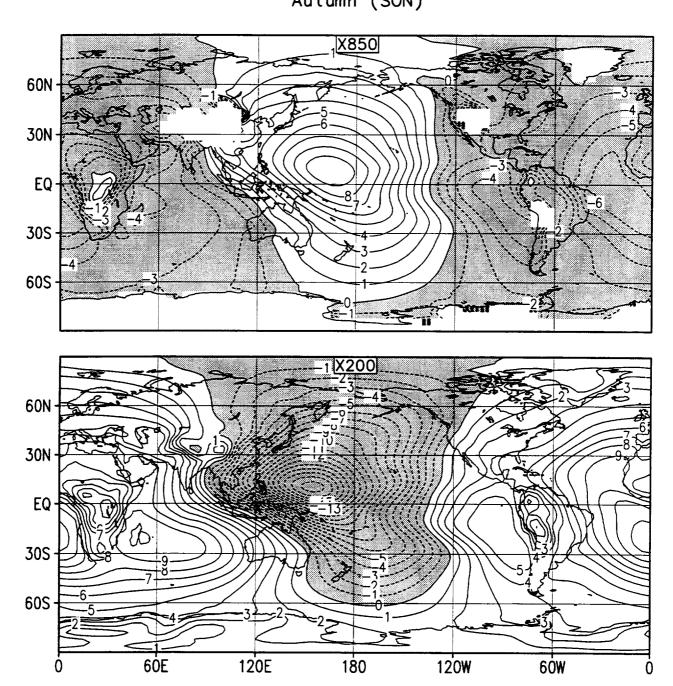
850 mb q (g/kg) and 500 mb W (Pa/s)
10 Year Mean (1979-88)
Autumn (SON)

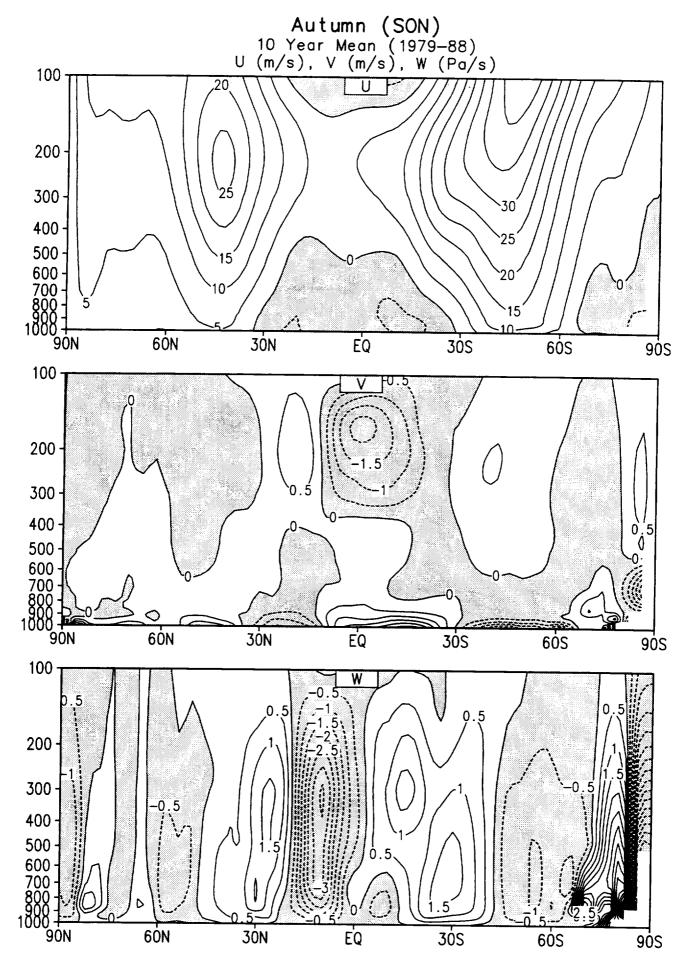


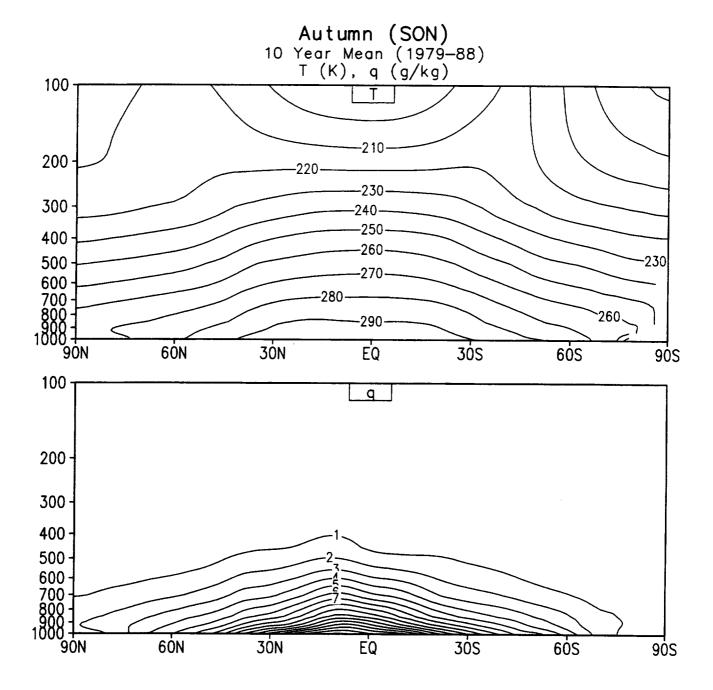
200 mb Stream Function (10E6 m**2/s) 10 Year Mean (1979-88) Autumn (SON)



Velocity Potential (10E6 m**2/s) 10 Year Mean (1979-88) Autumn (SON)

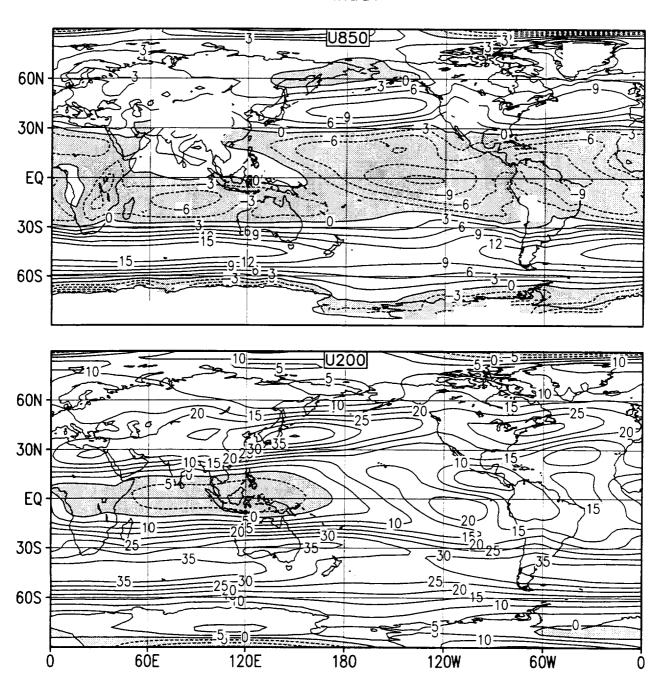




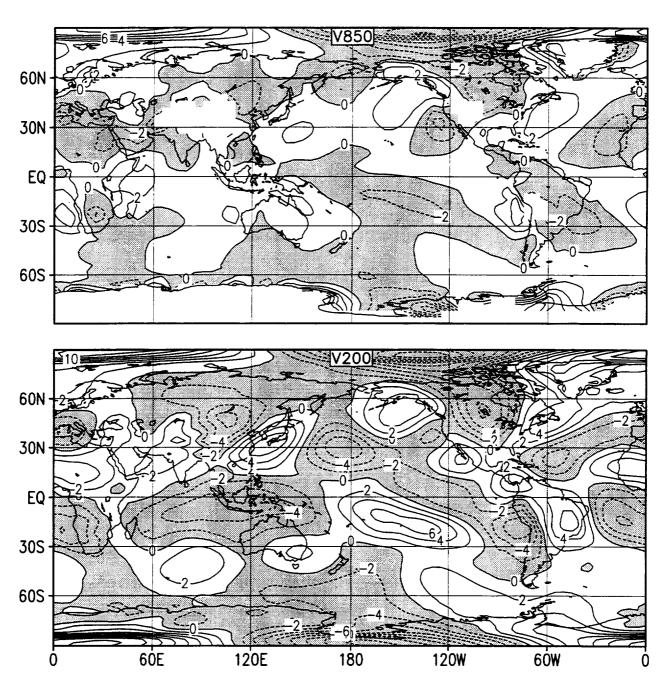


B. ANNUAL AVERAGES

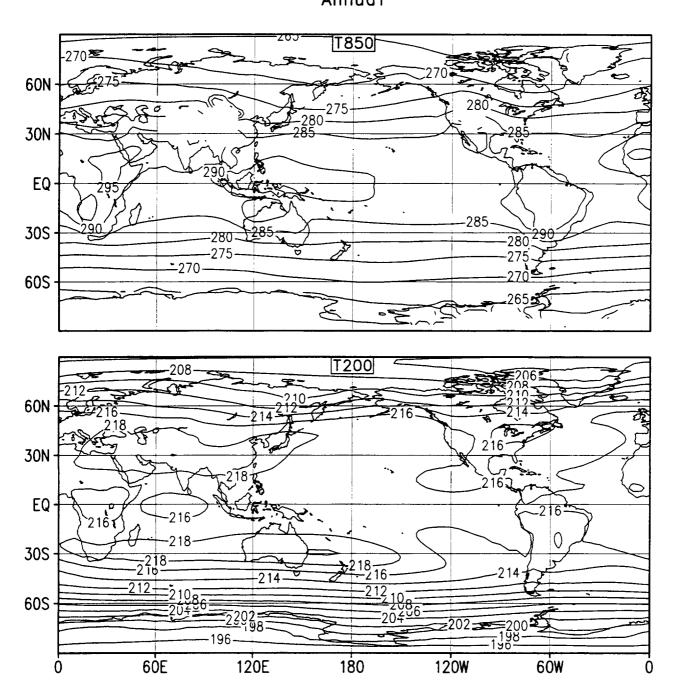
Zonal Wind (m/s)
10 Year Mean (1979-88)
Annual



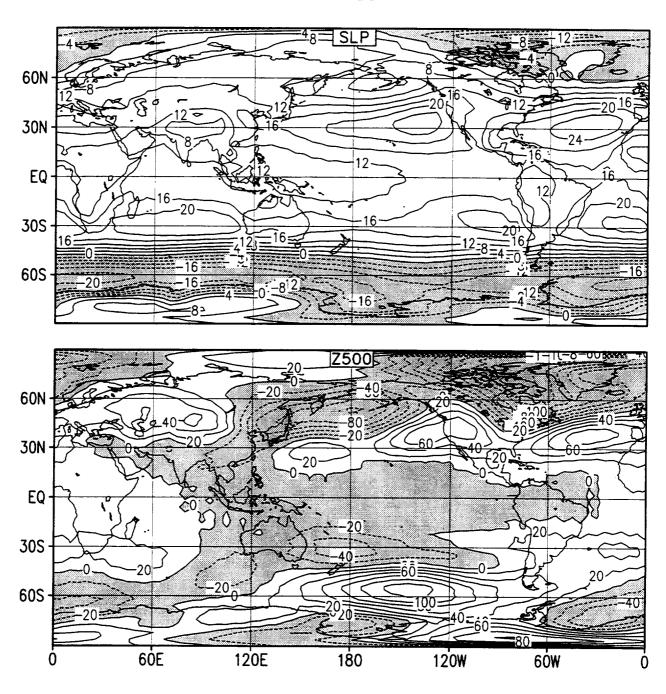
Meridional Wind (m/s)
10 Year Mean (1979-88)
Annual



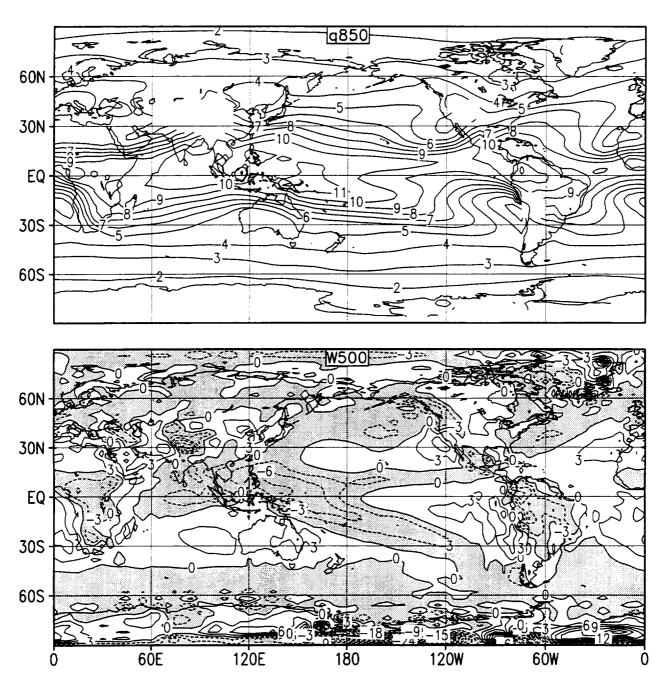
Temperature (K)
10 Year Mean (1979-88)
Annual



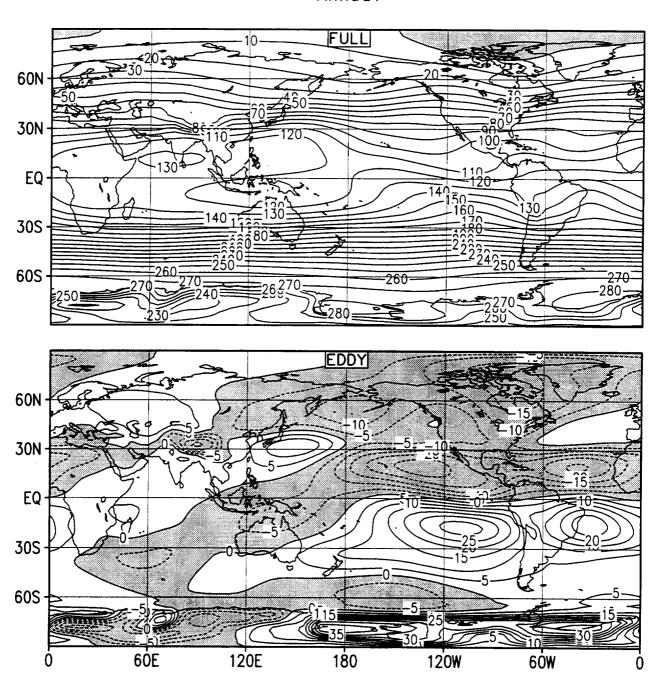
SLP-1000 (mb) and 500 mb eddy Z (m)
10 Year Mean (1979-88)
Annual



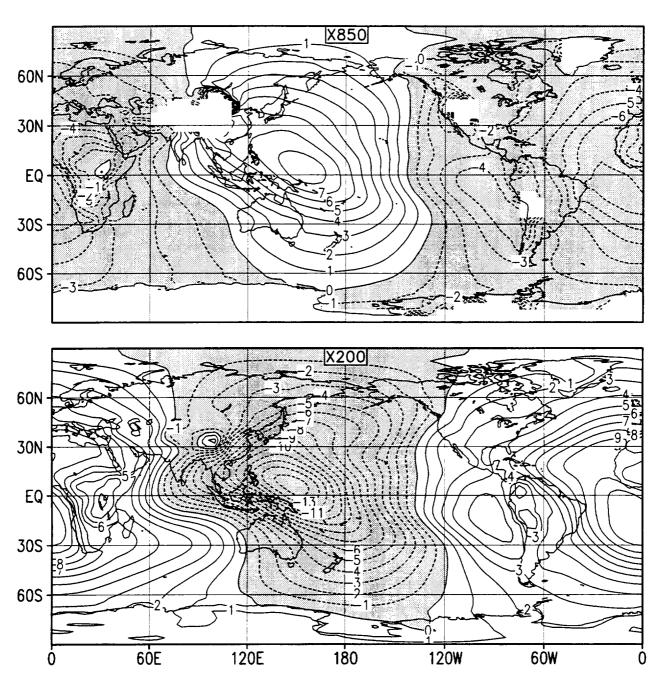
850 mb q (g/kg) and 500 mb W (Pa/s) 10 Year Mean (1979-88) Annual

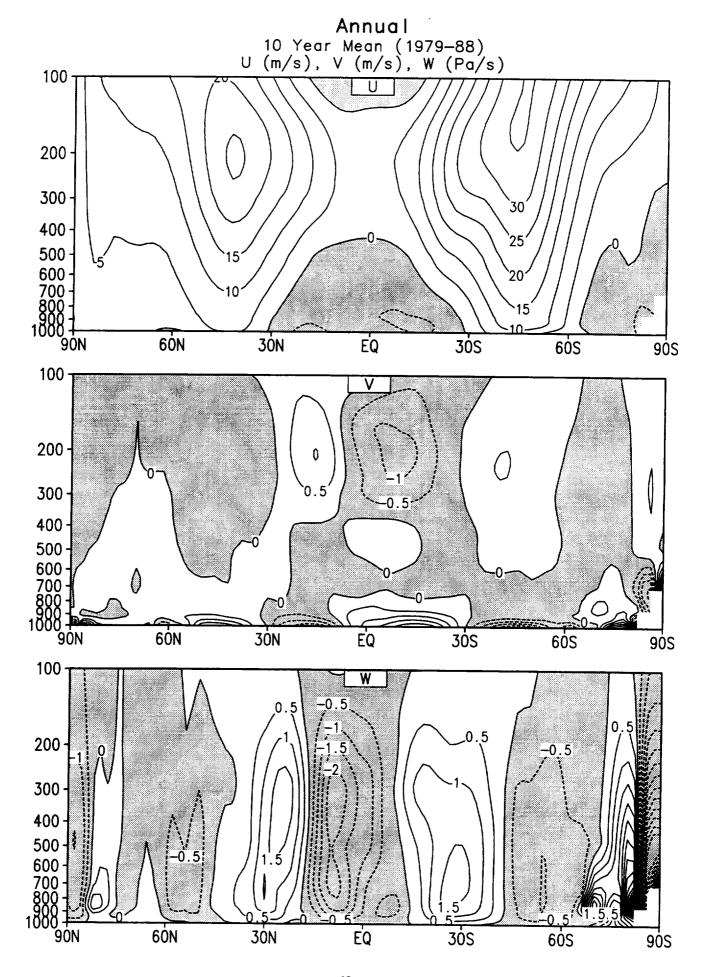


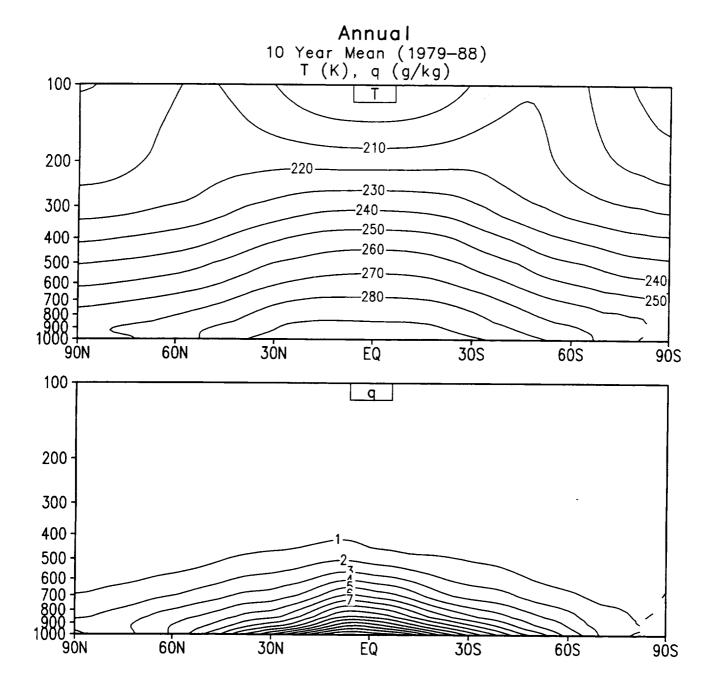
200 mb Stream Function (10E6 m**2/s)
10 Year Mean (1979-88)
Annual



Velocity Potential (10E6 m**2/s) 10 Year Mean (1979-88) Annual

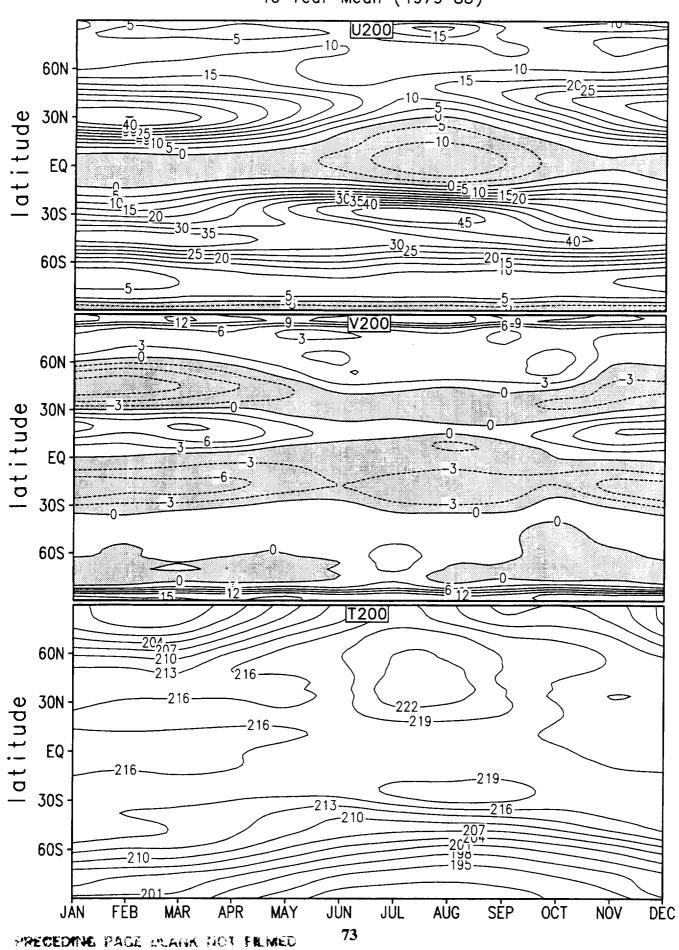




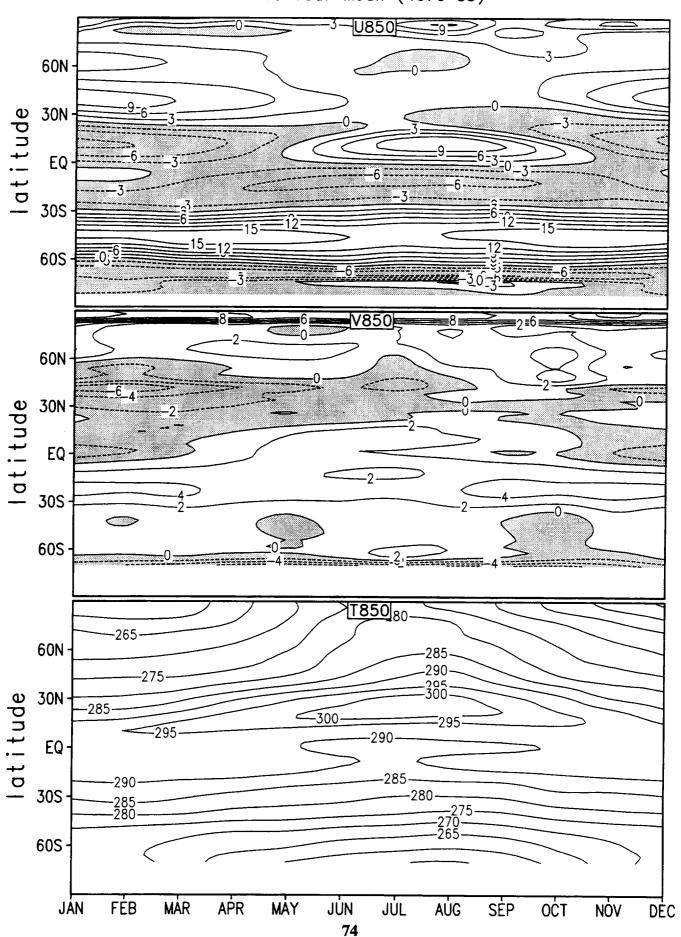


C. SEASONAL CYCLE

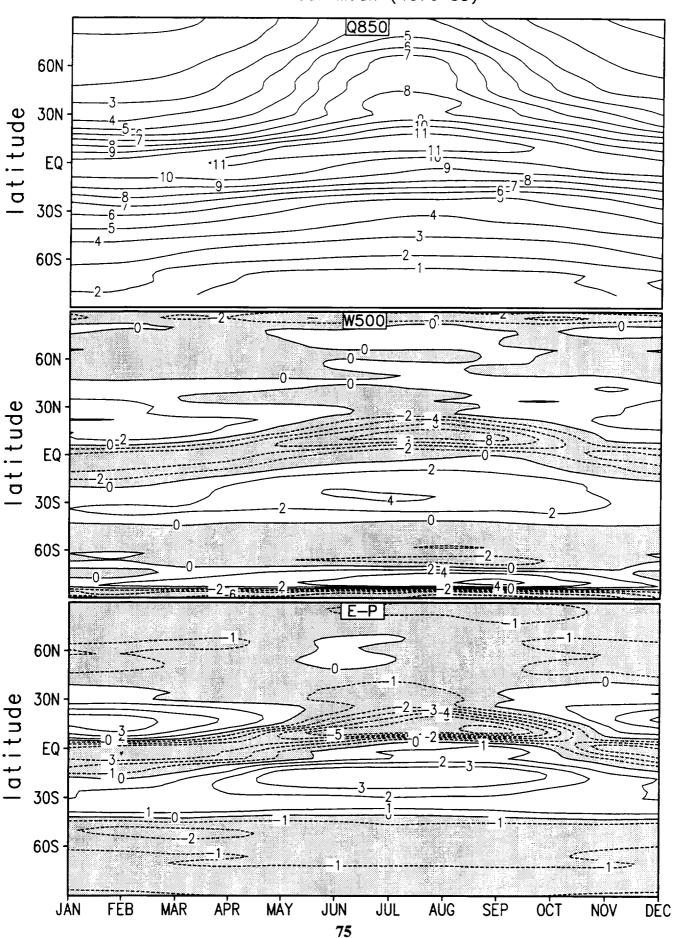
Seasonal Cycle 10 Year Mean (1979-88)



Seasonal Cycle 10 Year Mean (1979-88)



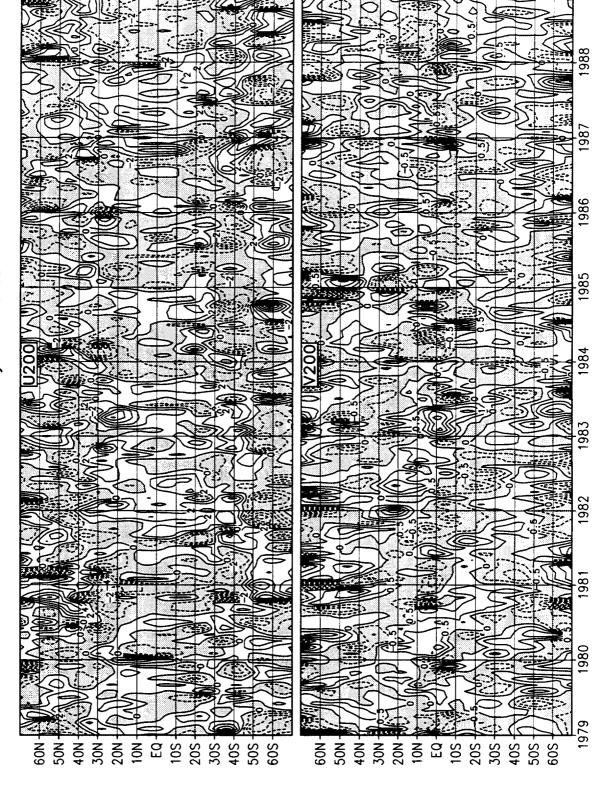
Seasonal Cycle 10 Year Mean (1979-88)



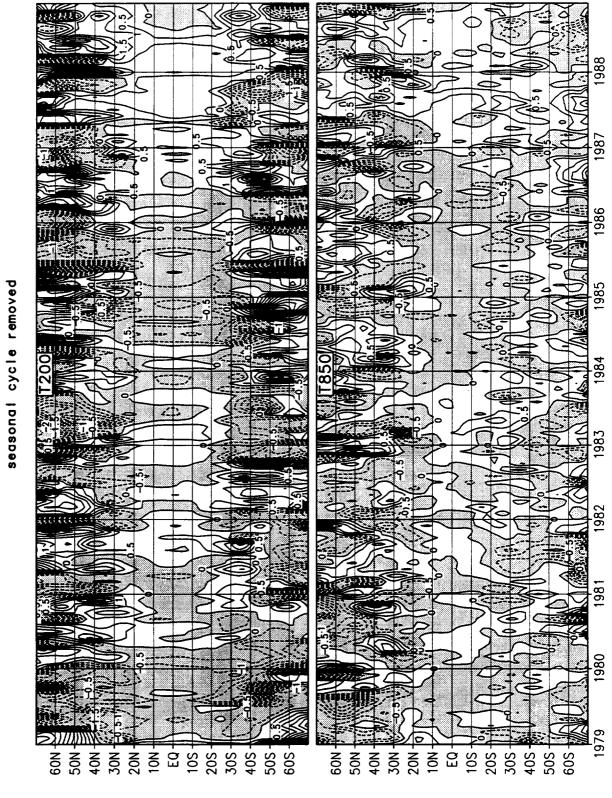
D. ZONAL MEAN ANOMALIES

Anomaly Zonal Mean Wind (m/sec)





Anomaly Zonal Mean T (deg K)



Anomaly Zonal Mean Q (g/kg) and W (Pa/s) 40S -50S -60S -20N-30S 30N-20N-30N 10N EQ -20S 60N 50N 40N Ē Š 10S 20S 30S -40S -

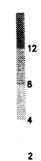
 $\xi \leq t$

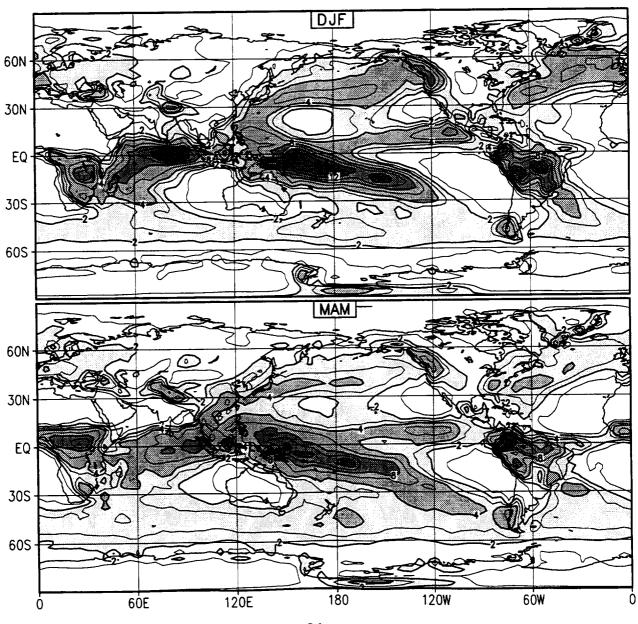
VII. <u>HYDROLOGY</u>

A. PRECIPITATION

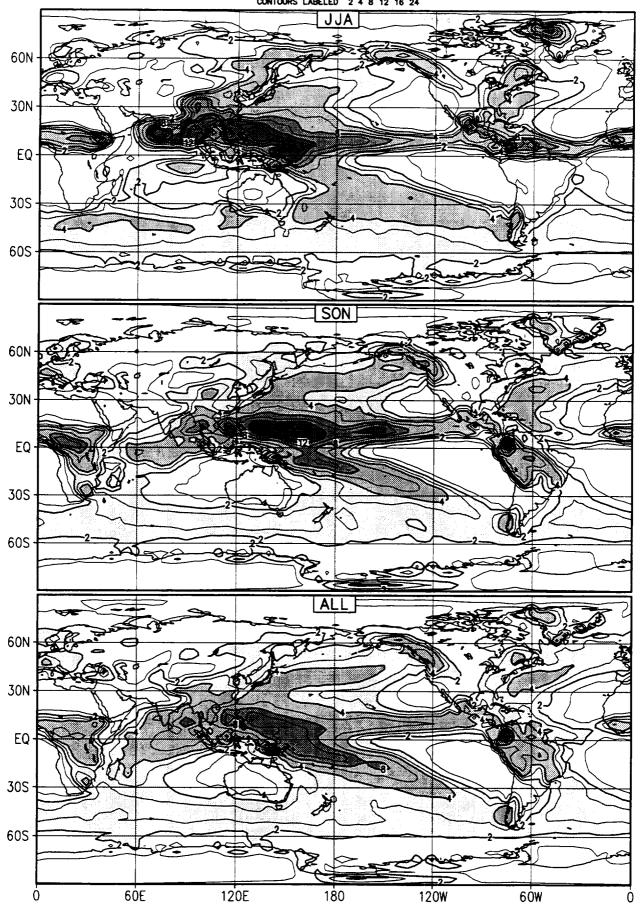
Total Precipitation (mm/day) 10 Year Mean (1979-88)

A set of simulated precipitation fields. Panel labels show seasonal means: December, January, February (DJF), March, April, May (MAM), June, July, August (JJA), September, October, November (SON), and annual mean (ALL). Thick (thin) contours are 2, 4, 8, 12, and 16 (1, 3, 6, 10, and 14) mm/day. Bar on the right shows range of the shaded regions. Area weighted global mean values are DJF: 2.89, MAM: 3.03, JJA: 3.45, SON: 2.94, and ALL: 3.08, respectively. Tropics are relatively well simulated. Orographically induced precipitation shows deficiencies. Excessive rainfall appears over Antarctica.





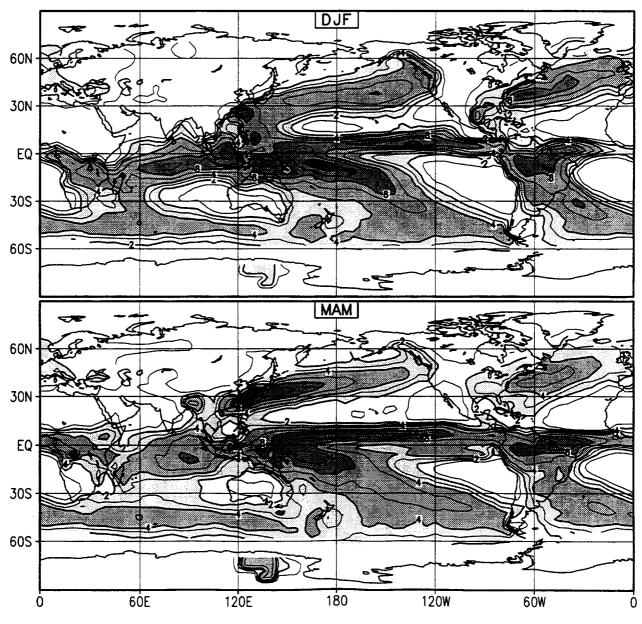
Total Precipitation (mm/day) 10 Year Mean (1979-88) CONTOURS LABELED 2 4 8 12 16 24



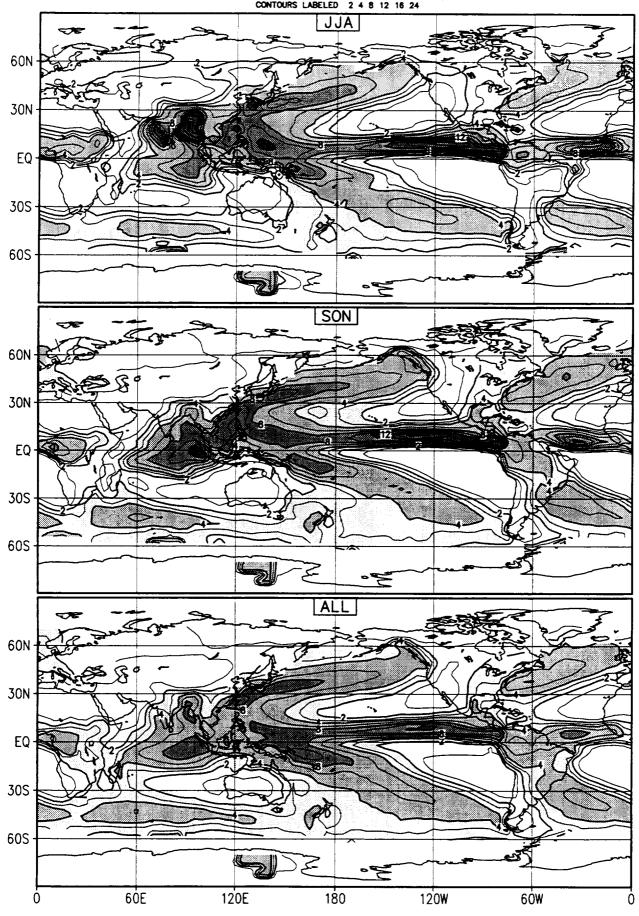
Observed Precipitation (mm/day) 10 Year Mean (1979-88)

A set of observed precipitation fields. Panel labels show seasonal means: December, January, February (DJF), March, April, May (MAM), June, July, August (JJA), September, October, November (SON), and annual mean (ALL). Raingauge data over land and MSU analysis over ocean (Spencer,1993) are merged together. Thick(thin) contours are 2, 4, 8, 12, and 16 (1, 3, 6, 10, and 14) mm/day. Bar on the right shows range of the shaded regions. Area weighted global mean values are DJF: 3.13, MAM: 3.12, JJA: 3.60, SON: 3.20, and ALL: 3.26, respectively.



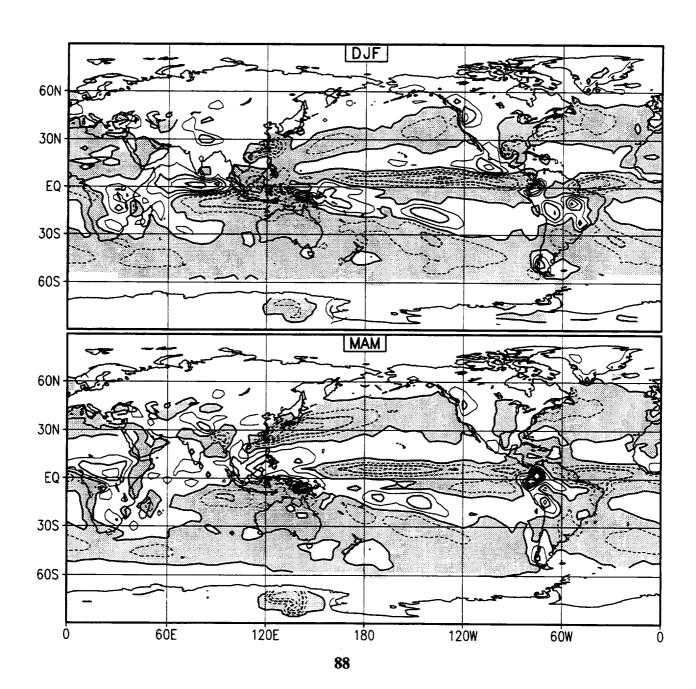


Observed Precipitation (mm/day) 10 Year Mean (1979-88) CONTOURS LABELED 2 4 8 12 16 24

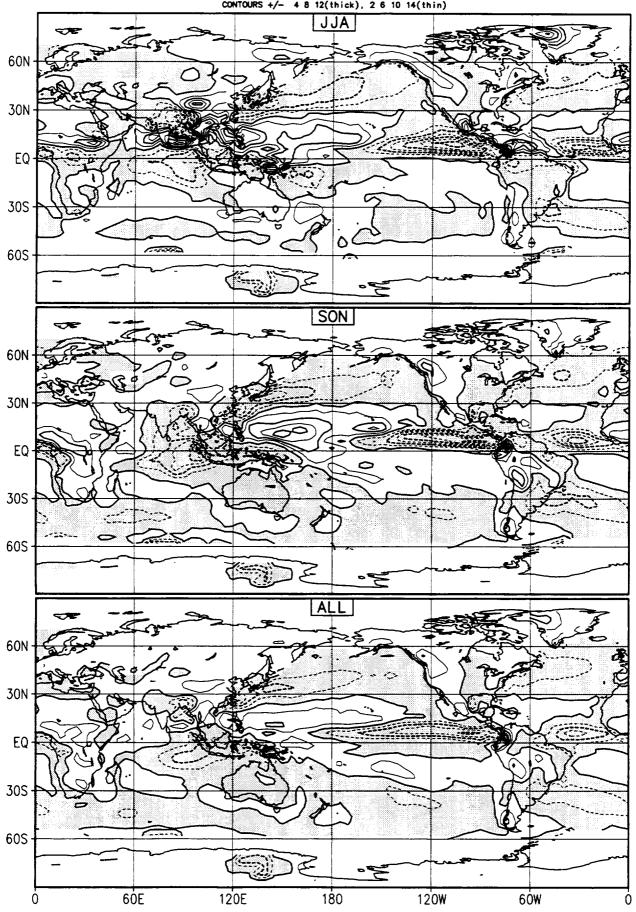


Precipitation AMIP—MSU (mm/day) 10 Year Mean (1979—88)

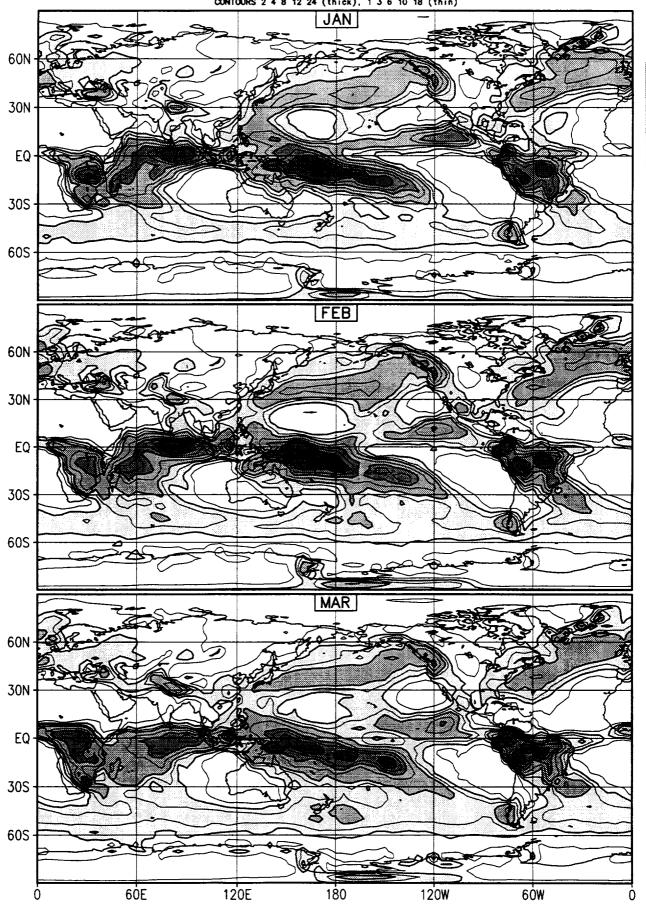
Simulated minus observed differences for precipitation fields. Panel labels show seasonal means: December, January, February (DJF), March, April, May (MAM), June, July, August (JJA), September, October, November (SON), and annual mean (ALL). Thick (thin) contours are ± 4 , 8, and $12 \dots (2, 6,$ and $10 \dots)$ mm/day. The differences are not necessarily caused by the simulation errors because of the well known biases in the analyzed precipitation.

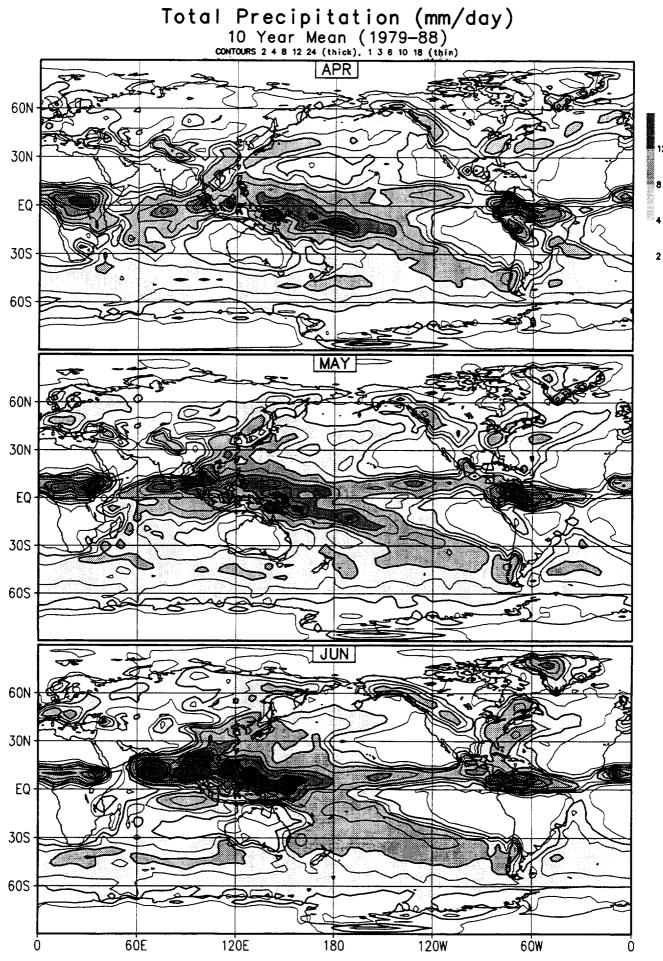


Precipitation AMIP—MSU (mm/day) 10 Year Mean (1979—88) contours +/- 4 8 12(thick), 2 6 10 14(thin)

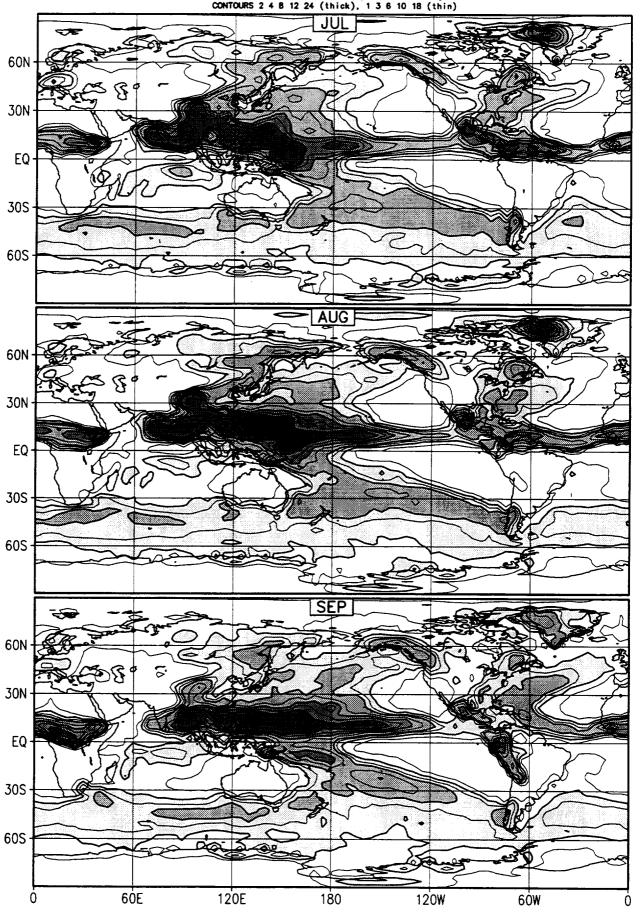


Total Precipitation (mm/day) 10 Year Mean (1979-88) contours 2 4 8 12 24 (thick), 1 3 6 10 18 (thin)

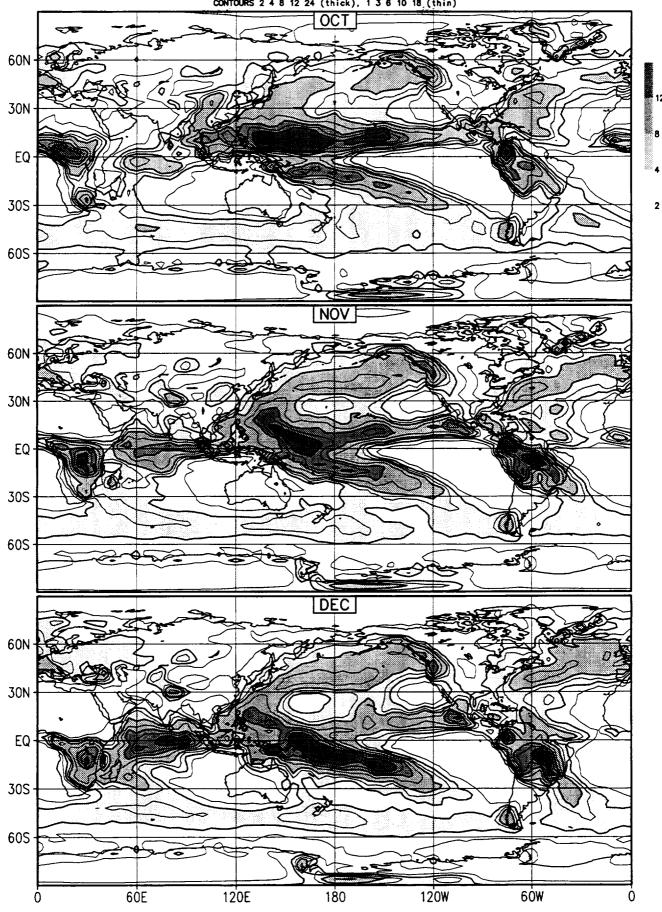




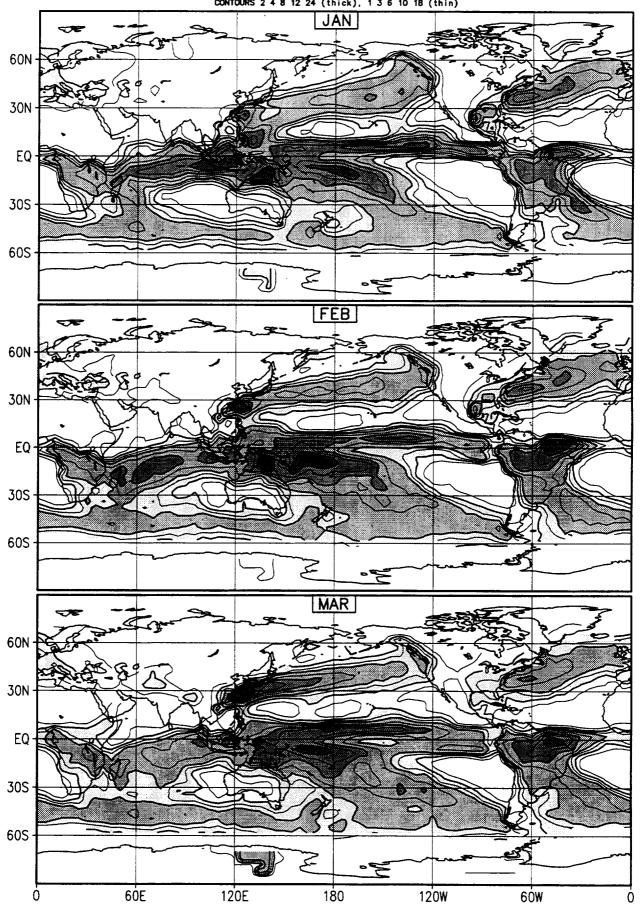
Total Precipitation (mm/day) 10 Year Mean (1979-88) CONTOURS 2 4 B 12 24 (thick), 1 3 6 10 18 (thin)



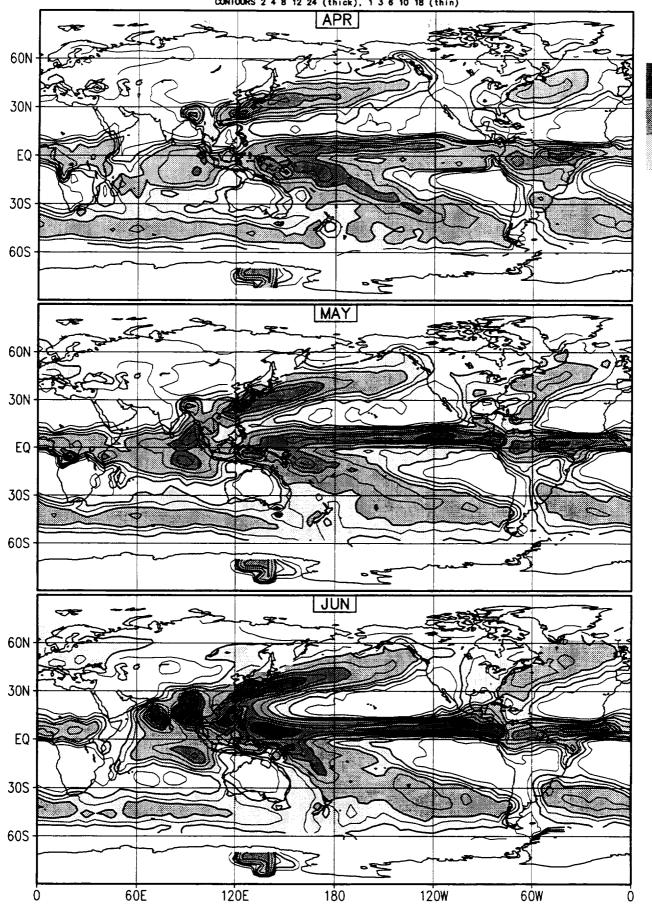
Total Precipitation (mm/day) 10 Year Mean (1979-88) contours 2 4 8 12 24 (thick), 1 3 6 10 18 (thin)



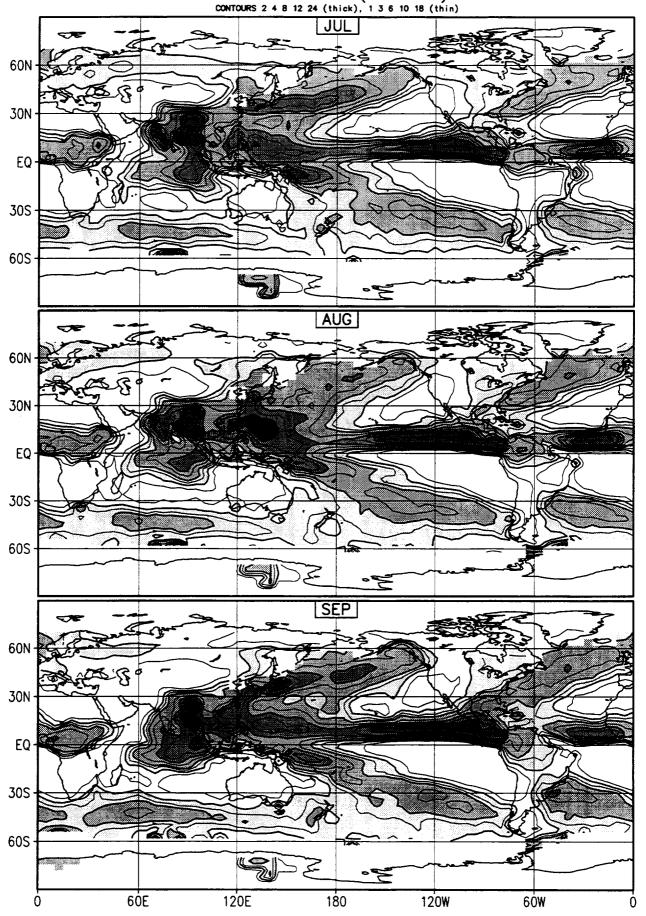
Observed Precipitation (mm/day) 10 Year Mean (1979-88) contours 2 + 8 12 24 (thick), 1 3 6 10 18 (thin)



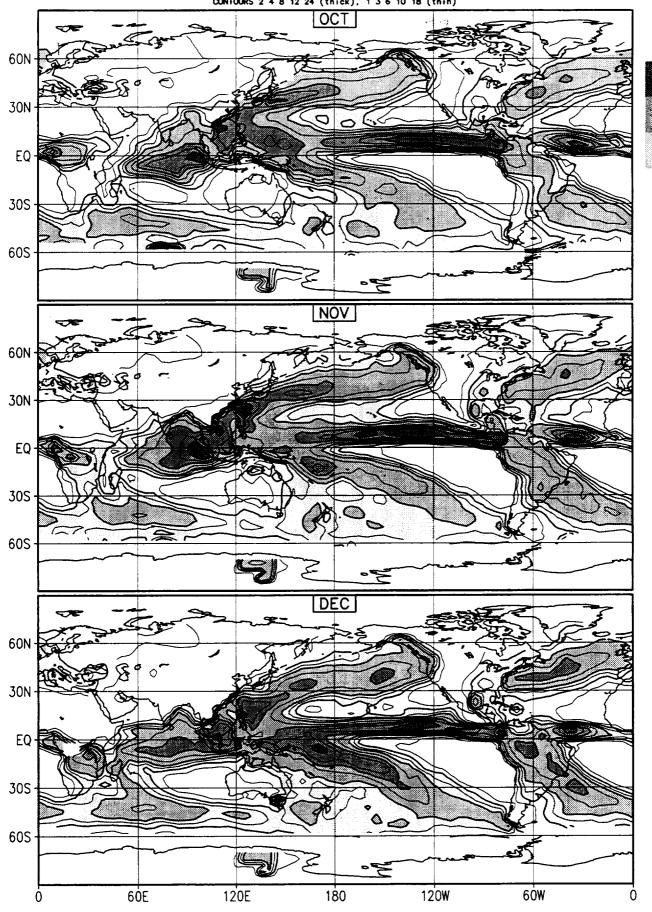
Observed Precipitation (mm/day) 10 Year Mean (1979-88) contours 2 + 8 12 24 (thick), 1 3 6 10 18 (thin)



Observed Precipitation (mm/day) 10 Year Mean (1979-88) contrours 2 4 8 12 24 (thick), 1 3 6 10 18 (thin)

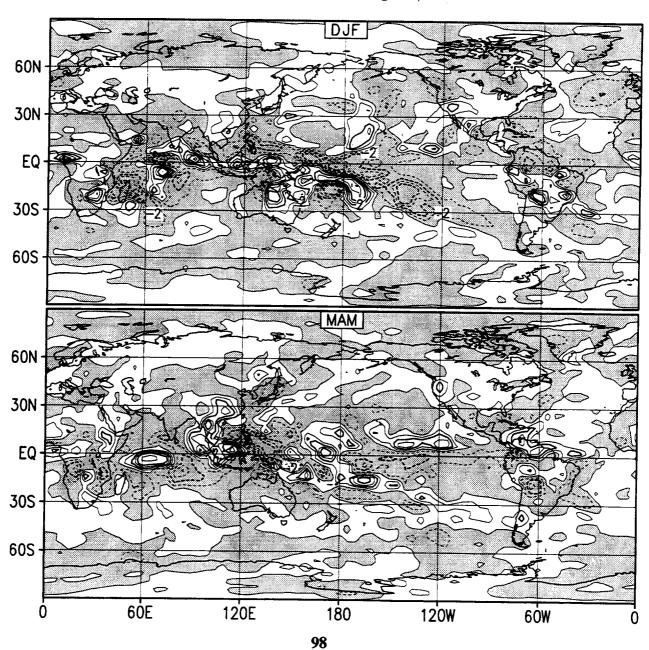


Observed Precipitation (mm/day) 10 Year Mean (1979-88) contrours 2 4 8 12 24 (thick), 1 3 6 10 18 (thin)

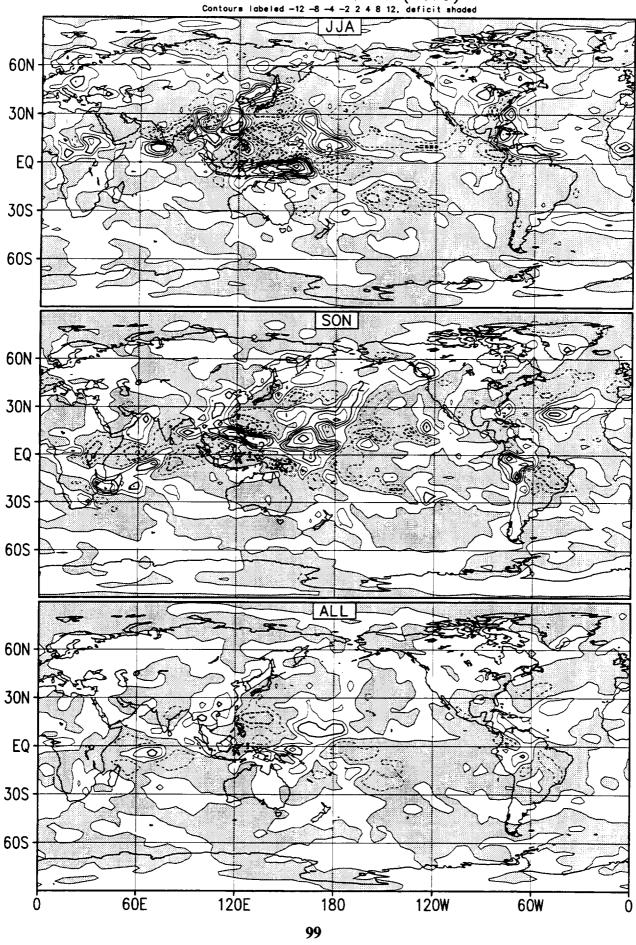


Anomaly Precipitation (mm/day) Simulation Year 1 (1979)

Deviations from the seasonal and annual averages (10 year means) for the simulated precipitation fields. Panel labels show seasonal means: December, January, February (DJF), March, April, May (MAM), June, July, August (JJA), September, October, November (SON), and annual mean (ALL). Thick (thin) contours are \pm 2, 4, 8, and 12 (1, 3, 6, and 10) mm/day. Seasonal anomalies over tropical Pacific are relatively well simulated especially during El Niño/La Niña periods. For example, MAM and SON/1982 versus 1983 and JJA 1987 versus 1988; however the anomalies for DJF 1982 versus 1983 are weaker than the observed (see next set of figures).

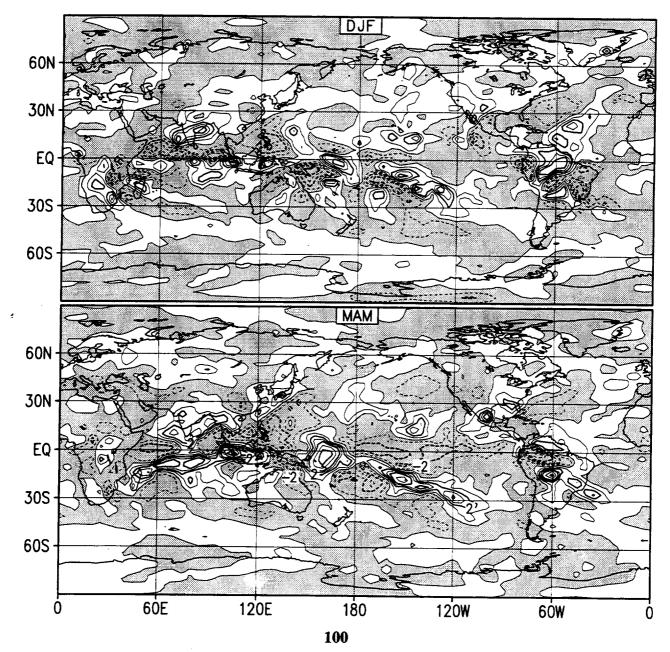


Anomaly Precipitation (mm/day) Simulation Year 1 (1979) Contours labeled -12 -8 -4 -2 2 4 8 12, deficit shaded

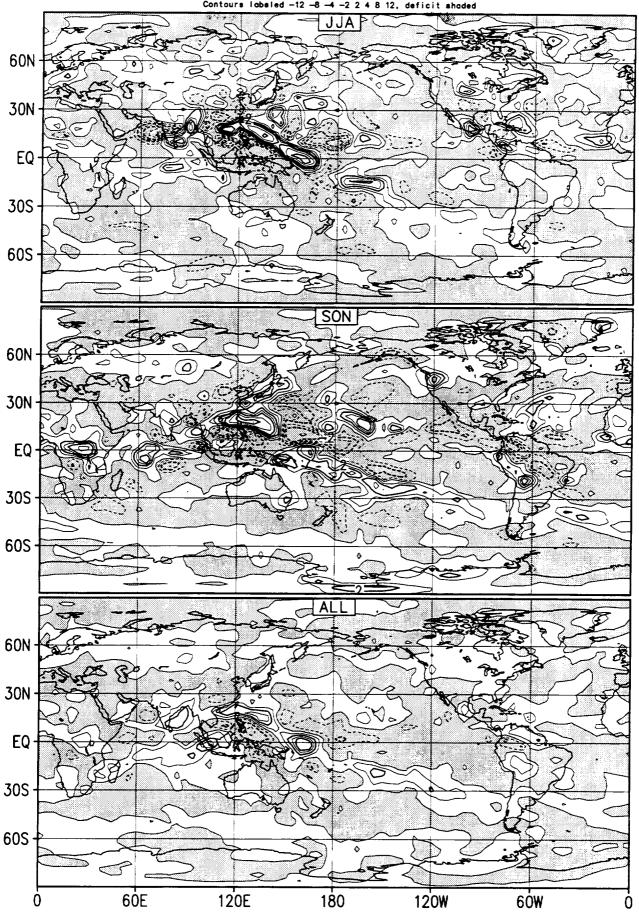


Anomaly Precipitation (mm/day) Simulation Year 2 (1980)

Deviations from the seasonal and annual averages (10 year means) for the simulated precipitation fields. Panel labels show seasonal means: December, January, February (DJF), March, April, May (MAM), June, July, August (JJA), September, October, November (SON), and annual mean (ALL). Thick (thin) contours are \pm 2, 4, 8, and 12 (1, 3, 6, and 10) mm/day. Seasonal anomalies over tropical Pacific are relatively well simulated especially during El Niño/La Niña periods. For example, MAM and SON/1982 versus 1983 and JJA 1987 versus 1988; however the anomalies for DJF 1982 versus 1983 are weaker than the observed (see next set of figures).

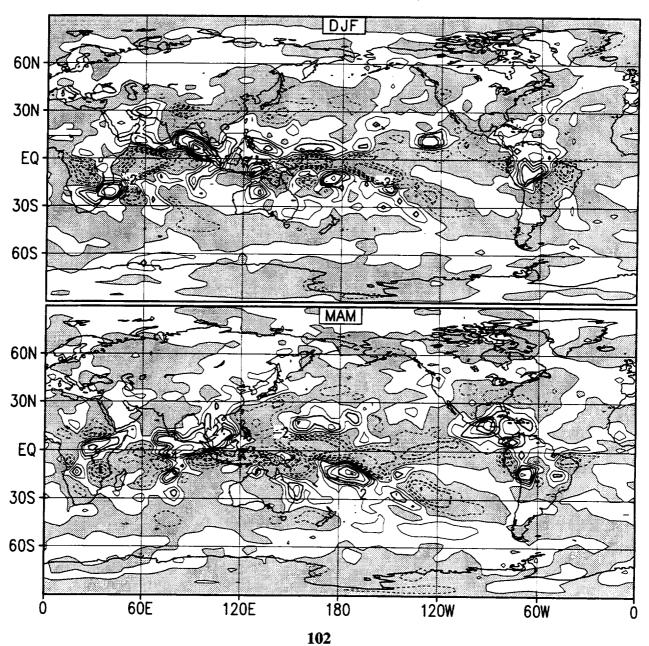


Anomaly Precipitation (mm/day) Simulation Year 2 (1980) Contours labeled -12 -8 -4 -2 2 4 8 12, deficit shaded

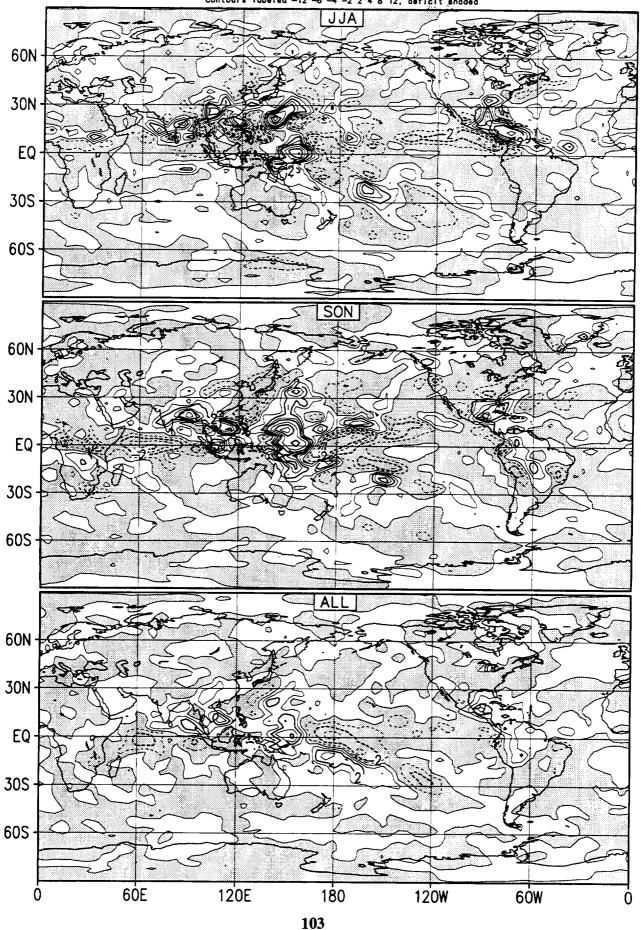


Anomaly Precipitation (mm/day) Simulation Year 3 (1981)

Deviations from the seasonal and annual averages (10 year means) for the simulated precipitation fields. Panel labels show seasonal means: December, January, February (DJF), March, April, May (MAM), June, July, August (JJA), September, October, November (SON), and annual mean (ALL). Thick (thin) contours are \pm 2, 4, 8, and 12 (1, 3, 6, and 10) mm/day. Seasonal anomalies over tropical Pacific are relatively well simulated especially during El Niño/La Niña periods. For example, MAM and SON/1982 versus 1983 and JJA 1987 versus 1988; however the anomalies for DJF 1982 versus 1983 are weaker than the observed (see next set of figures).



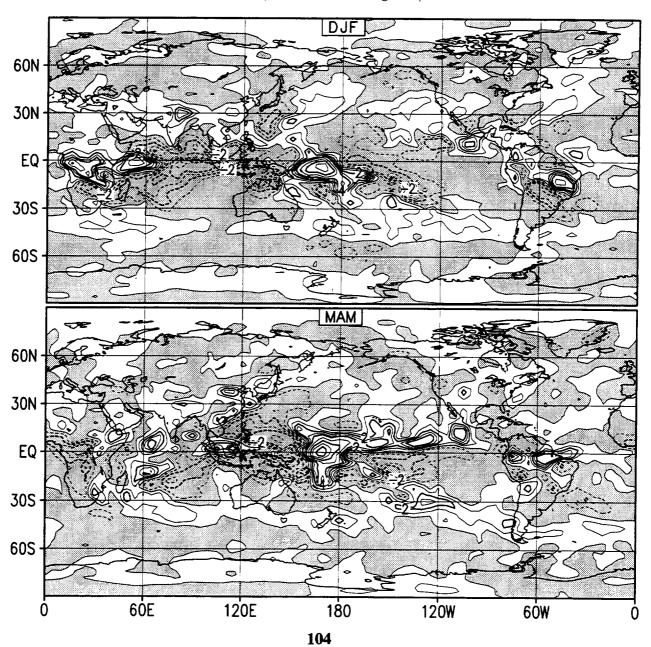
Anomaly Precipitation (mm/day) Simulation Year 3 (1981) Contours labeled -12 -8 -4 -2 2 4 8 12, deficit shaded



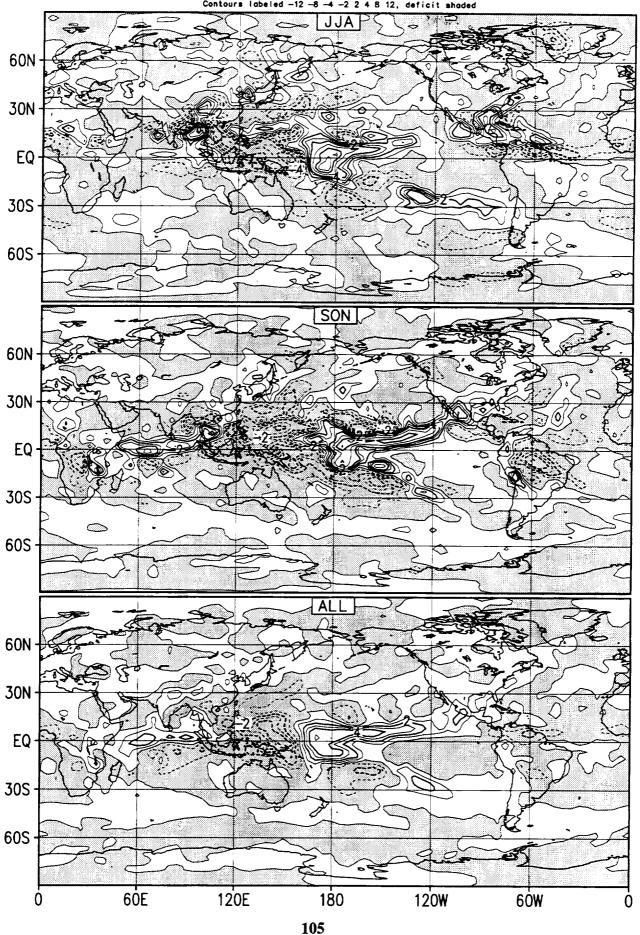
Anomaly Precipitation (mm/day)

Simulation Year 4 (1982) Contours labeled -12 -8 -4 -2 2 4 8 12, deficit shaded

Deviations from the seasonal and annual averages (10 year means) for the simulated precipitation fields. Panel labels show seasonal means: December, January, February (DJF), March, April, May (MAM), June, July, August (JJA), September, October, November (SON), and annual mean (ALL). Thick (thin) contours are \pm 2, 4, 8, and 12 (1, 3, 6, and 10) mm/day. Seasonal anomalies over tropical Pacific are relatively well simulated especially during El Niño/La Niña periods. For example, MAM and SON/1982 versus 1983 and JJA 1987 versus 1988; however the anomalies for DJF 1982 versus 1983 are weaker than the observed (see next set of figures).

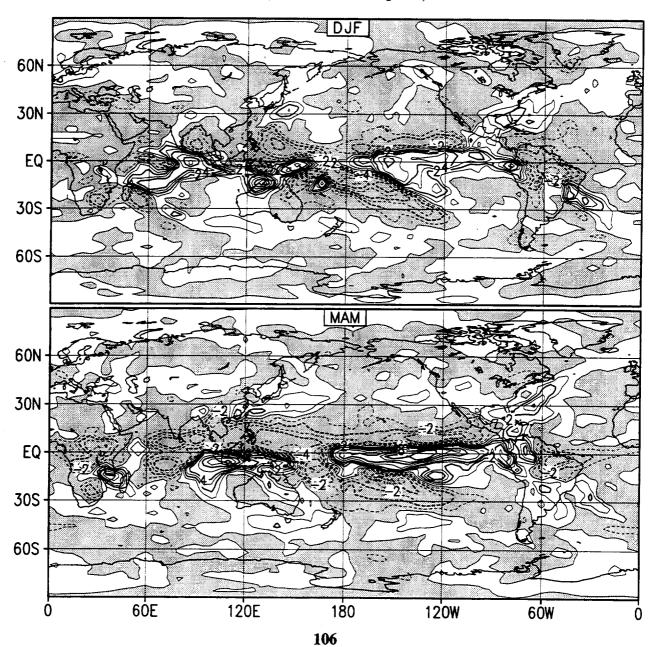


Anomaly Precipitation (mm/day) Simulation Year 4 (1982) Contours labeled -12 -8 -4 -2 2 4 8 12, deficit shaded

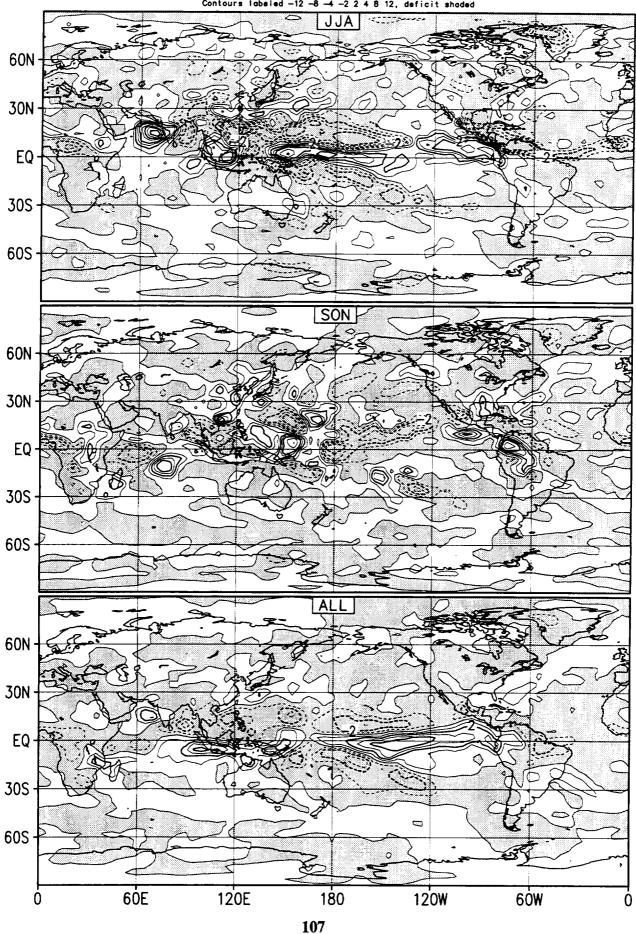


Anomaly Precipitation (mm/day) Simulation Year 5 (1983) Contours labeled -12 -8 -4 -2 2 4 8 12, deficit shaded

Deviations from the seasonal and annual averages (10 year means) for the simulated precipitation fields. Panel labels show seasonal means: December, January, February (DJF), March, April, May (MAM), June, July, August (JJA), September, October, November (SON), and annual mean (ALL). Thick (thin) contours are \pm 2, 4, 8, and 12 (1, 3, 6, and 10) mm/day. Seasonal anomalies over tropical Pacific are relatively well simulated especially during El Niño/La Niña periods. For example, MAM and SON/1982 versus 1983 and JJA 1987 versus 1988; however the anomalies for DJF 1982 versus 1983 are weaker than the observed (see next set of figures).



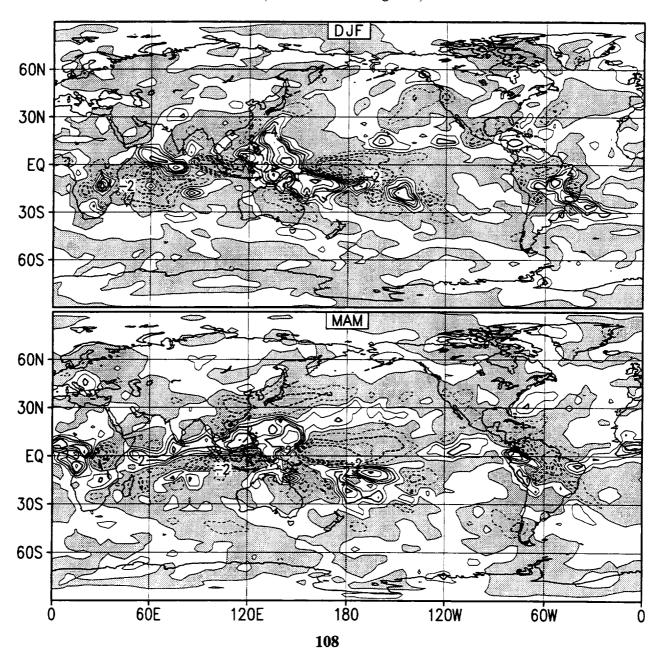
Anomaly Precipitation (mm/day) Simulation Year 5 (1983) Contours labeled -12 -8 -4 -2 2 4 8 12, deficit shaded



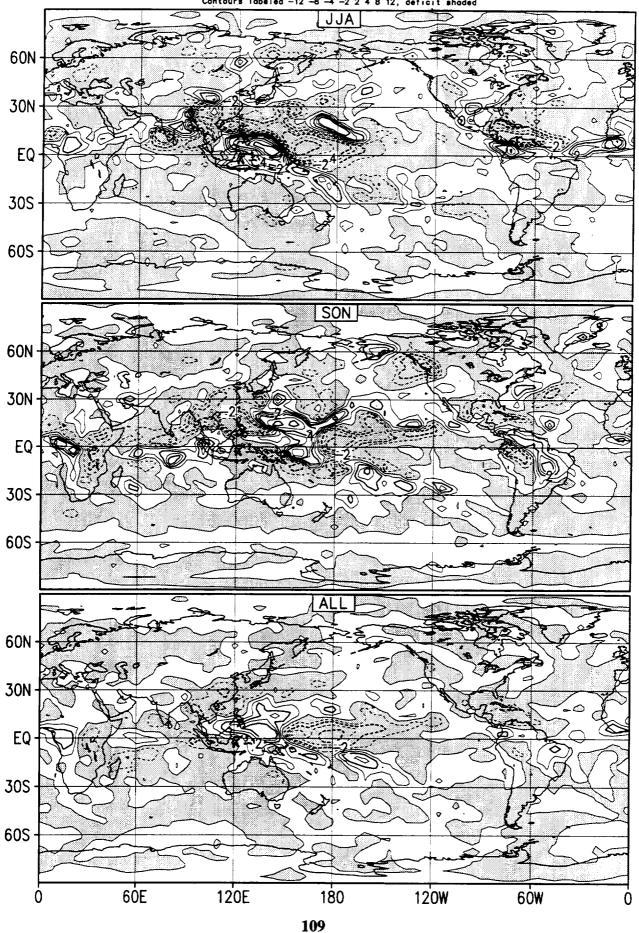
Anomaly Precipitation (mm/day) Simulation Year 6 (1984)

Contours labeled -12 -8 -4 -2 2 4 B 12, deficit shaded

Deviations from the seasonal and annual averages (10 year means) for the simulated precipitation fields. Panel labels show seasonal means: December, January, February (DJF), March, April, May (MAM), June, July, August (JJA), September, October, November (SON), and annual mean (ALL). Thick (thin) contours are \pm 2, 4, 8, and 12 (1, 3, 6, and 10) mm/day. Seasonal anomalies over tropical Pacific are relatively well simulated especially during El Niño/La Niña periods. For example, MAM and SON/1982 versus 1983 and JJA 1987 versus 1988; however the anomalies for DJF 1982 versus 1983 are weaker than the observed (see next set of figures).

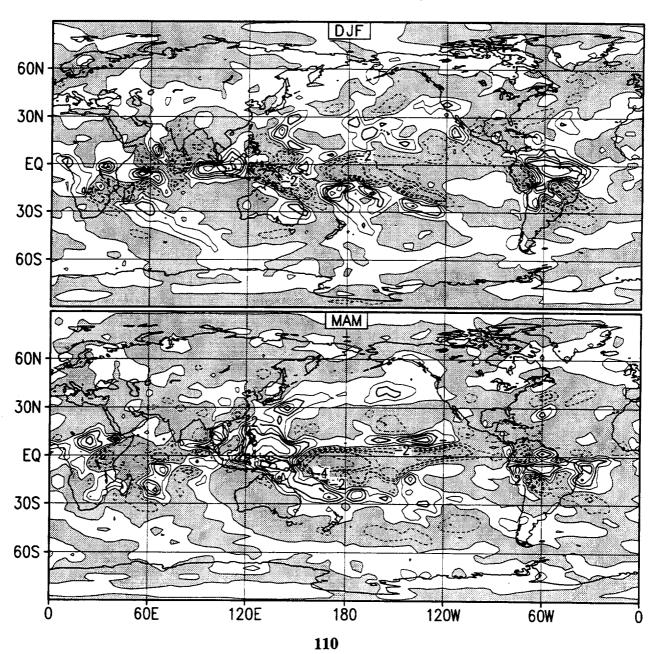


Anomaly Precipitation (mm/day) Simulation Year 6 (1984) Contours labeled -12 -8 -4 -2 2 4 8 12, deficit shaded

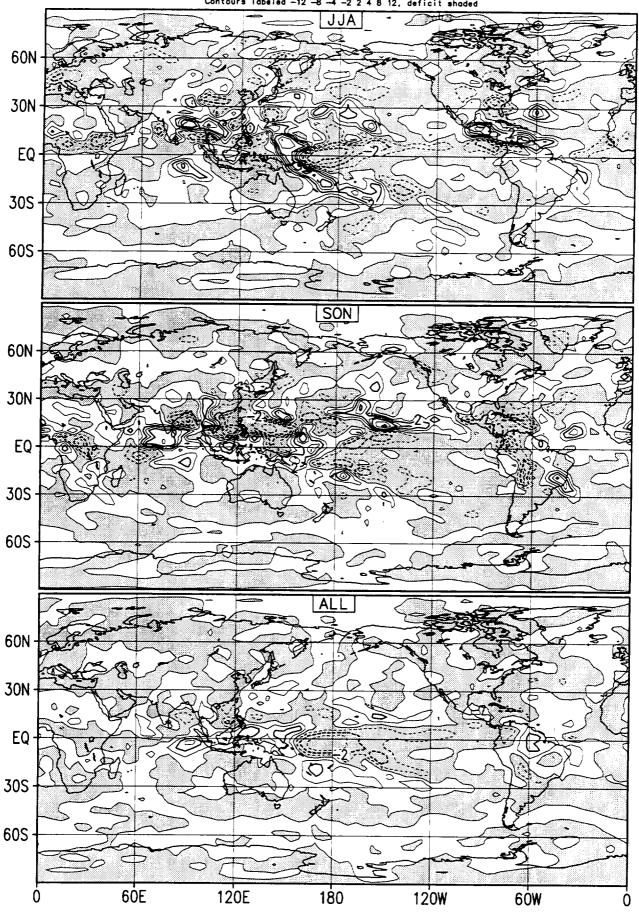


Anomaly Precipitation (mm/day) Simulation Year 7 (1985)

Deviations from the seasonal and annual averages (10 year means) for the simulated precipitation fields. Panel labels show seasonal means: December, January, February (DJF), March, April, May (MAM), June, July, August (JJA), September, October, November (SON), and annual mean (ALL). Thick (thin) contours are \pm 2, 4, 8, and 12 (1, 3, 6, and 10) mm/day. Seasonal anomalies over tropical Pacific are relatively well simulated especially during El Niño/La Niña periods. For example, MAM and SON/1982 versus 1983 and JJA 1987 versus 1988; however the anomalies for DJF 1982 versus 1983 are weaker than the observed (see next set of figures).



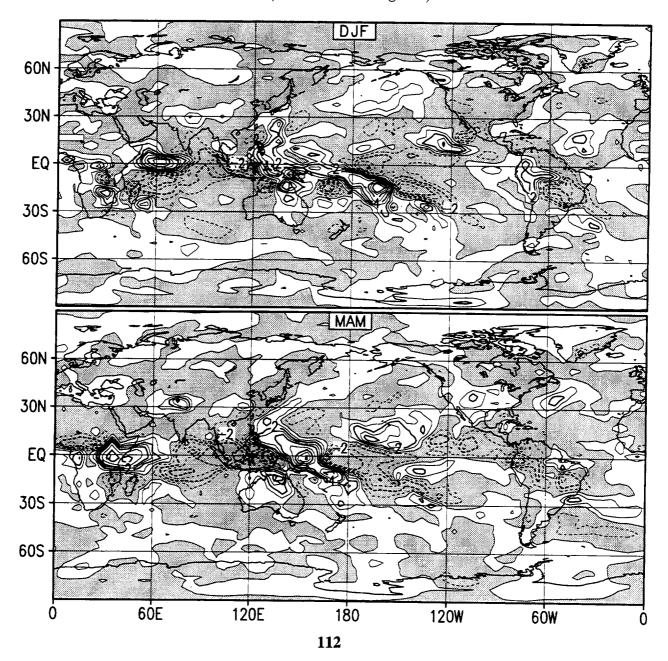
Anomaly Precipitation (mm/day) Simulation Year 7 (1985) Contours labeled -12 -8 -4 -2 2 4 8 12, deficit shaded



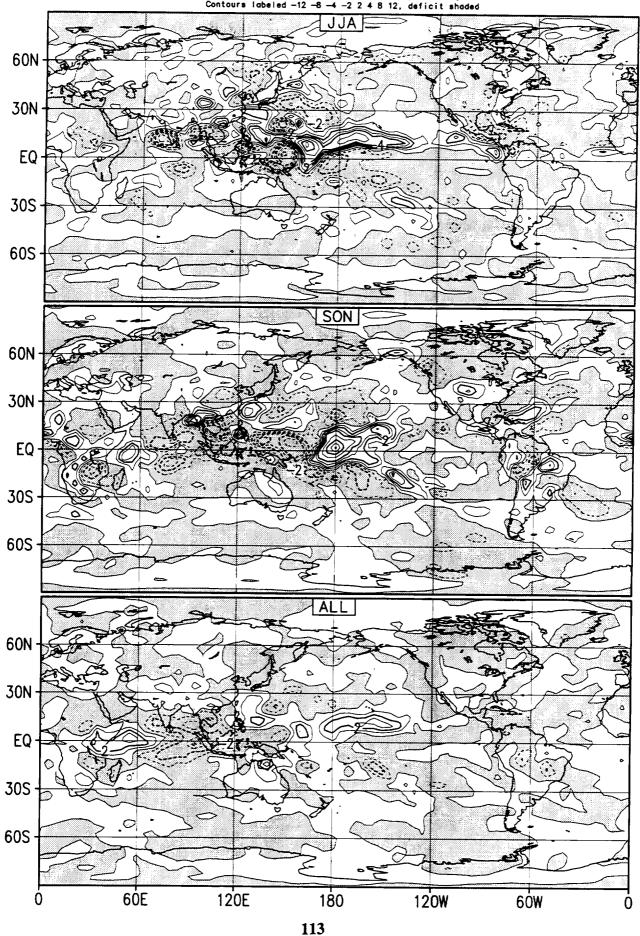
Anomaly Precipitation (mm/day) Simulation Year 8 (1986)

Contours labeled -12 -8 -4 -2 2 4 8 12, deficit shaded

Deviations from the seasonal and annual averages (10 year means) for the simulated precipitation fields. Panel labels show seasonal means: December, January, February (DJF), March, April, May (MAM), June, July, August (JJA), September, October, November (SON), and annual mean (ALL). Thick (thin) contours are \pm 2, 4, 8, and 12 (1, 3, 6, and 10) mm/day. Seasonal anomalies over tropical Pacific are relatively well simulated especially during El Niño/La Niña periods. For example, MAM and SON/1982 versus 1983 and JJA 1987 versus 1988; however the anomalies for DJF 1982 versus 1983 are weaker than the observed (see next set of figures).

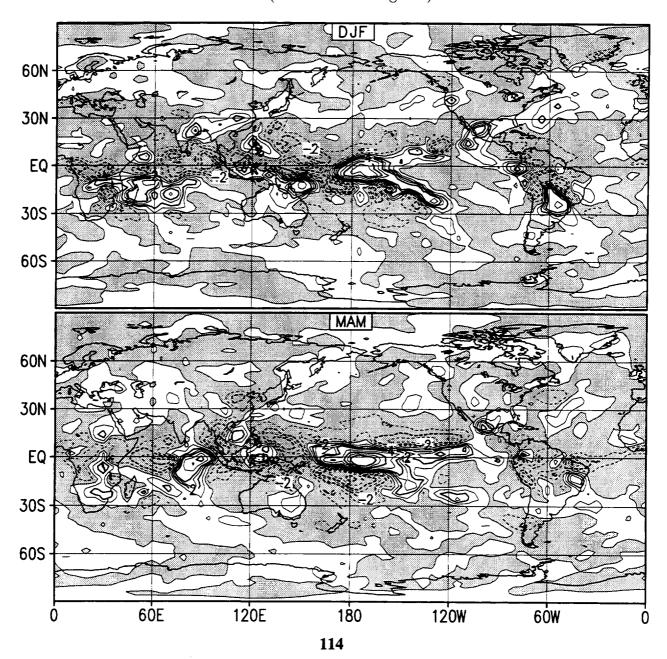


Anomaly Precipitation (mm/day) Simulation Year 8 (1986) Contours labeled -12 -8 -4 -2 2 4 8 12, deficit shaded

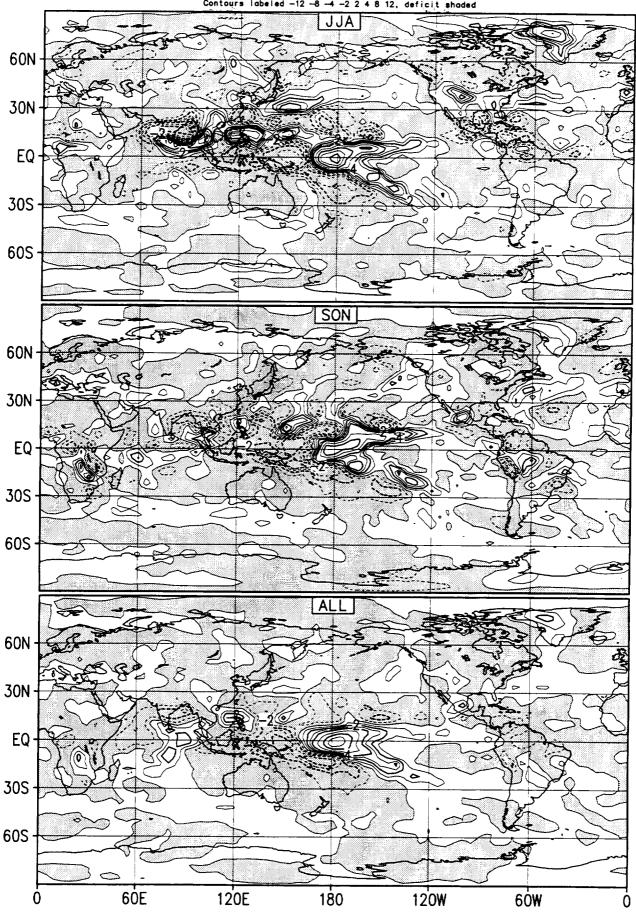


Anomaly Precipitation (mm/day) Simulation Year 9 (1987)

Deviations from the seasonal and annual averages (10 year means) for the simulated precipitation fields. Panel labels show seasonal means: December, January, February (DJF), March, April, May (MAM), June, July, August (JJA), September, October, November (SON), and annual mean (ALL). Thick (thin) contours are \pm 2, 4, 8, and 12 (1, 3, 6, and 10) mm/day. Seasonal anomalies over tropical Pacific are relatively well simulated especially during El Niño/La Niña periods. For example, MAM and SON/1982 versus 1983 and JJA 1987 versus 1988; however the anomalies for DJF 1982 versus 1983 are weaker than the observed (see next set of figures).

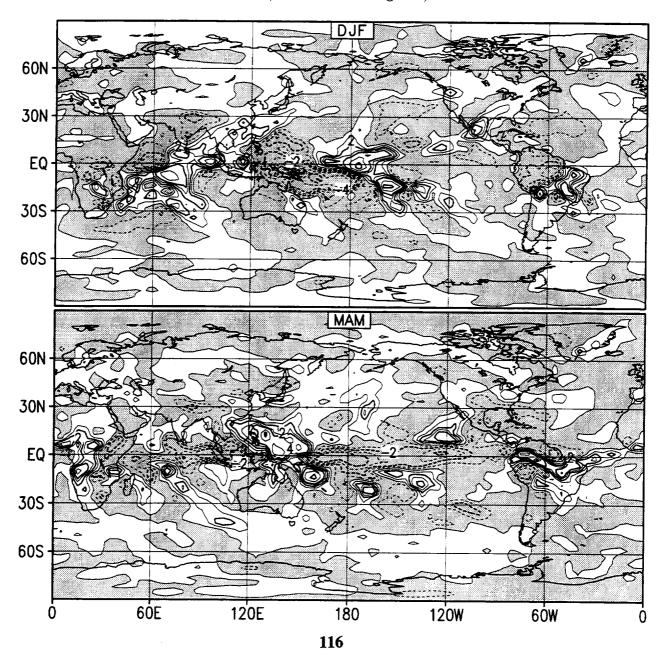


Anomaly Precipitation (mm/day) Simulation Year 9 (1987) Contours labeled -12 -8 -4 -2 2 4 8 12, deficit shoded

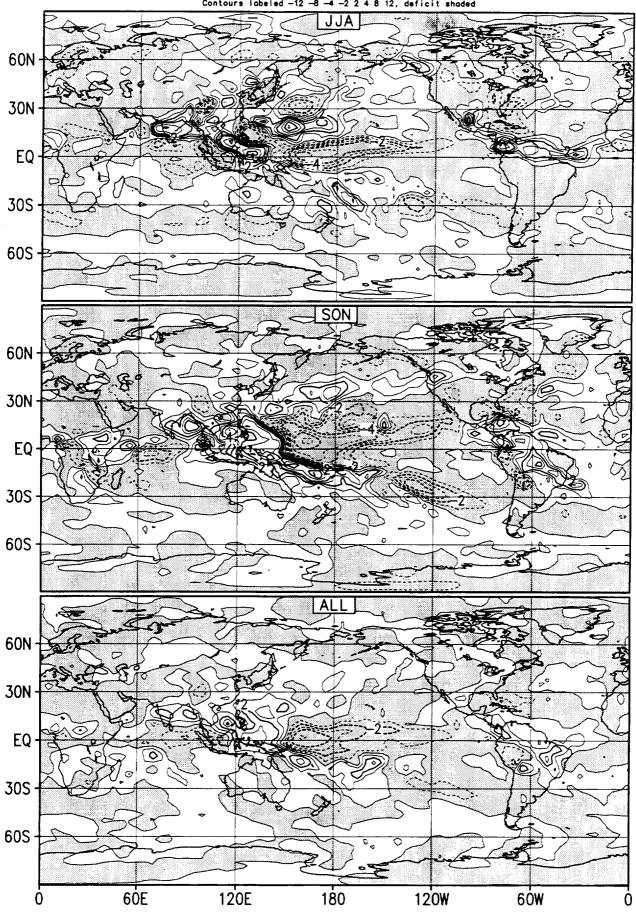


Anomaly Precipitation (mm/day) Simulation Year 10 (1988) Contours lobeled 12 28 4 22 24 8 12 definite photos

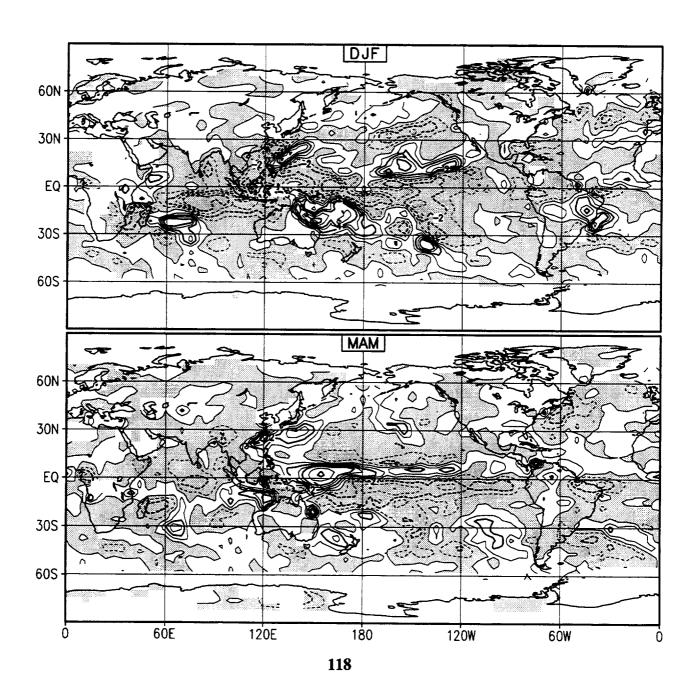
Deviations from the seasonal and annual averages (10 year means) for the simulated precipitation fields. Panel labels show seasonal means: December, January, February (DJF), March, April, May (MAM), June, July, August (JJA), September, October, November (SON), and annual mean (ALL). Thick (thin) contours are \pm 2, 4, 8, and 12 (1, 3, 6, and 10) mm/day. Seasonal anomalies over tropical Pacific are relatively well simulated especially during El Niño/La Niña periods. For example, MAM and SON/1982 versus 1983 and JJA 1987 versus 1988; however the anomalies for DJF 1982 versus 1983 are weaker than the observed (see next set of figures).



Anomaly Precipitation (mm/day) Simulation Year 10 (1988) Contours labeled -12 -8 -4 -2 2 4 8 12, deficit shaded



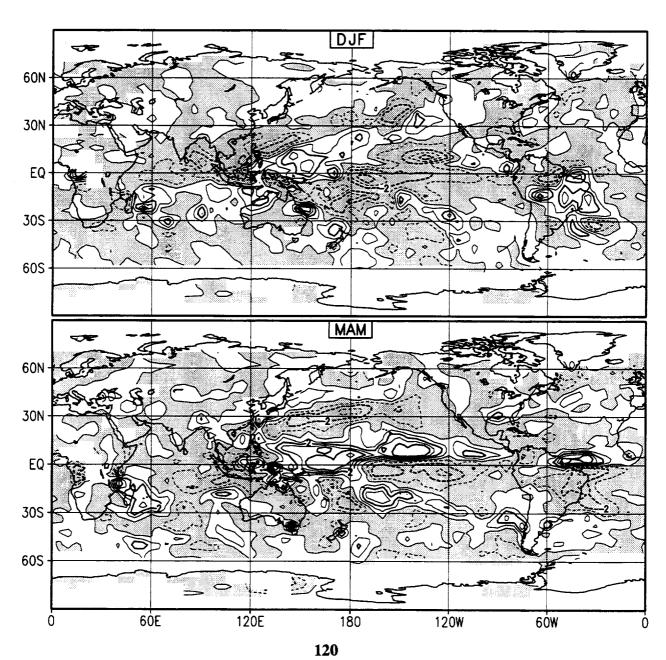
Observed Anomaly Rainfall (mm/day) Year 1 (1979)



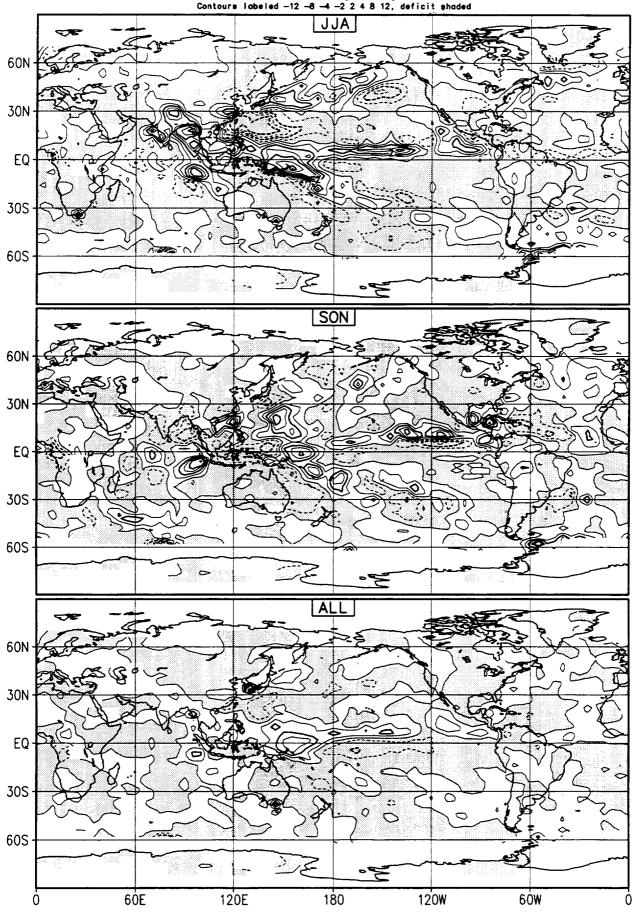
Observed Anomaly Rainfall (mm/day) Year 1 (1979) Contours labeled -12 -8 -4 -2 2 4 8 12, deficit shaded

60N -30N EQ 30S 60S SON 60N 30N EQ-30S -60S ALL 60N 30N · EQ-30S 60S J.0 6ÓE 120W 120E 180 6ÓW

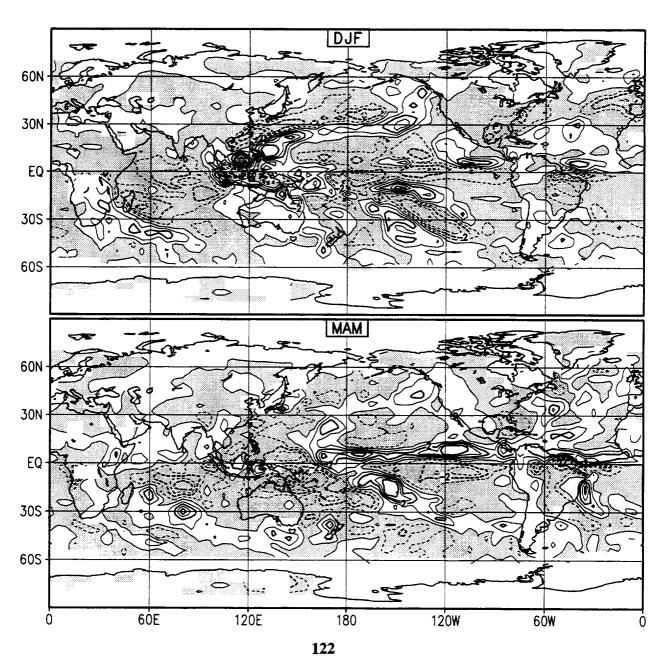
Observed Anomaly Rainfall (mm/day) Year 2 (1980) Contours labeled -12 -8 -4 -2 2 4 8 12, deficit shaded



Observed Anomaly Rainfall (mm/day) Year 2 (1980) Contours labeled -12 -8 -4 -2 2 4 8 12, deficit shaded



Observed Anomaly Rainfall (mayear 3 (1981) Contours labeled -12 -8 -4 -2 2 4 8 12, deficit shaded (mm/day)



Observed Anomaly Rainfall (mm/day)

Year 3 (1981)

Contours labeled -12 -8 -4 -2 2 4 8 12, deficit shaded JJA 60N 30N -EQ-**30**S 60S -SON 60N -30N EQ-30S 60S ALL 60N -30N EQ-30S 605 -

180

120E

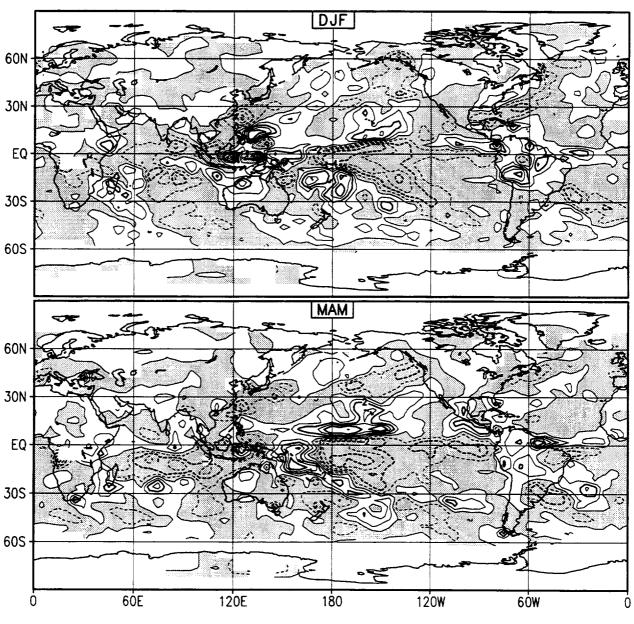
60W

120W

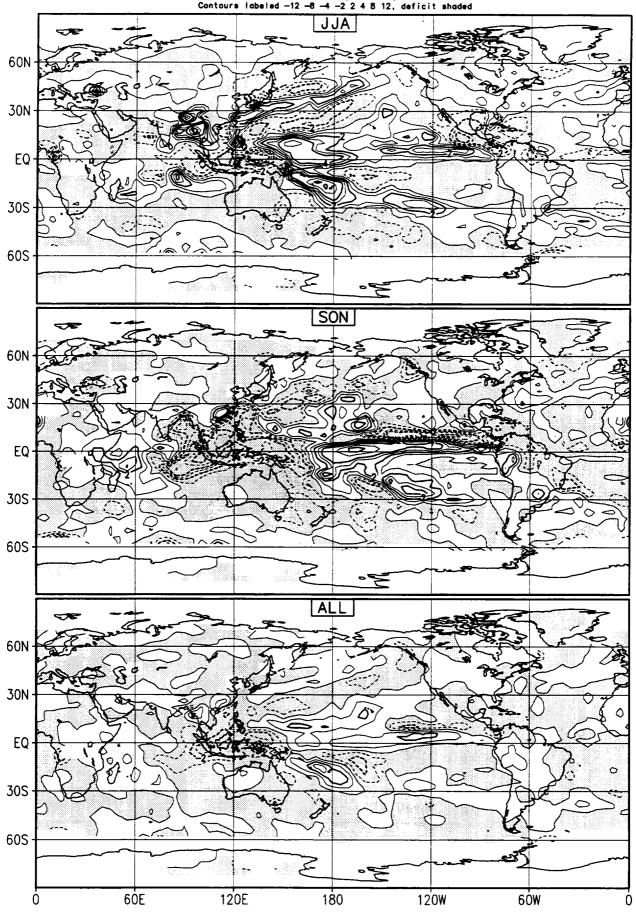
60E

Observed Anomaly Rainfall (mm/day) Year 4 (1982)

Contours labeled -12 -8 -4 -2 2 4 8 12, deficit shaded

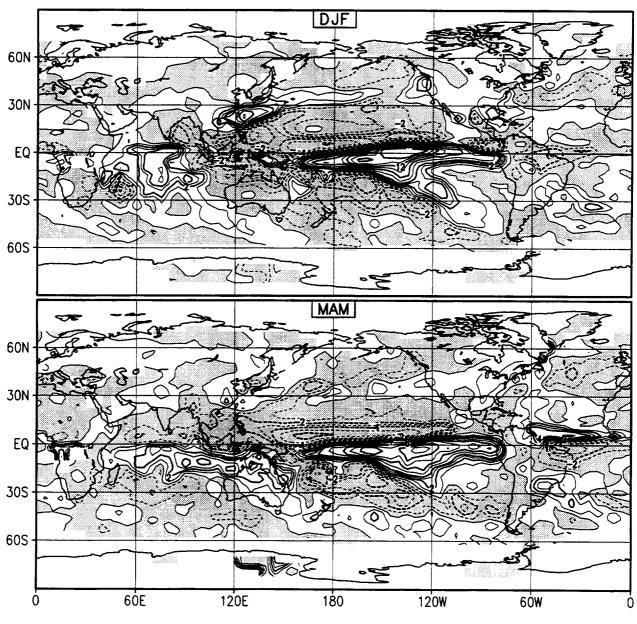


Observed Anomaly Rainfall (mm/day) Year 4 (1982) Contours labeled -12 -8 -4 -2 2 4 8 12, deficit shaded



Observed Anomaly Rainfall (mm/day) Year 5 (1983)

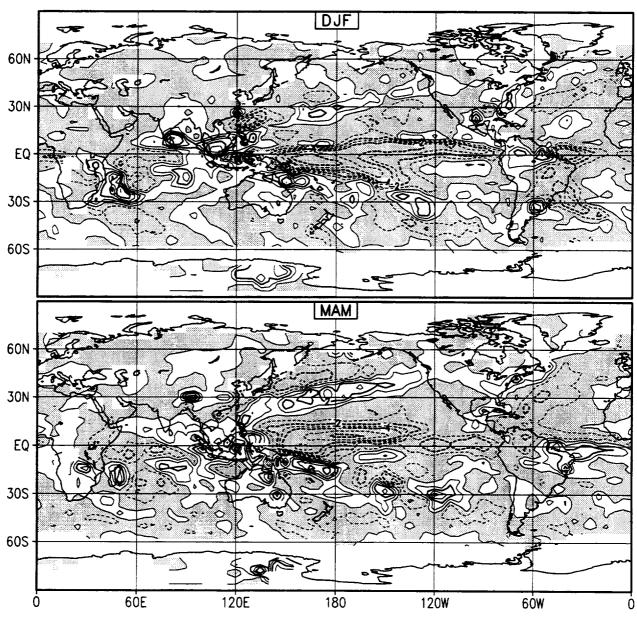
Contours labeled -12 -8 -4 -2 2 4 8 12, deficit shaded



Observed Anomaly Rainfall (mm/day)
Year 5 (1983)
Contours labeled -12 -8 -4 -2 2 4 8 12, definit shaded 60N 30N EQ-30S 605 SON 60N -30N EQ: 30S 60S 60N 30N EQ-30S · 60S -60E 120E 180 120W 6ÓW

Observed Anomaly Rainfall (mm/day)

Contours labeled -12 -8 -4 -2 2 4 8 12, deficit shaded



Observed Anomaly Rainfall (mm/day)
Year 6 (1984)
Contours labeled -12 -8 -4 -2 2 4 8 12, deficit shaded 60N -30N EQ: 30S 60S SON 60N-30N EQ-30S 60S ALL 60N 30N EQ-30S · 60S

180

120W

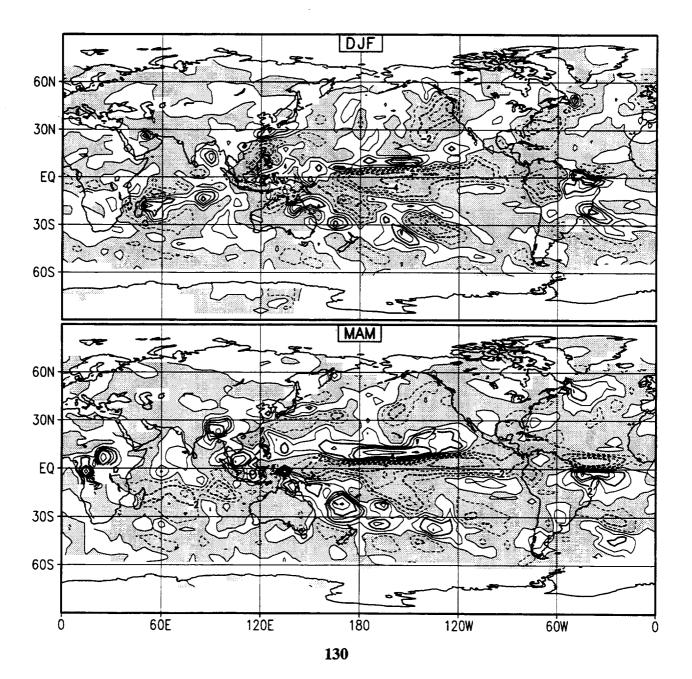
60W

120E

6ÓE

Observed Anomaly Rainfall (mm/day) Year 7 (1985)

Contours labeled -12 -8 -4 -2 2 4 8 12, deficit shaded



Observed Anomaly Rainfall (mm/day)
Year 7 (1985)
Contours labeled -12 -8 -4 -2 2 4 8 12, deficit shaded 60N 30N EQ-30S 60S -SON 60N 30N EQ-30S 60S ALI 60N 30N EQ. 30S 60S

180

120W

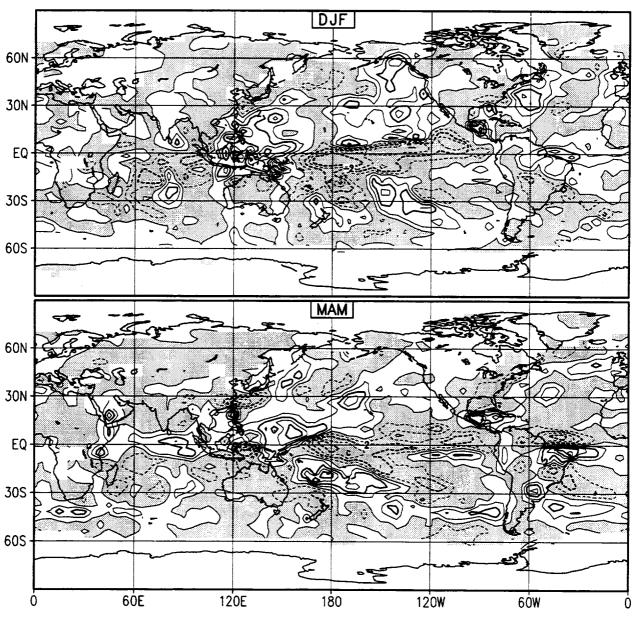
6ÒW

120E

6ÓE

Observed Anomaly Rainfall (mm/day) Year 8 (1986)

Contours labeled -12 -8 -4 -2 2 4 8 12, deficit shaded



Observed Anomaly Rainfall (mm/day)
Year 8 (1986)
Contours labeled -12 -8 -4 -2 2 4 8 12, deficit shaded 60N 30N EQ: 30S 60S SON 60N 30N EQ: 30S 60S 60N 30N -EQ-30S -60S -

180

120W

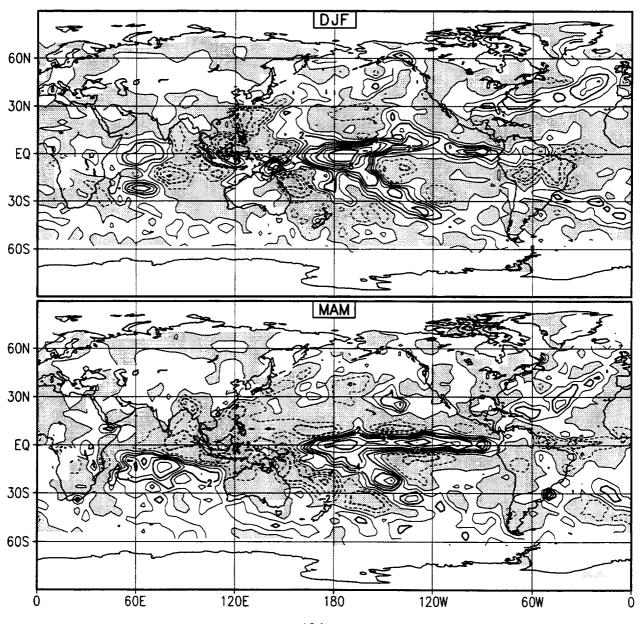
6ÒW

120E

6ÒE

Observed Anomaly Rainfall (mm/day) Year 9 (1987)

Contours | abeled -12 -8 -4 -2 2 4 8 12, deficit shaded



Observed Anomaly Rainfall (mm/day)

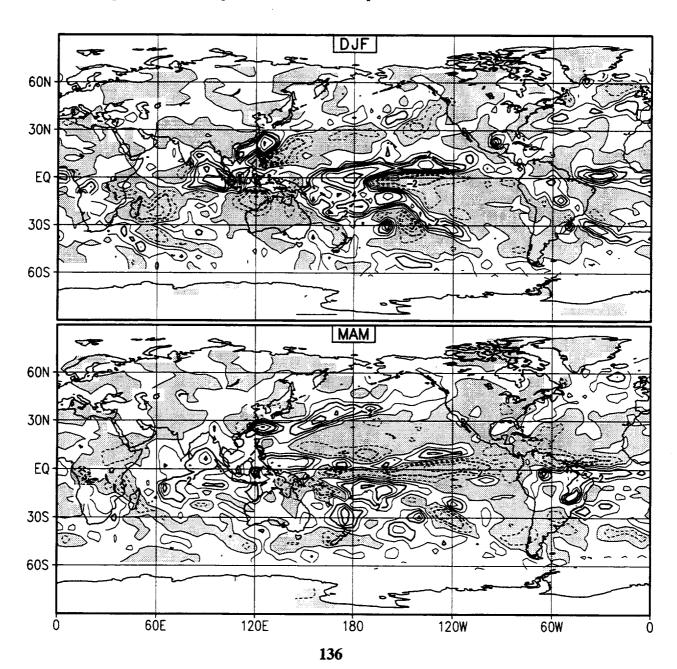
Year 9 (1987)

Contours labeled -12 -8 -4 -2 2 4 8 12, deficit shaded 60N -30N EQ-**30S** 60S SON 60N 30N EQ 30S 60S 60N 30N EQ-30S 60S 60E 120E 180 120W 6ÓW

Observed Anomaly Rainfall (mm/day)

Year 10 (1988)

Contours labeled -12 -8 -4 -2 2 4 8 12, deficit shaded



Observed Anomaly Rainfall (mm/day)
Year 10 (1988)
Contours labeled -12 -8 -4 -2 2 4 8 12, deficit shaded 60N -30N EQ-30S 605 SON 60N 30N EQ-30S 60S 60N 30N EQ. 30S 60S

180

120E

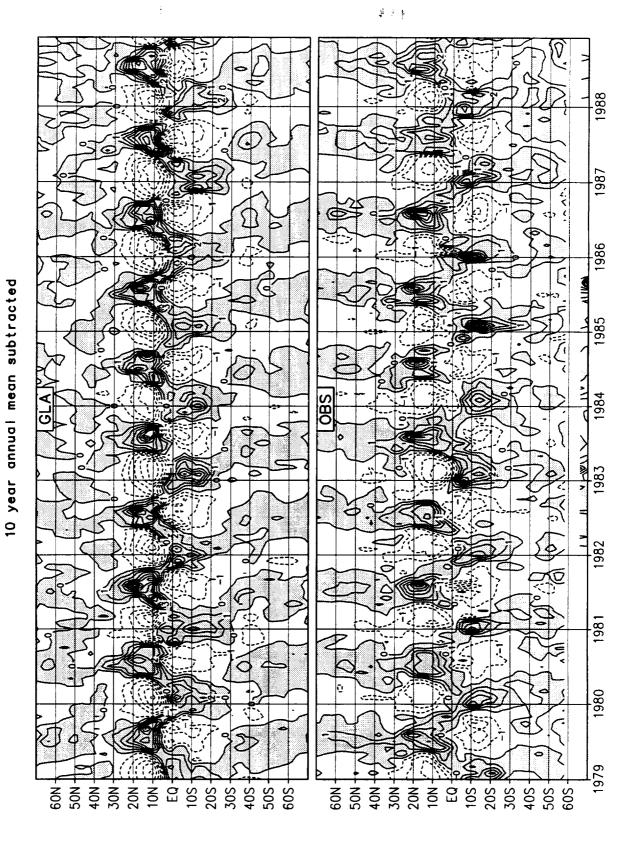
60E

120W

6ÓW

1988 1987 Zonal Mean Precipitation (mm/day) 1986 1985 Total 1984 1983 1982 1981 1980 40N-50S -60S -- N09 50N-30N-20N-10N - 10S - 20S - 30S - 40S - 50S - 60S - 20N-10N - 10S - 20S - 30S -40S-40N-30N

Zonal Mean Precipitation (mm/day)



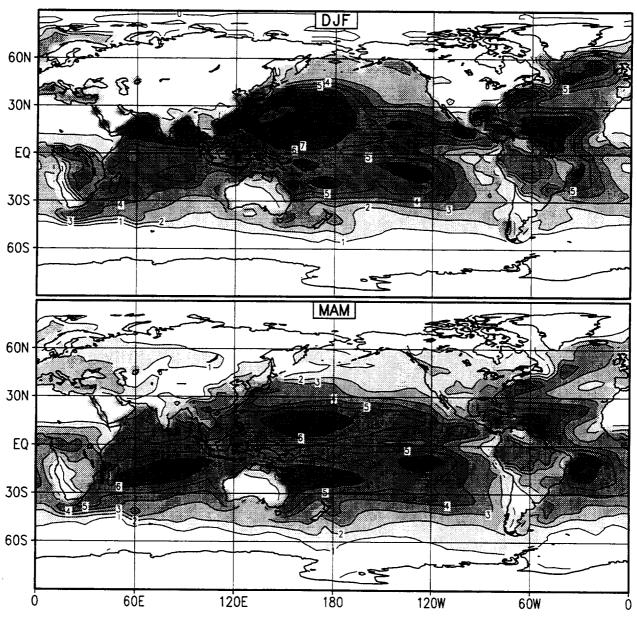
1988 1987 10 year monthly mean subtracted 1985 کے 1984 > 1W V 1983 1982 1981 1980 1979 20N -40N-30N-20N-10N -EQ -10S -20S -30S -40S--N09 30N-10N-EQ-20S -30S -50S -60S -40S-50N-40N-

Zonal Mean Precipitation (mm/day)

B. EVAPORATION

Evaporation (mm/day) 10 Year Mean (1979-88)

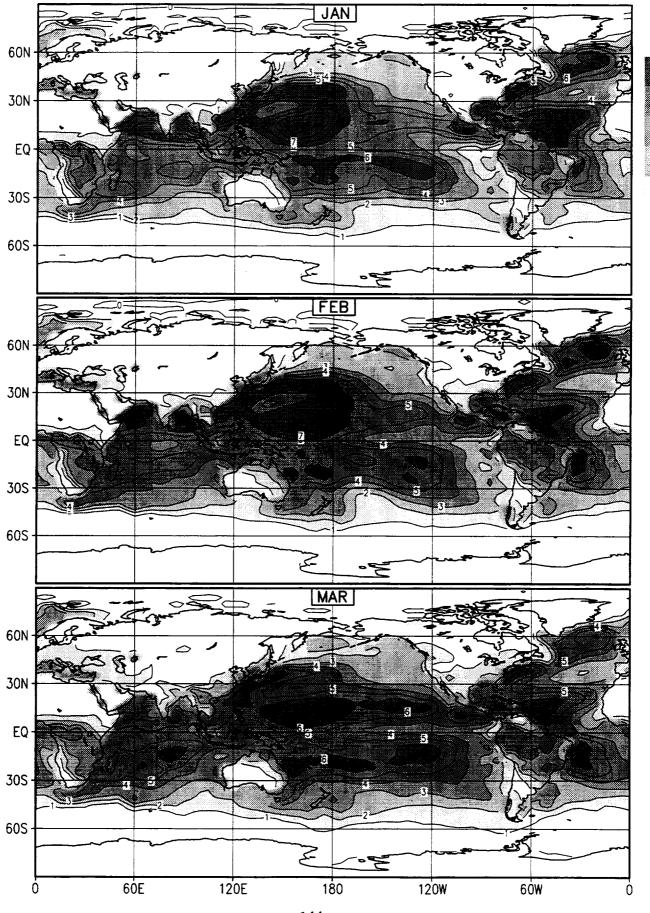
A set of simulated evaporation fields. Panel labels show seasonal means: December, January, February (DJF), March, April, May (MAM), June, July, August (JJA), September, October, November (SON), and annual mean (ALL). Contour interval is 1 mm/day. Bar on the right shows range of the shaded regions. Area weighted global mean values are DJF: 2.77, MAM: 2.84, JJA: 3.11, SON: 2.79, and ALL: 2.88, respectively.



Evaporation (mm/day) 10 Year Mean (1979-88) shaded 1 2 3 4 6, contour interval 1

60N 30N -EQ-30S 60S SON 60N 30N EQ-30S 60S -ALL 60N 30N EQ-5 30S 60S 60E 120E 180 120W 60W

Evaporation (mm/day) 10 Year Mean (1979-88) shoded 1 2 3 4 6, contour interval 1



Evaporation (mm/day) 10 Year Mean (1979-88) shaded 1 2 3 4 6, contour interval 1

APR 60N 30N EQ-30S -60S MAY 60N 30N EQ-30S -60S JUN 60N 30N EQ-30S -60S 120E 6ÓE 180 120W 60W

Evaporation (mm/day) 10 Year Mean (1979-88) shoded 1 2 3 4 6, contour interval 1

60N 30N EQ 5 30S 60S AUG 60N 30N EQ 30S 60S SEP 60N 30N 5 5 EQ 30S 60S

180

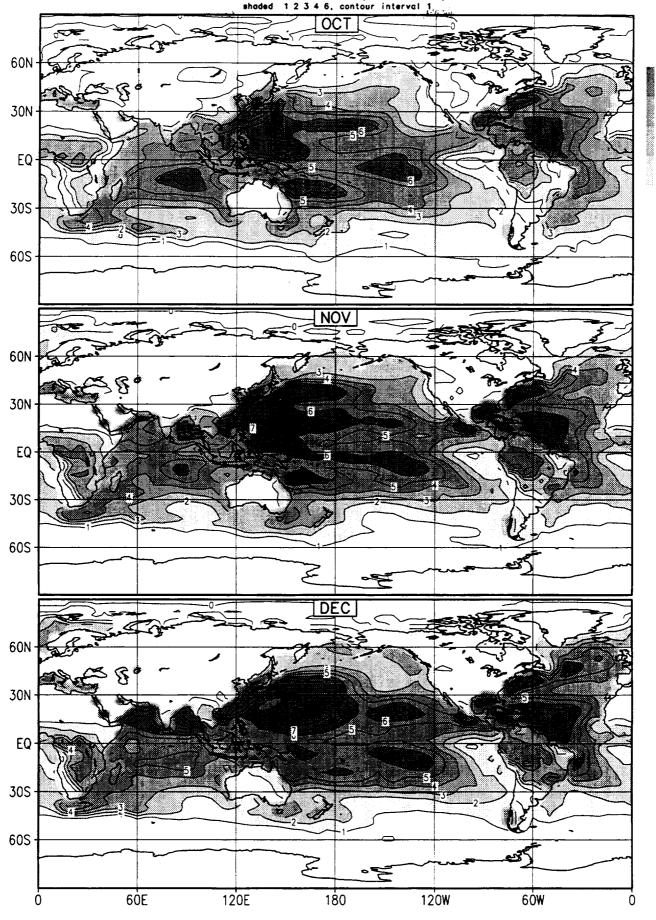
120W

6ÓW

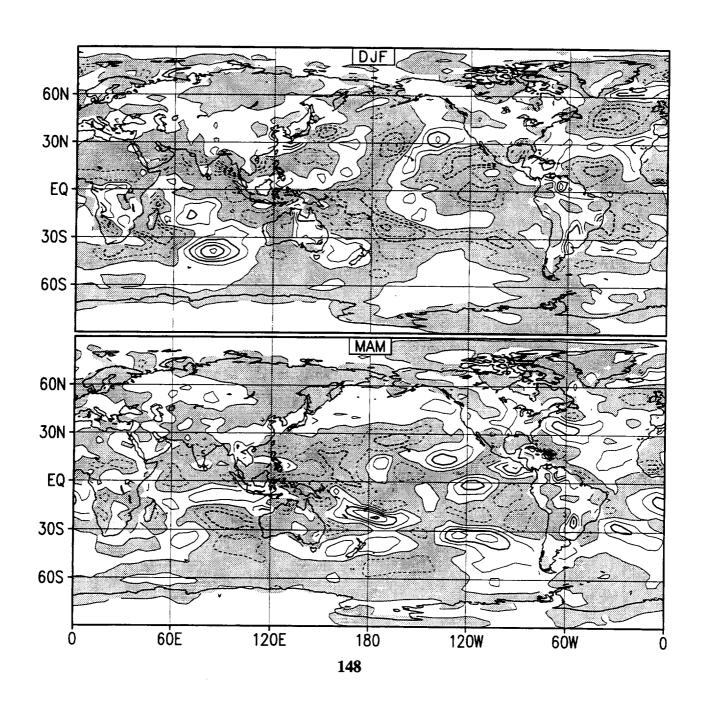
120E

60E

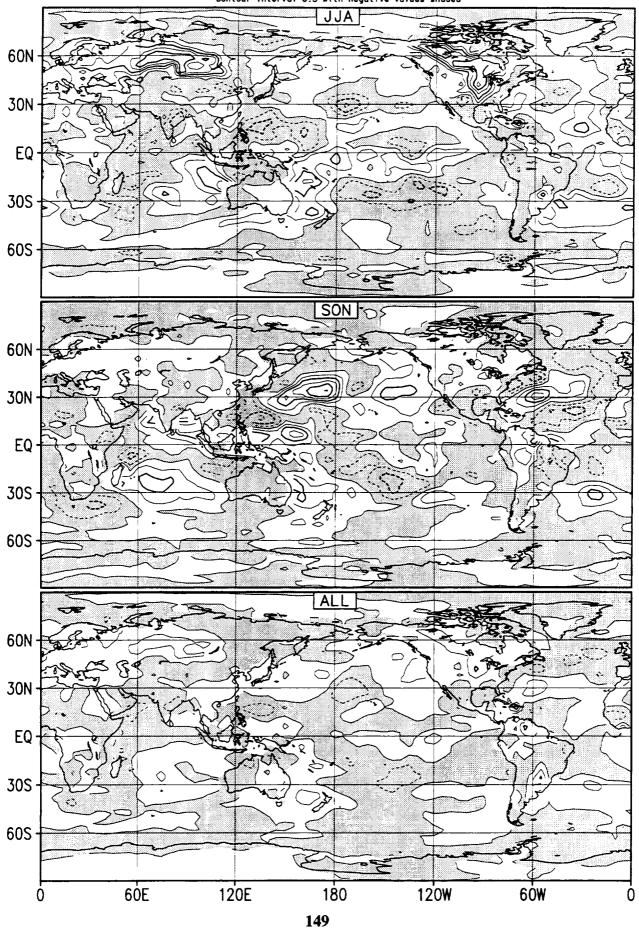
Evaporation (mm/day)
10 Year Mean (1979-88)
shoded 1 2 3 4 6, contour interval 1



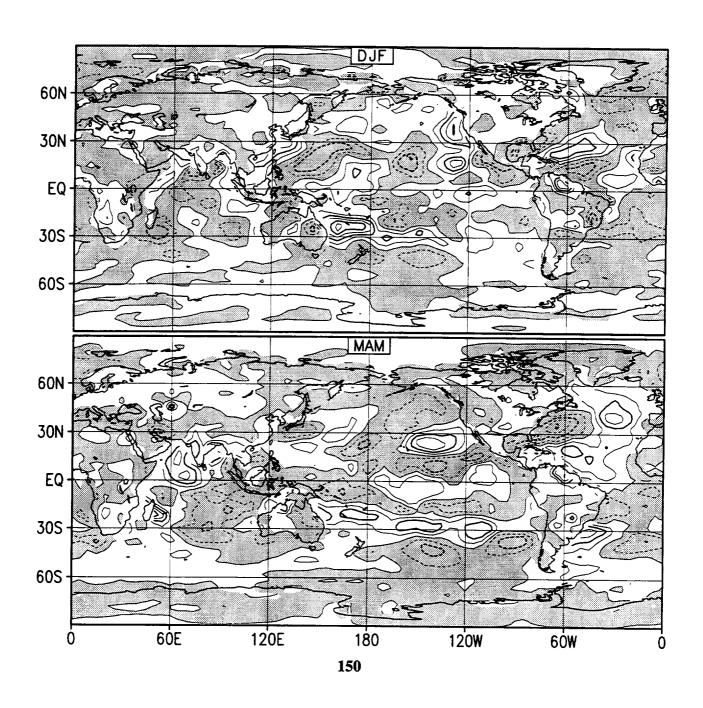
Anomaly Evaporation (mm/day) Simulation Year 1 (1979)



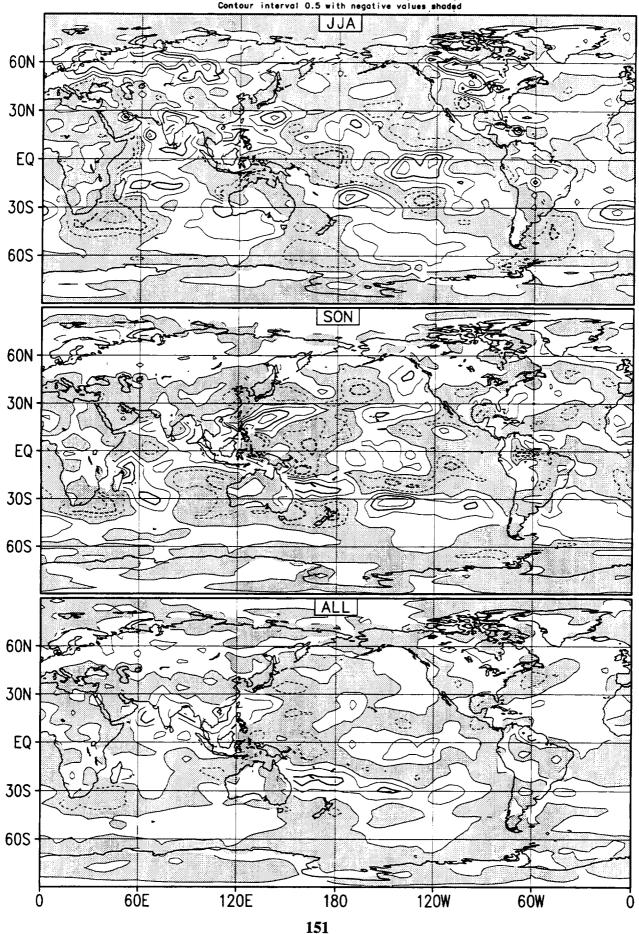
Anomaly Evaporation (mm/day) Simulation Year 1 (1979) Contour interval 0.5 with negative values shaded



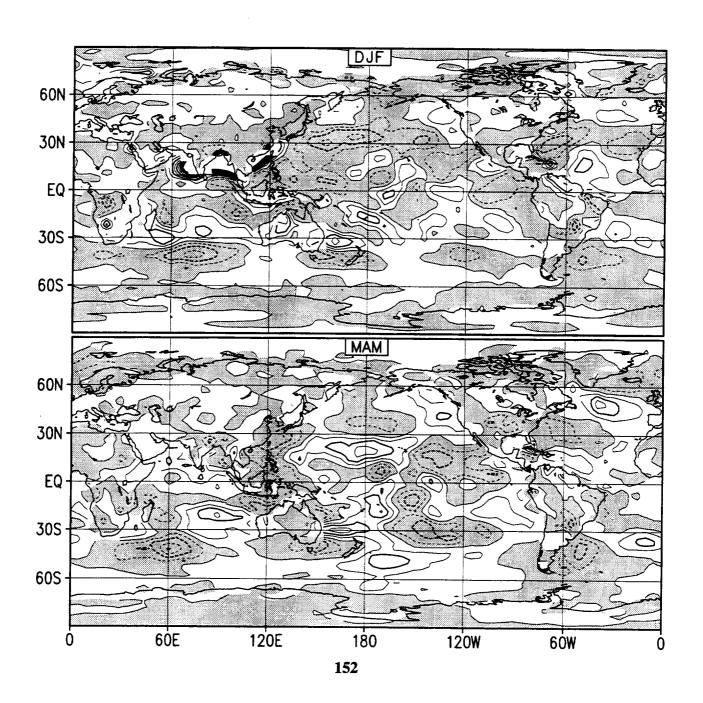
Anomaly Evaporation (mm/day) Simulation Year 2 (1980) Contour interval 0.5 with negative values shaded



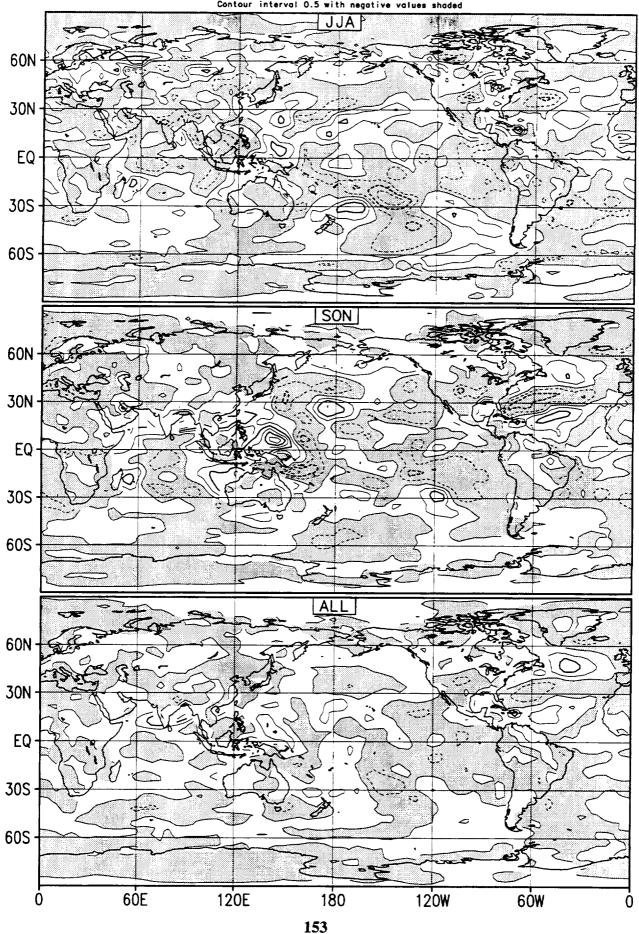
Anomaly Evaporation (mm/day) Simulation Year 2 (1980) Contour interval 0.5 with negative values shaded



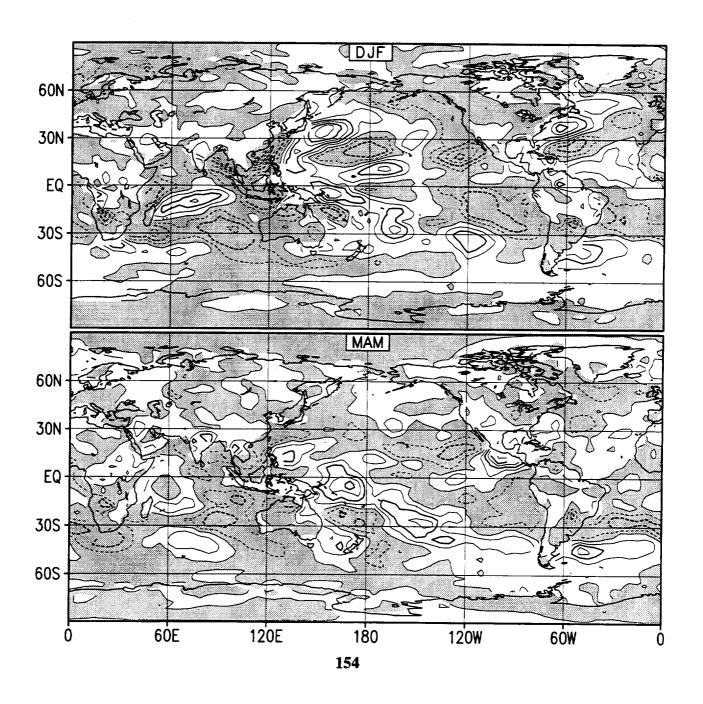
Anomaly Evaporation (mm/day) Simulation Year 3 (1981) Contour interval 0.5 with negative values shaded



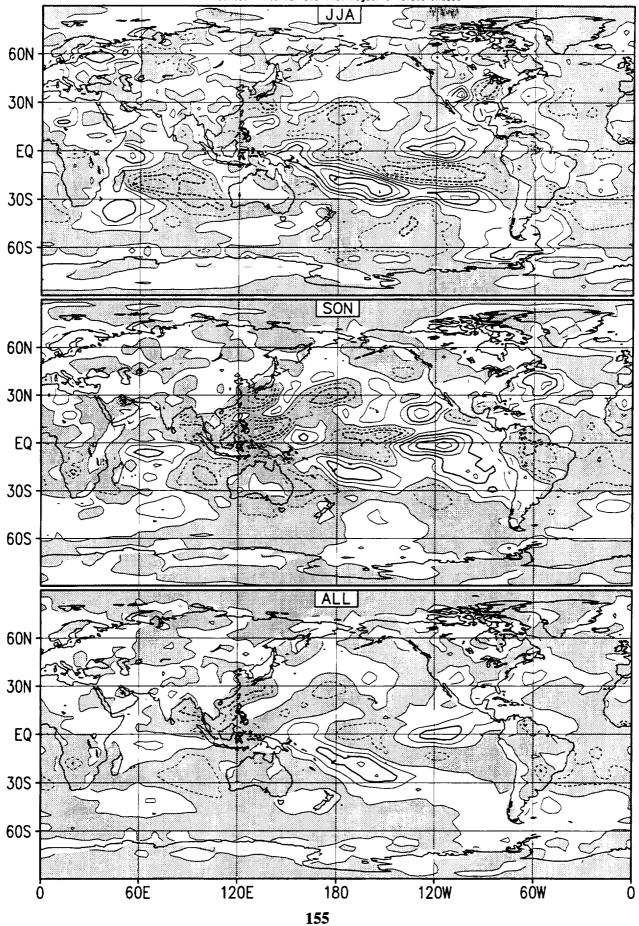
Anomaly Evaporation (mm/day) Simulation Year 3 (1981) Contour interval 0.5 with negative values shaded



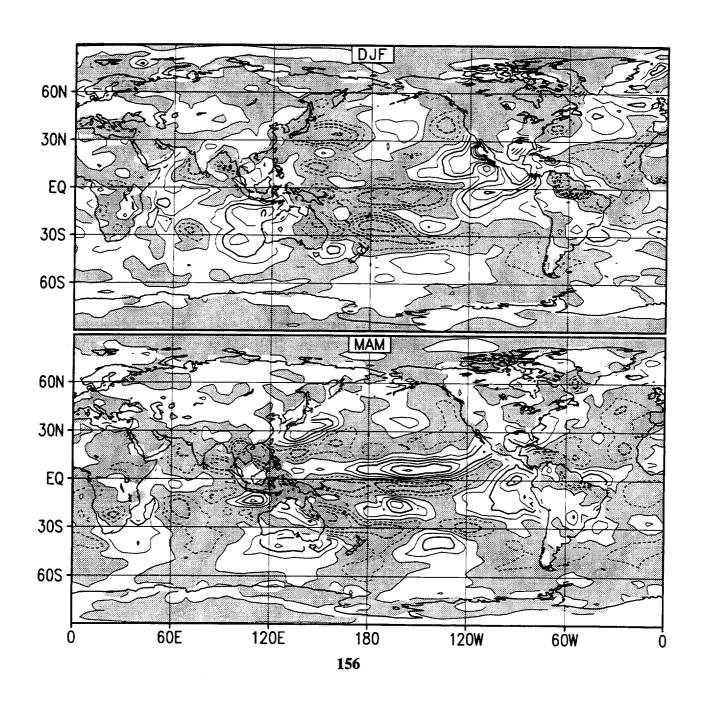
Anomaly Evaporation (mm/day) Simulation Year 4 (1982) Contour interval 0.5 with negative values shaded



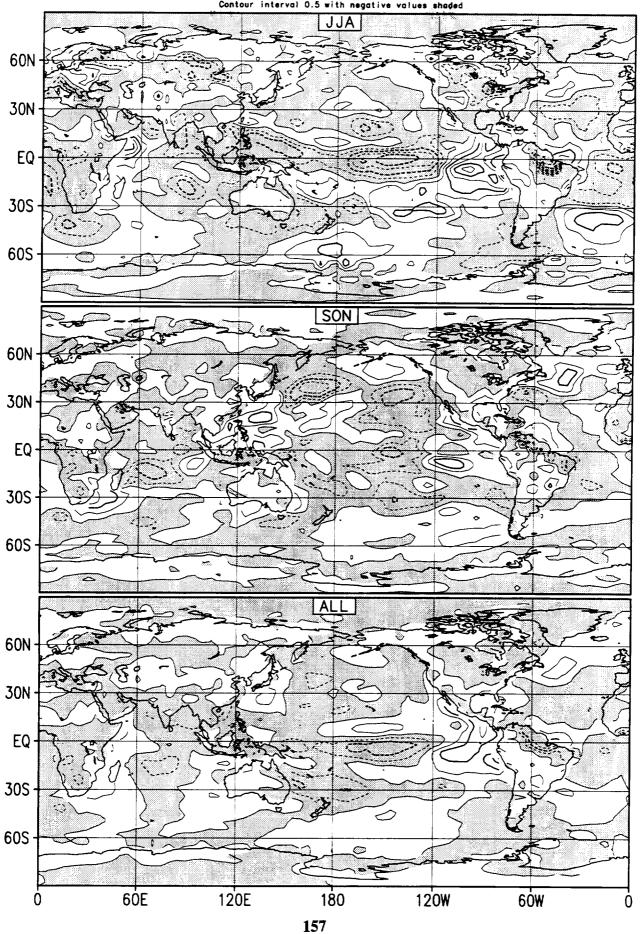
Anomaly Evaporation (mm/day) Simulation Year 4 (1982) Contour interval 0.5 with negative values shaded



Anomaly Evaporation (mm/day) Simulation Year 5 (1983) Contour interval 0.5 with negative values shaded

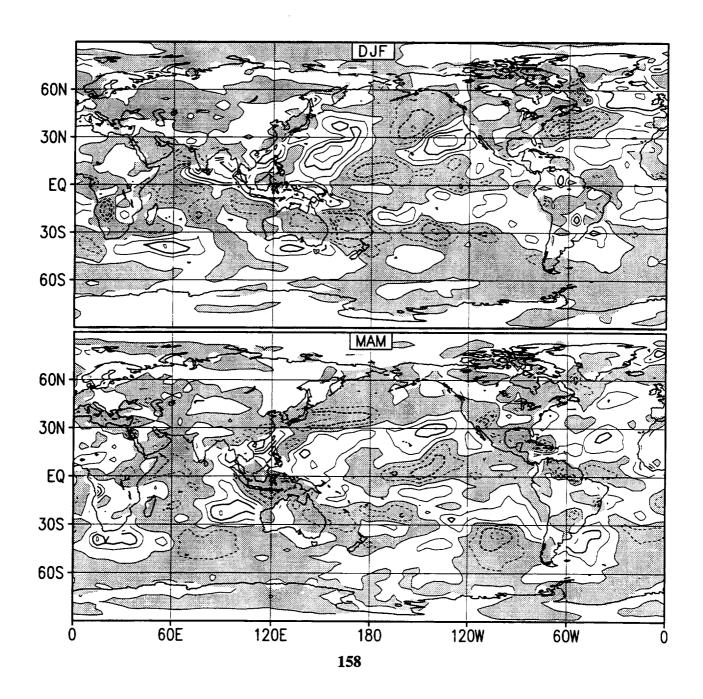


Anomaly Evaporation (mm/day) Simulation Year 5 (1983) Contour interval 0.5 with negative values shaded

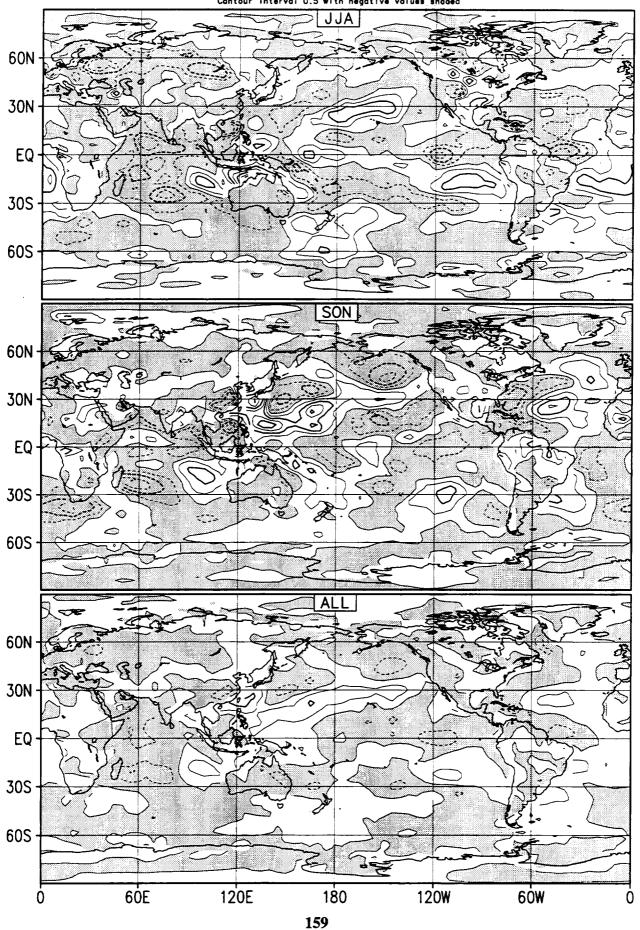


Anomaly Evaporation (mm/day) Simulation Year 6 (1984)

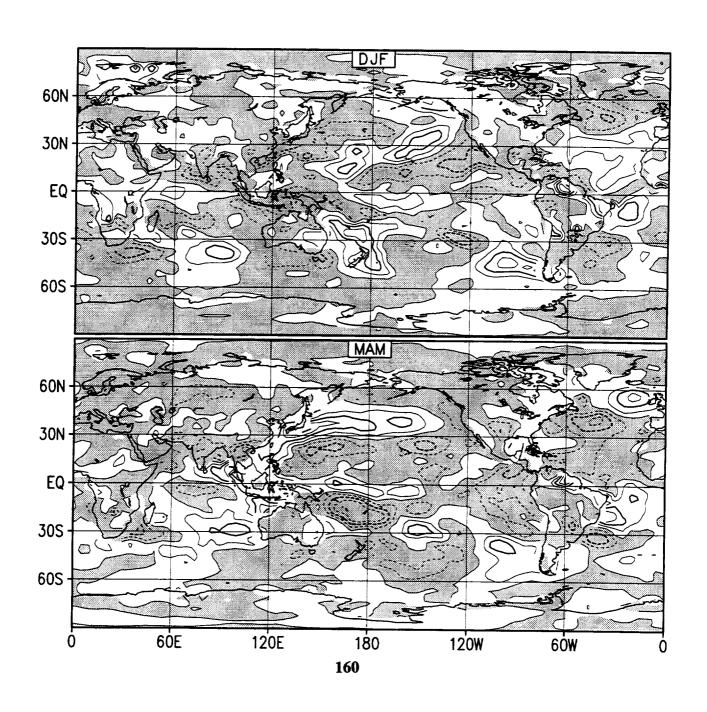
Contour interval 0.5 with negative values shaded



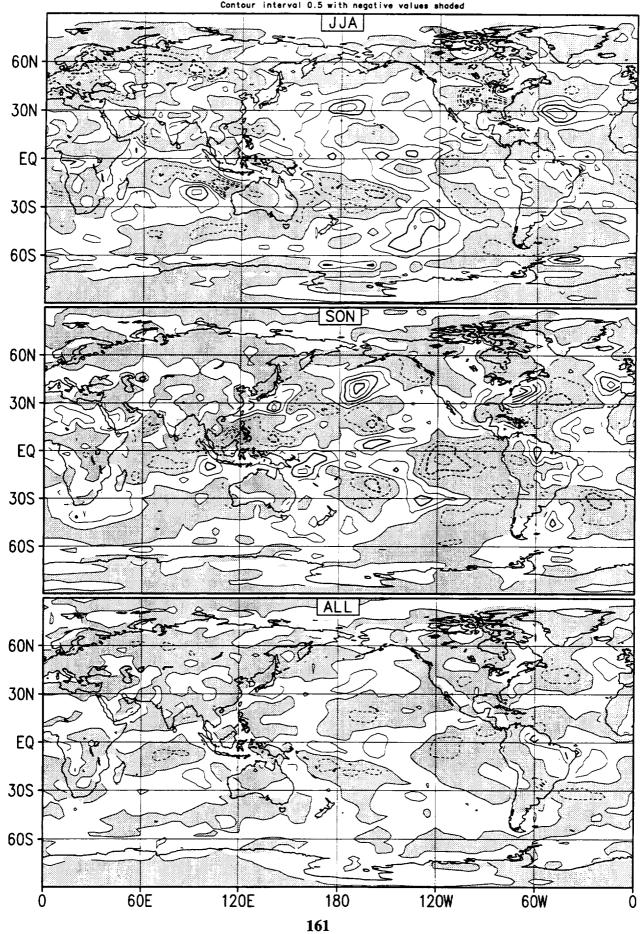
Anomaly Evaporation (mm/day) Simulation Year 6 (1984) Cantour interval 0.5 with negative values shaded



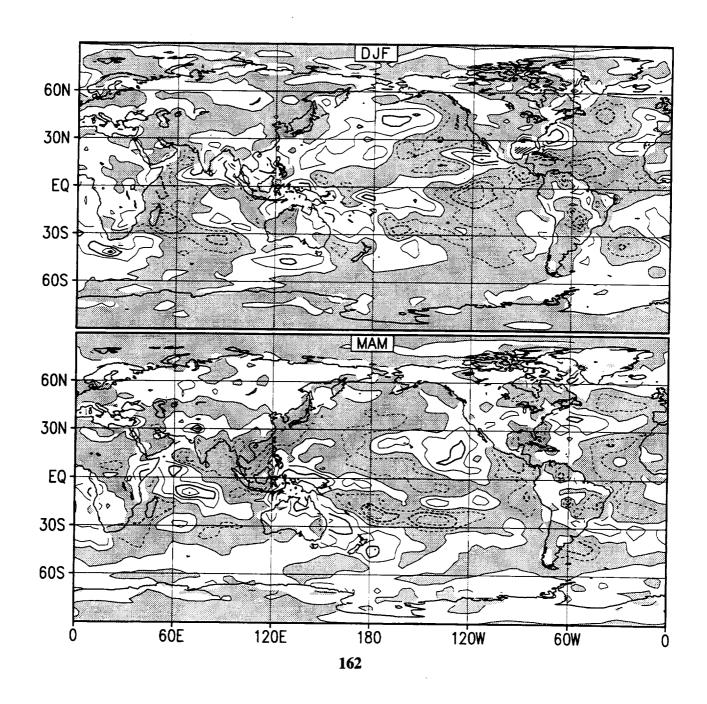
Anomaly Evaporation (mm/day) Simulation Year 7 (1985) Contour interval 0.5 with negative values shaded



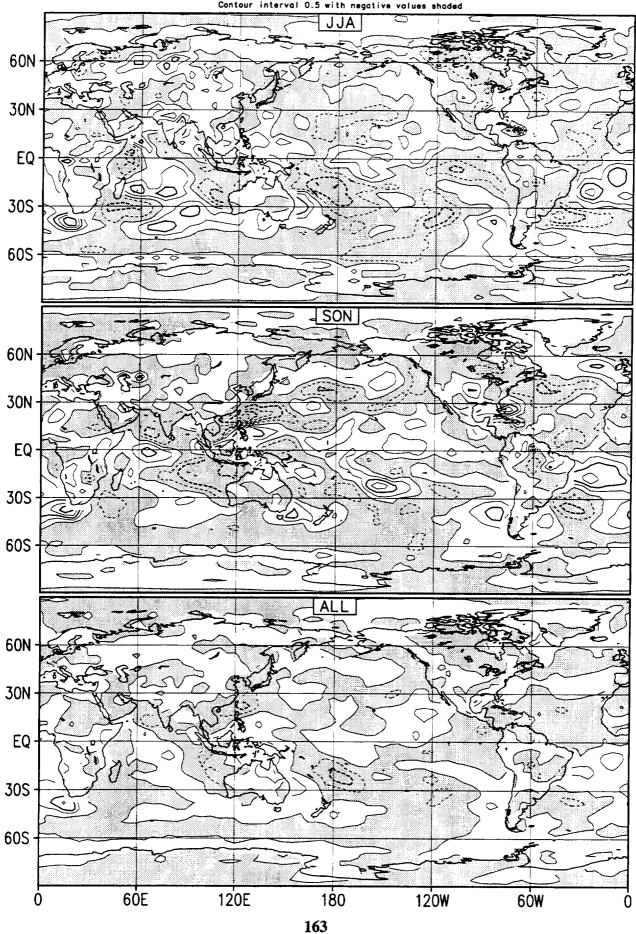
Anomaly Evaporation (mm/day) Simulation Year 7 (1985) Contour interval 0.5 with negative values shaded



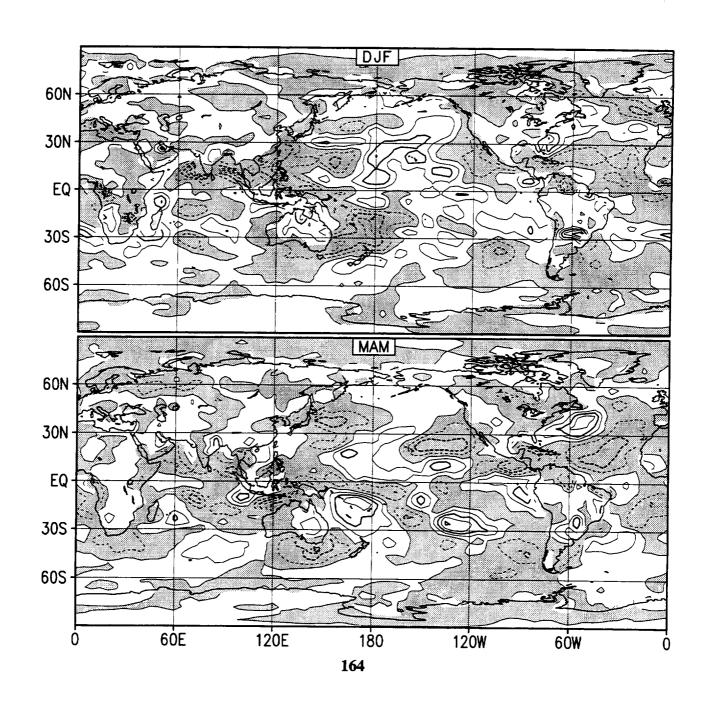
Anomaly Evaporation (mm/day) Simulation Year 8 (1986) Contour interval 0.5 with negative values shaded



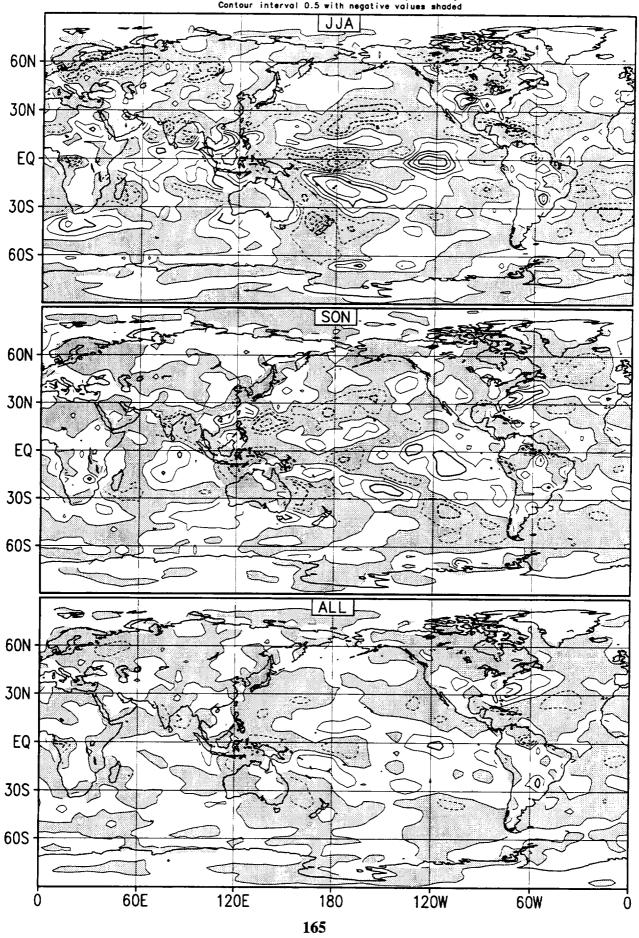
Anomaly Evaporation (mm/day) Simulation Year 8 (1986) Contour interval 0.5 with negative values shaded



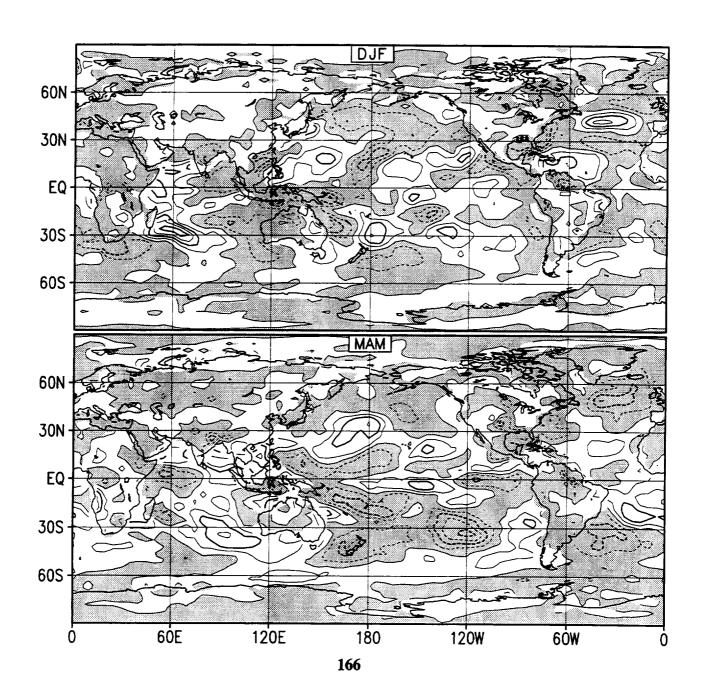
Anomaly Evaporation (mm/day) Simulation Year 9 (1987) Contour interval 0.5 with profitive values shaded



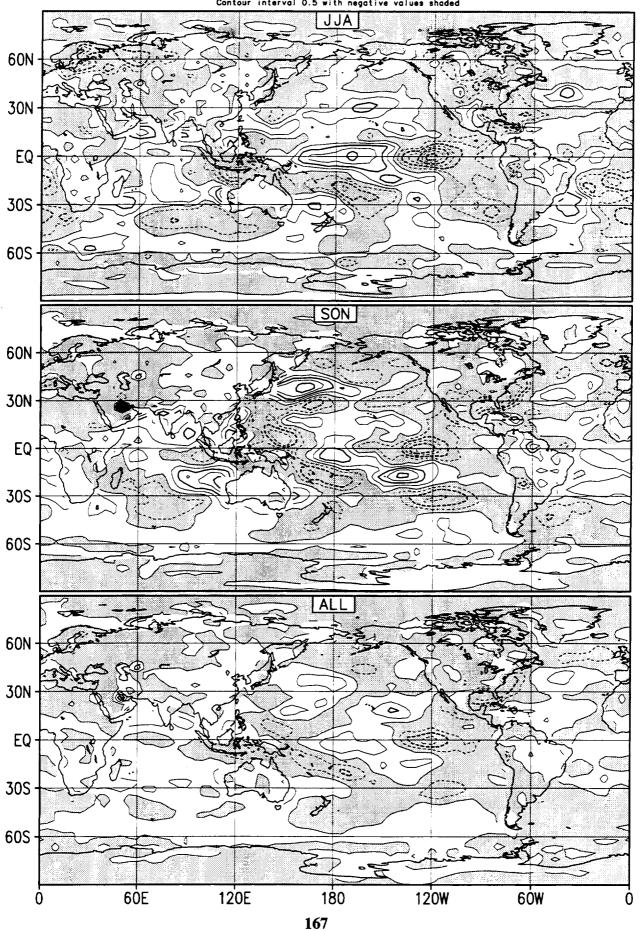
Anomaly Evaporation (mm/day) Simulation Year 9 (1987) Contour interval 0.5 with negative values shaded



Anomaly Evaporation (mm/day) Simulation Year 10 (1988) Contour interval 0.5 with negative values shaded



Anomaly Evaporation (mm/day) Simulation Year 10 (1988) Contour interval 0.5 with negative values shaded

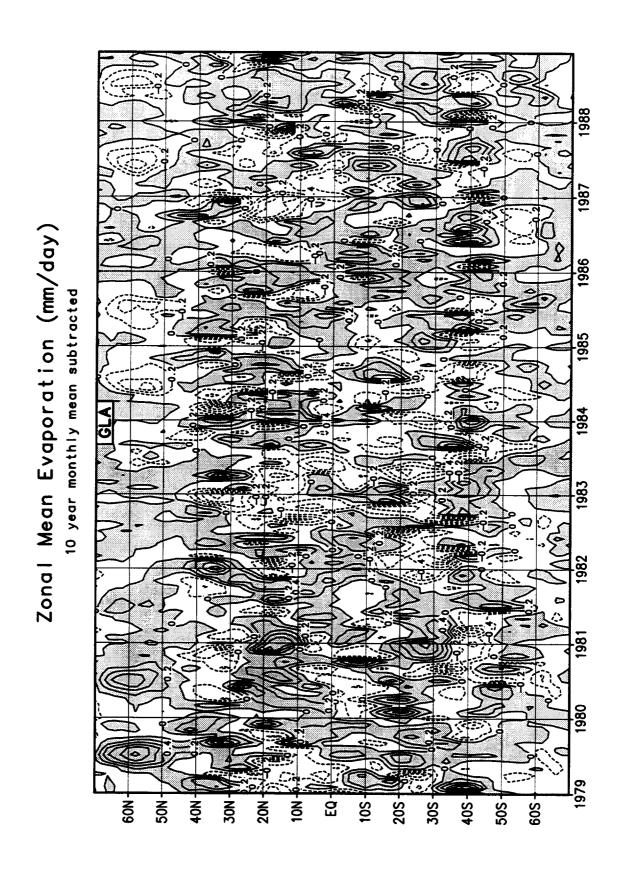


Zonal Mean Evaporation (mm/day) 1986 1983 1982 1980 30S-50N \$. 30N 20N 8 10S 20S

168

Zonal Mean Evaporation (mm/day) 10 year annual mean subtracted 10S 40S-20N 30S

1 4

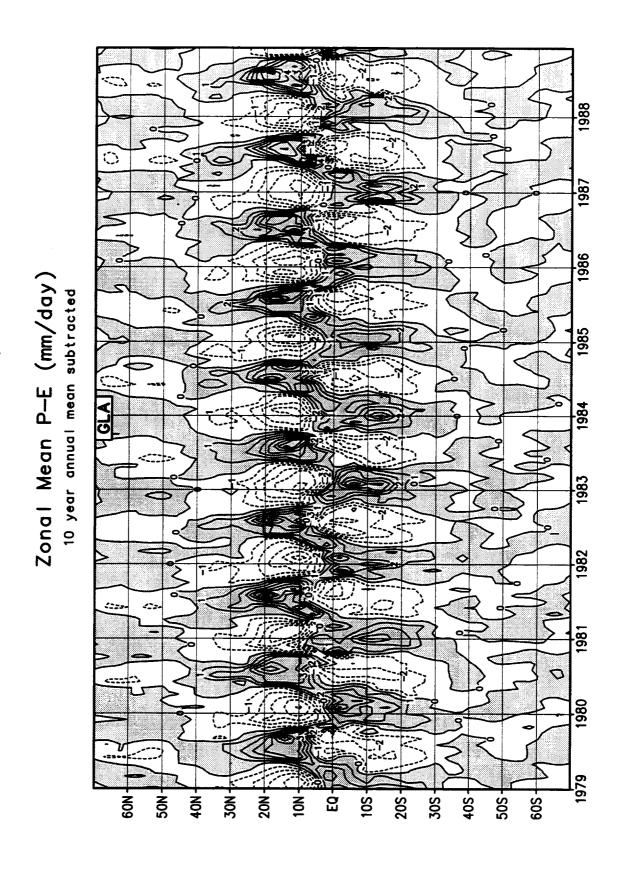


C. TIME SERIES P-E

€ + € 4

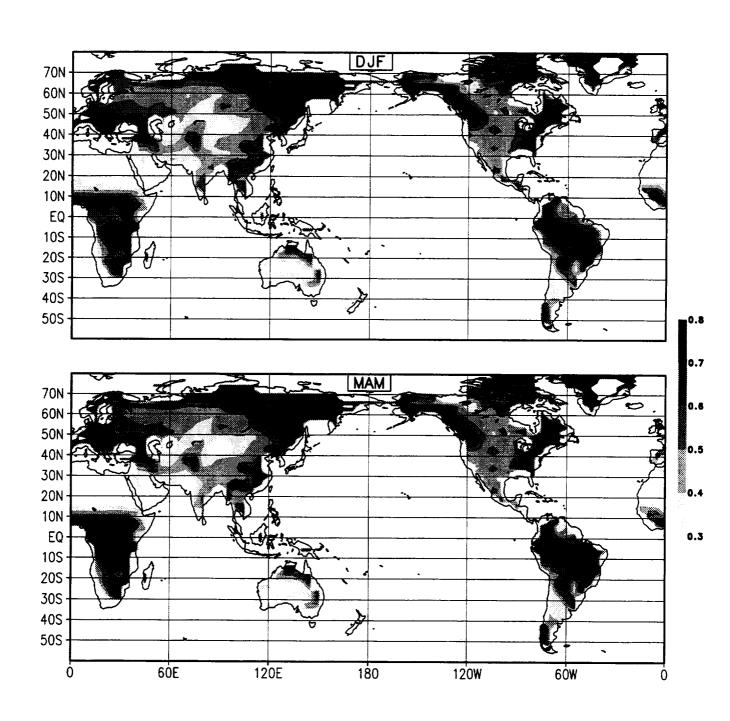
1987 Zonal Mean P—E (mm/day) 20S 30N 30S

PRECEDING PAGE PLANK NOT FILMED

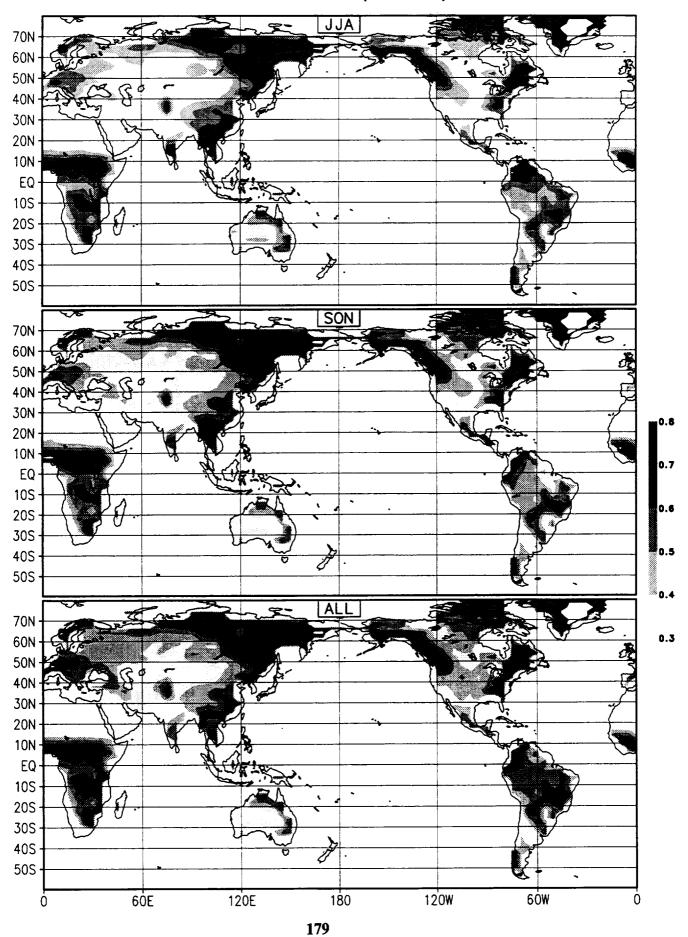


1987 1986 Zonal Mean P—E (mm/day)
10 year monthly mean subtracted 1984 1983 1982 1981 1980 30N-30S 40S 50S **4**04 ∙ 20N **20S**

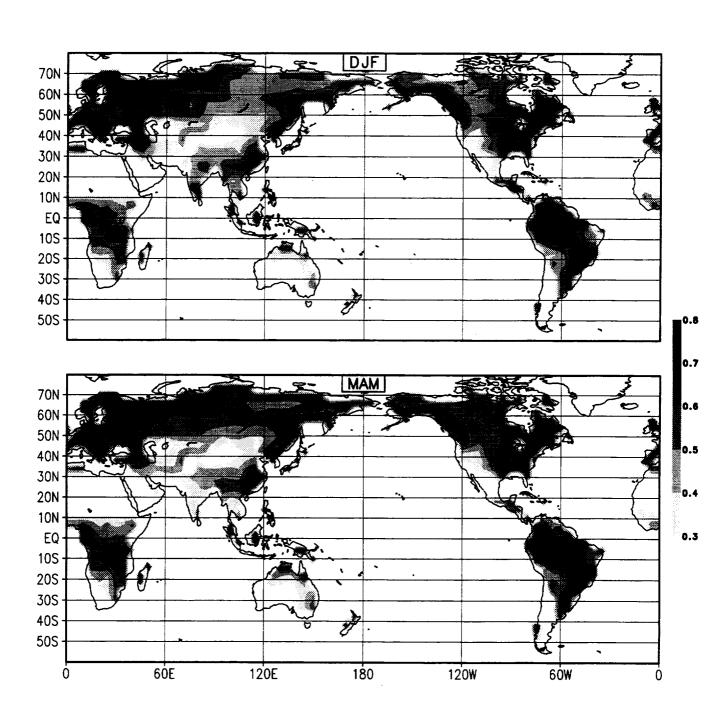
D. SOIL MOISTURE



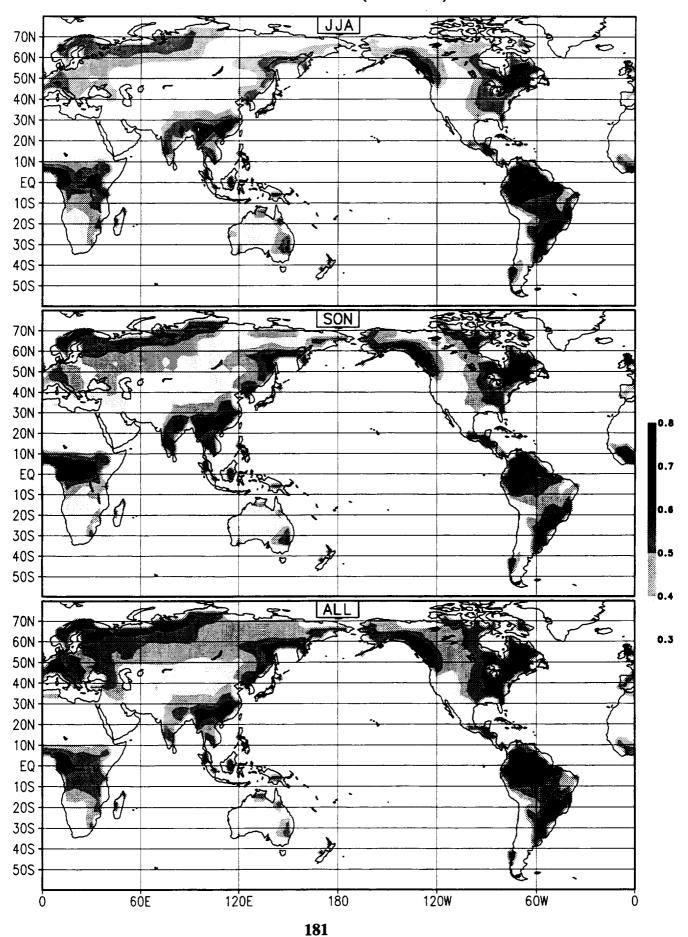
Soil Wetness in Layer 2 10 Year Mean (1979-88)



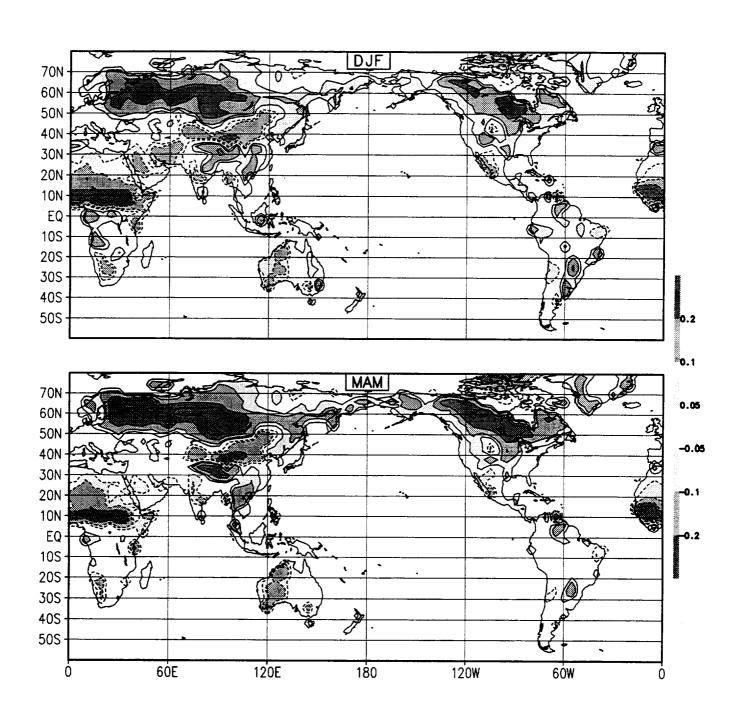
Estimated Soil Wetness L2 10 Year Mean (1979-88)



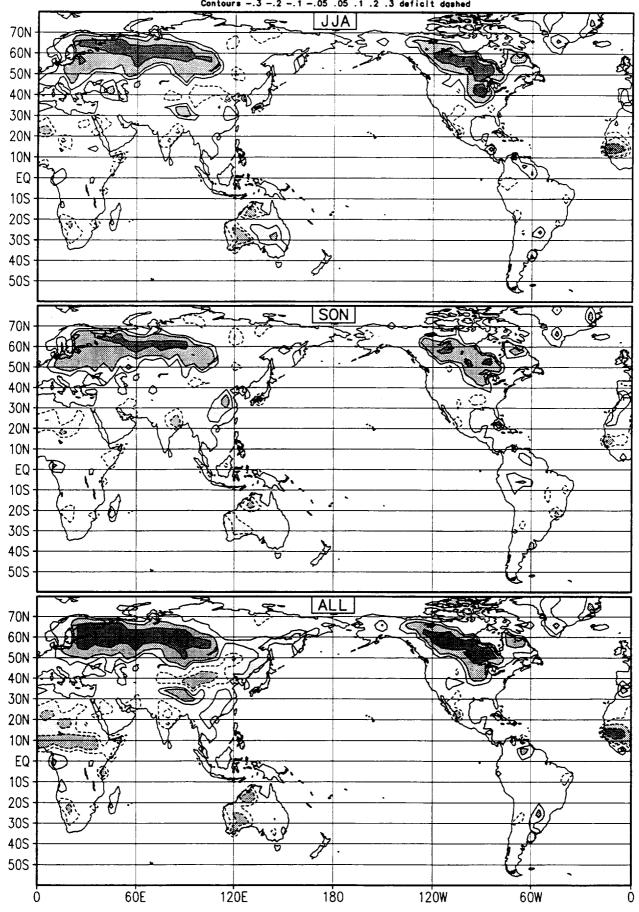
Estimated Soil Wetness L2 10 Year Mean (1979-88)



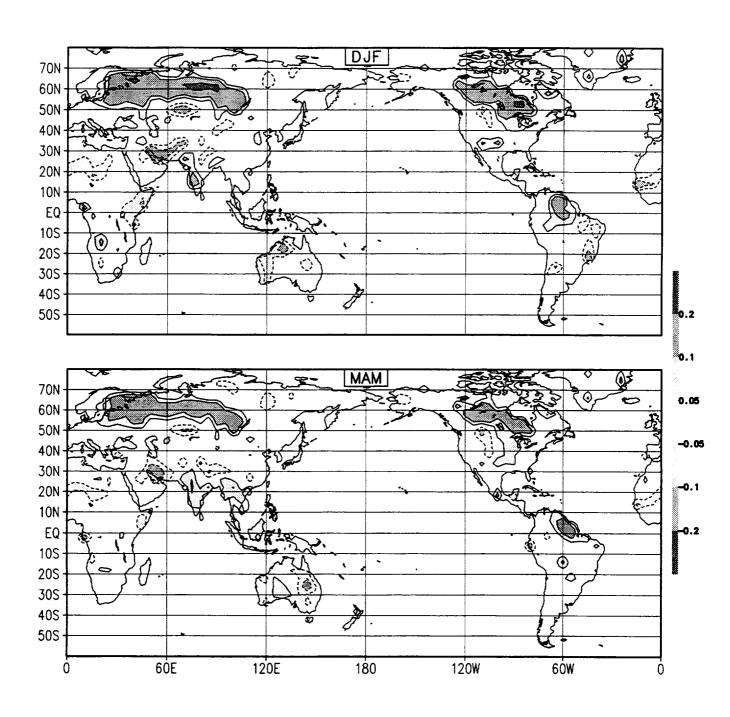
Anomaly Soil Moisture Simulation Year 1 (1979) Contours -.3 -.2 -.1 -.05 .05 .1 .2 .3 deficit dashed



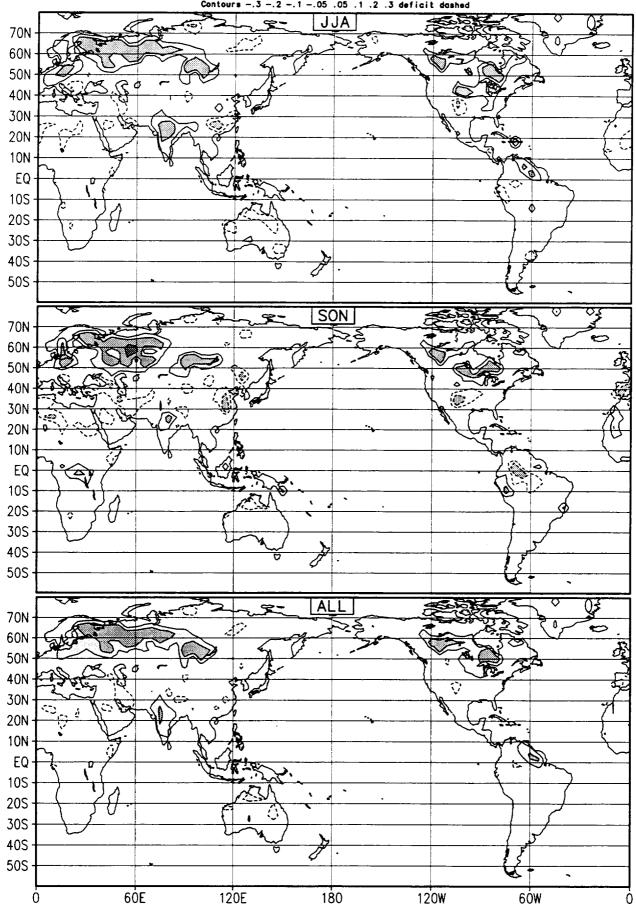
Anomaly Soil Moisture Simulation Year 1 (1979) Contours -.3 -.2 -.1 -.05 .05 .1 .2 .3 deficit dashed



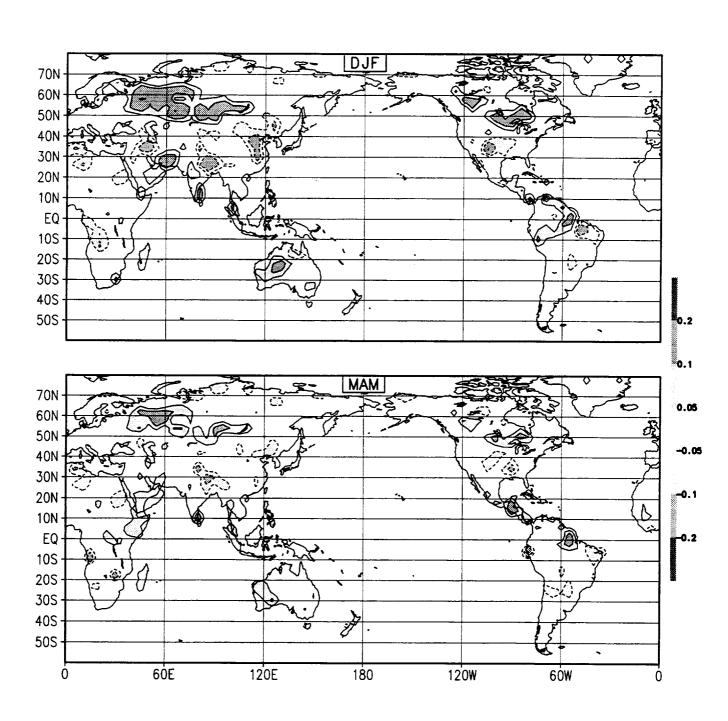
Anomaly Soil Moisture Simulation Year 2 (1980) Contours -.3 -.2 -.1 -.05 .05 .1 .2 .3 deficit dashed



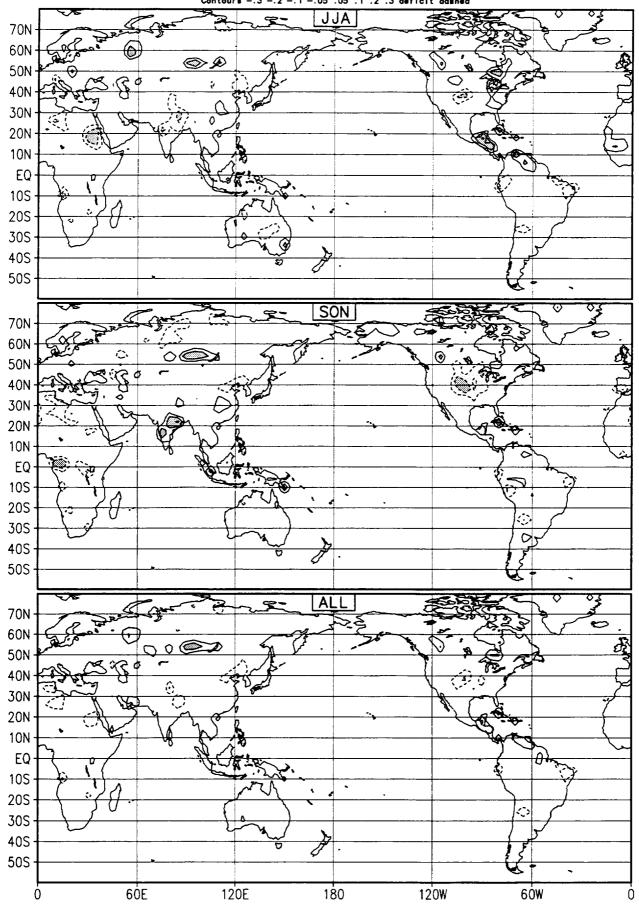
Anomaly Soil Moisture Simulation Year 2 (1980) Contours -.3 -.2 -.1 -.05 .05 .1 .2 .3 deficit dashed



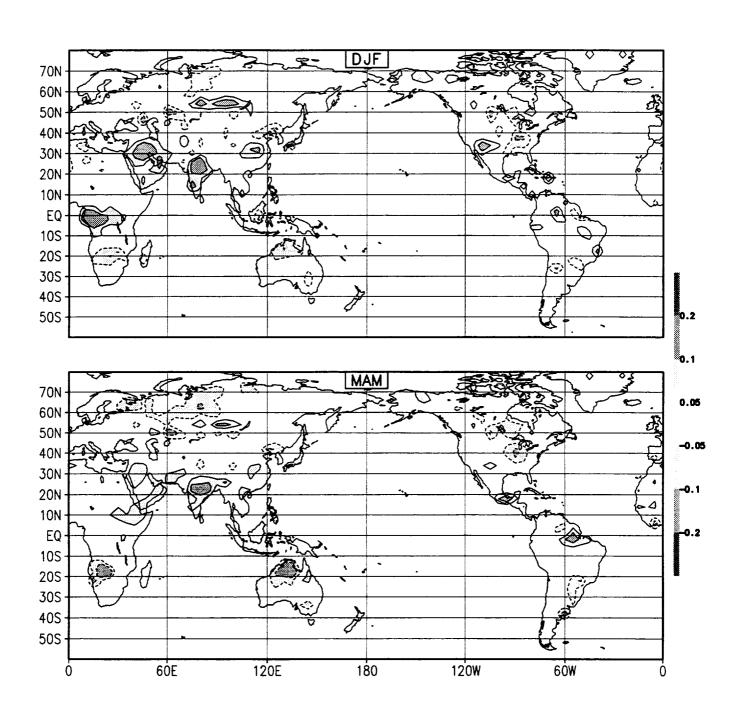
Anomaly Soil Moisture Simulation Year 3 (1981) Contours -.3 -.2 -.1 -.05 .05 .1 .2 .3 deficit dashed



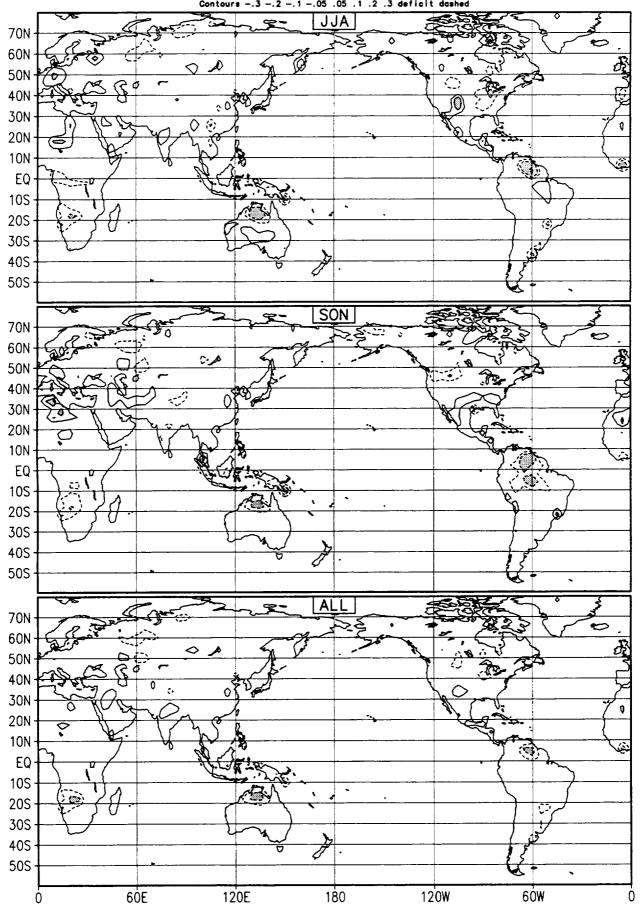
Anomaly Soil Moisture Simulation Year 3 (1981) Contours -.3 -.2 -.1 -.05 .05 .1 .2 .3 deficit dashed



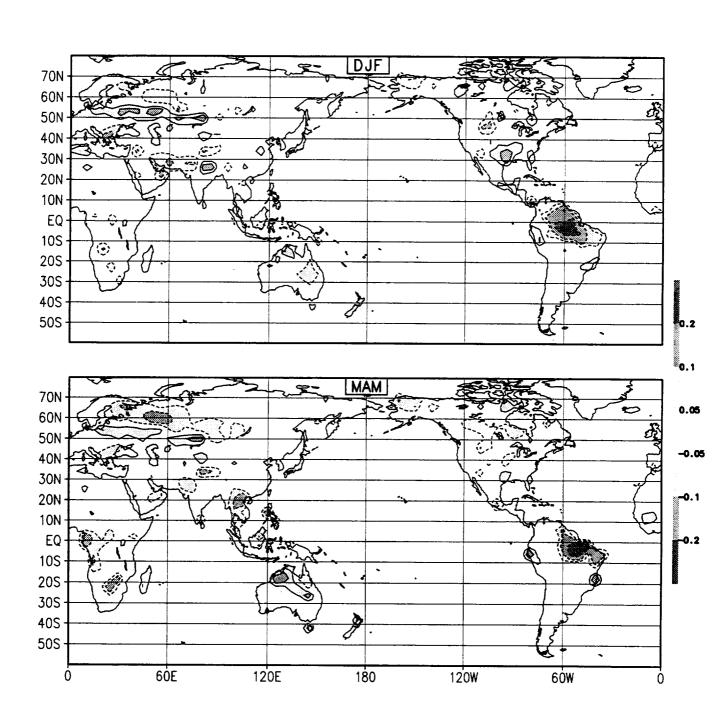
Anomaly Soil Moisture Simulation Year 4 (1982) Contours -.3 -.2 -.1 -.05 .05 .1 .2 .3 deficit dashed



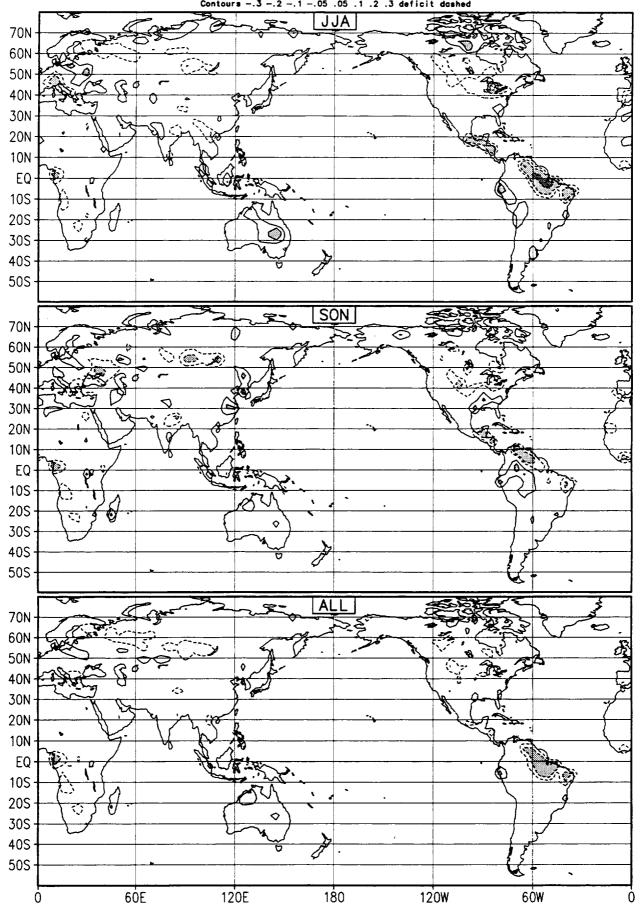
Anomaly Soil Moisture Simulation Year 4 (1982) Contours -.3 -.2 -.1 -.05 .05 .1 .2 .3 deficit dashed



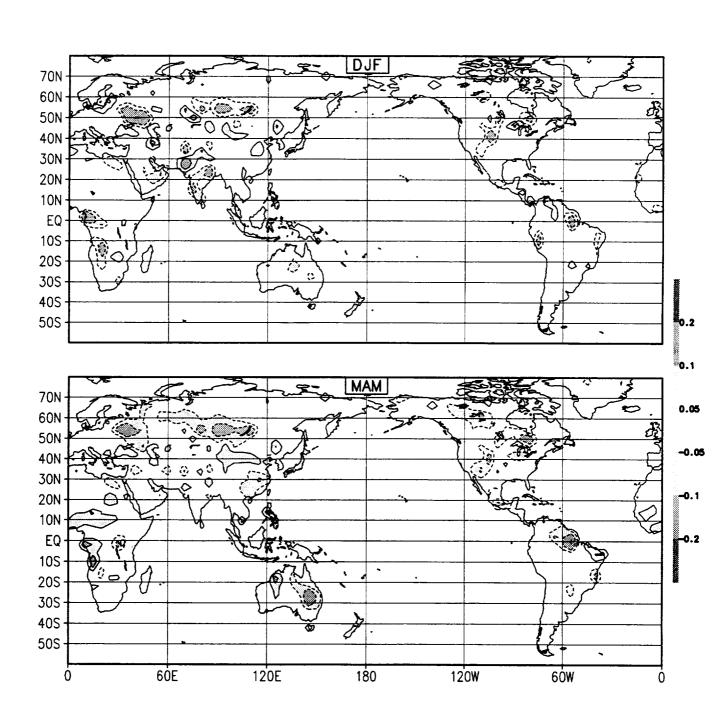
Anomaly Soil Moisture Simulation Year 5 (1983) Contours -.3 -.2 -.1 -.05 .05 .1 .2 .3 deficit dashed



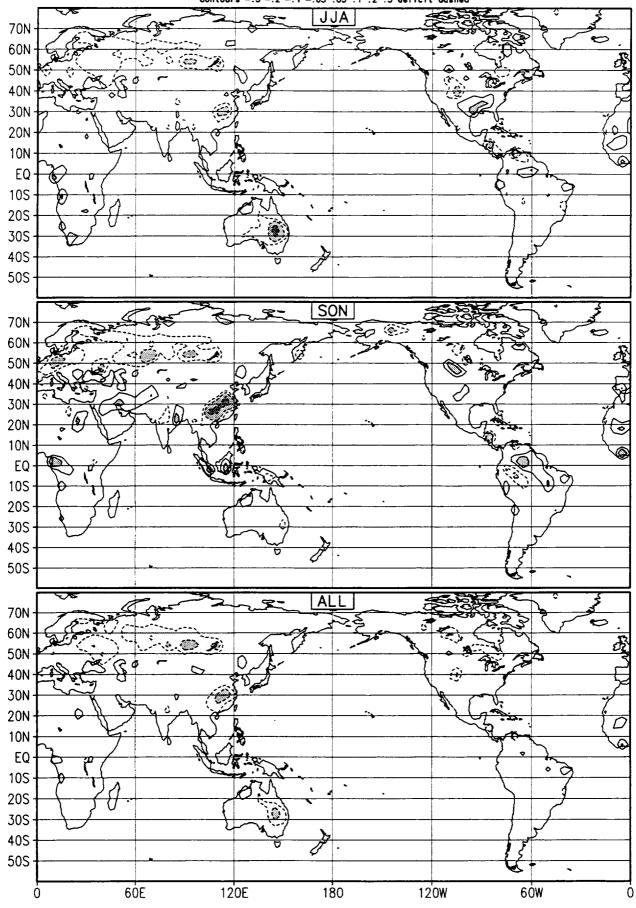
Anomaly Soil Moisture Simulation Year 5 (1983) Contours -.3 -.2 -.1 -.05 .05 .1 .2 .3 deficit dashed



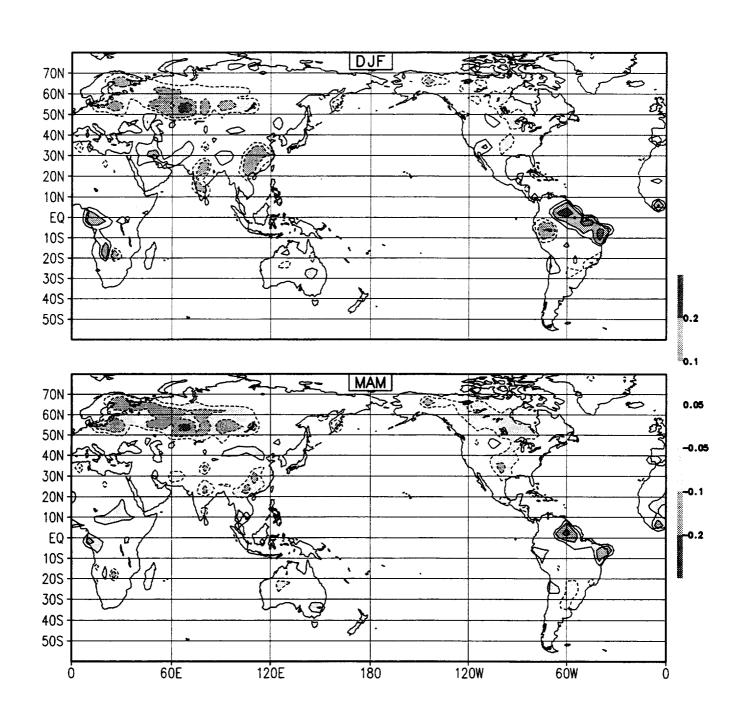
Anomaly Soil Moisture Simulation Year 6 (1984) Contours -.3 -.2 -.1 -.05 .05 .1 .2 .3 deficit dashed



Anomaly Soil Moisture Simulation Year 6 (1984) Contours -.3 -.2 -.1 -.05 .05 .1 .2 .3 deficit dashed



193



Anomaly Soil Moisture Simulation Year 7 (1985) Contours -.3 -.2 -.1 -.05 .05 .1 .2 .3 deficit doshed JJA 70N 60N 50N 40N 30N 20N 10N EQ **10S** 20S 30S 40S 50S SON 70N 60N 50N 40N 30N 20N 10N EQ **10S** 20S 30S 40S 50S ALL 70N 60N 50N 40N 30N 20N 10N EQ **10S 20S 30S 40S** 50S

120E

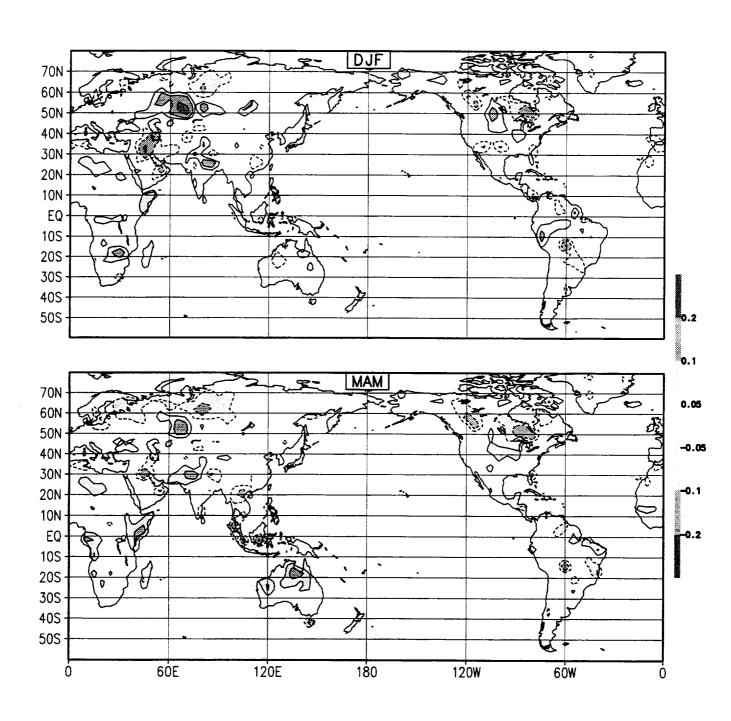
180

120W

6ÓW

60E

Anomaly Soil Moisture Simulation Year 8 (1986) Contours -.3 -.2 -.1 -.05 .05 .1 .2 .3 deficit dashed



Anomaly Soil Moisture Simulation Year 8 (1986) Contours -.3 -.2 -.1 -.05 .05 .1 .2 .3 deficit dashed

JJA 70N 60N 50N 40N 30N 20N 10N EQ 10S 20S 30S 40S 50S SON 70N 60N 50N 40N <. 30N 20N 10N EQ **10S** 20S \Diamond 30S 40\$ 50S ALL 70N 60N 50N 40N 30N 20N 10N EQ 10S **20S** 30S 40S 50S

180

120E

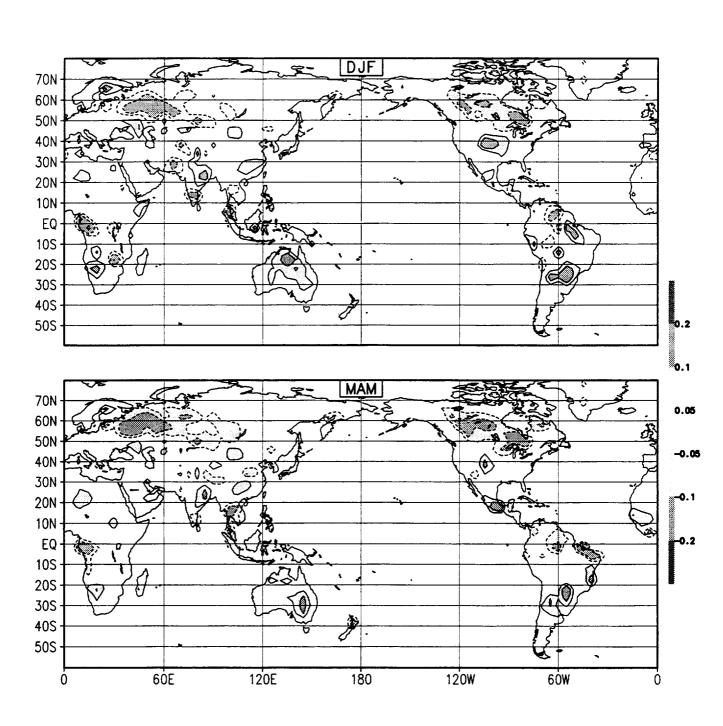
Ó

60E

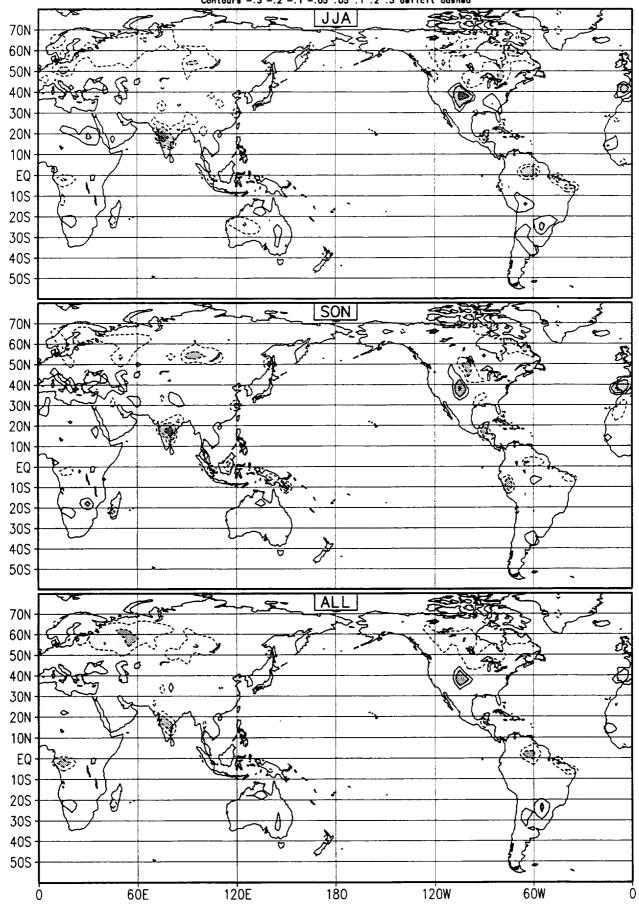
120W

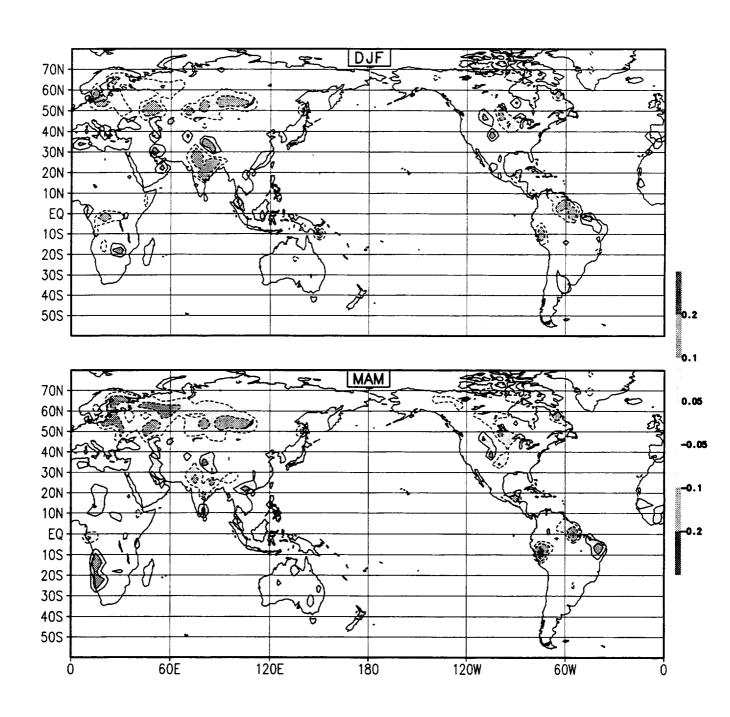
60W

Anomaly Soil Moisture Simulation Year 9 (1987) Contours -.3 -.2 -.1 -.05 .05 .1 .2 .3 deficit dashed



Anomaly Soil Moisture Simulation Year 9 (1987) Contours -.3 -.2 -.1 -.05 .05 .1 .2 .3 deficit dashed



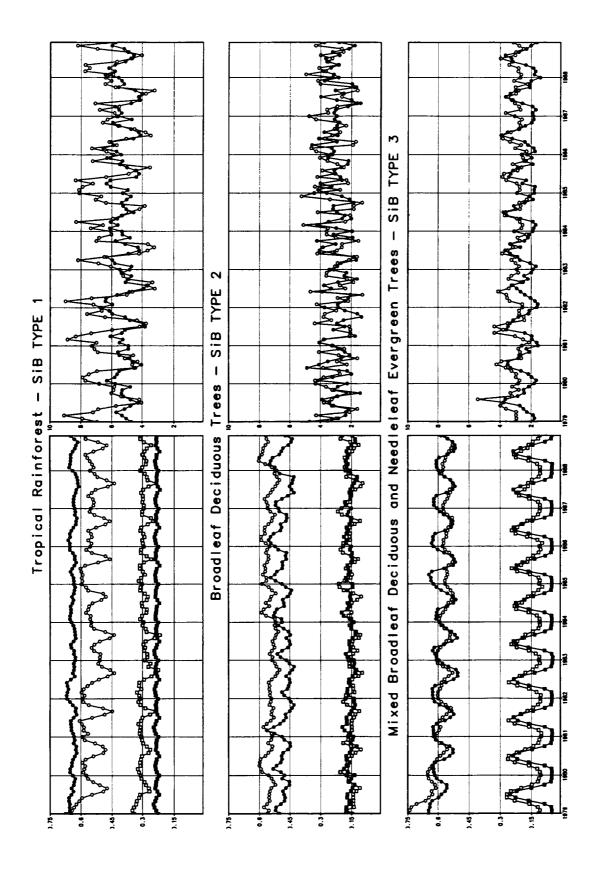


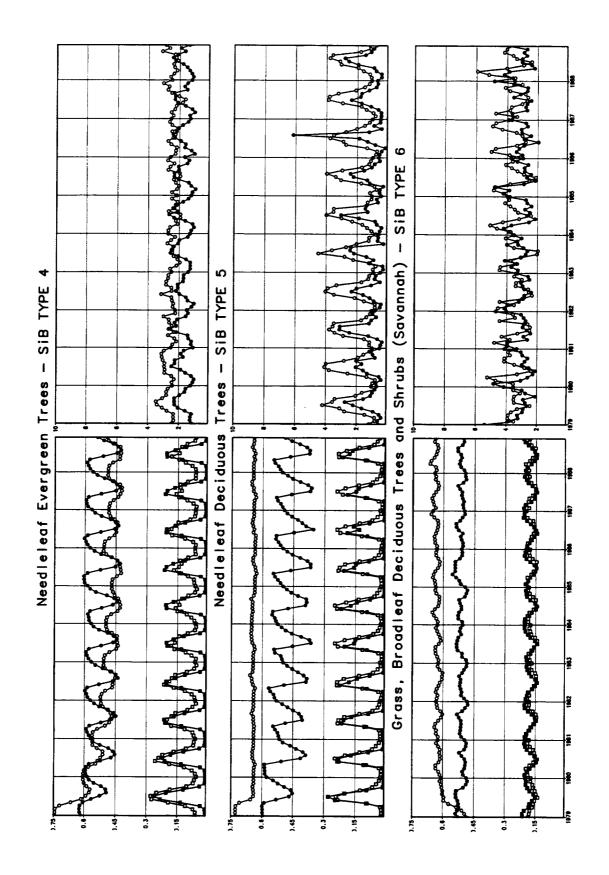
Anomaly Soil Moisture Simulation Year 10 (1988) Contours -.3 -.2 -.1 -.05 .05 .1 .2 .3 deficit dashed

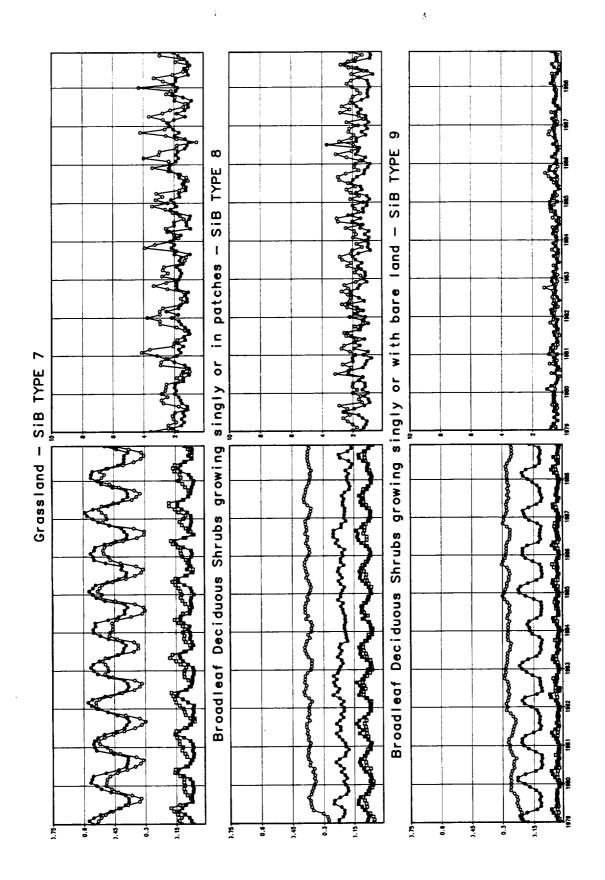
70N 60N 50N 40N 30N 20N 10N EQ 10S **20S** 30S 40S 50S SON 70N 60N 50N 40N 30N 20N 10N EQ 10S **20S** 30S 40S 50S ALL 70N 60N 50N 40N 30N 20N 10N EQ 105 20S 30S 40S 50S 6ÒE 120W 120E 180 6ÓW

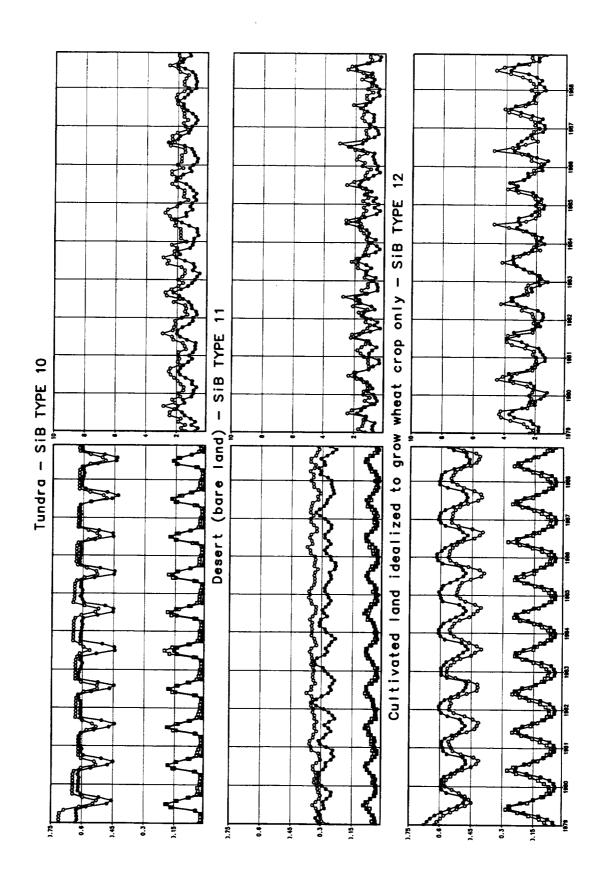
Ó

E. TIME SERIES P, E, SOIL MOISTURE







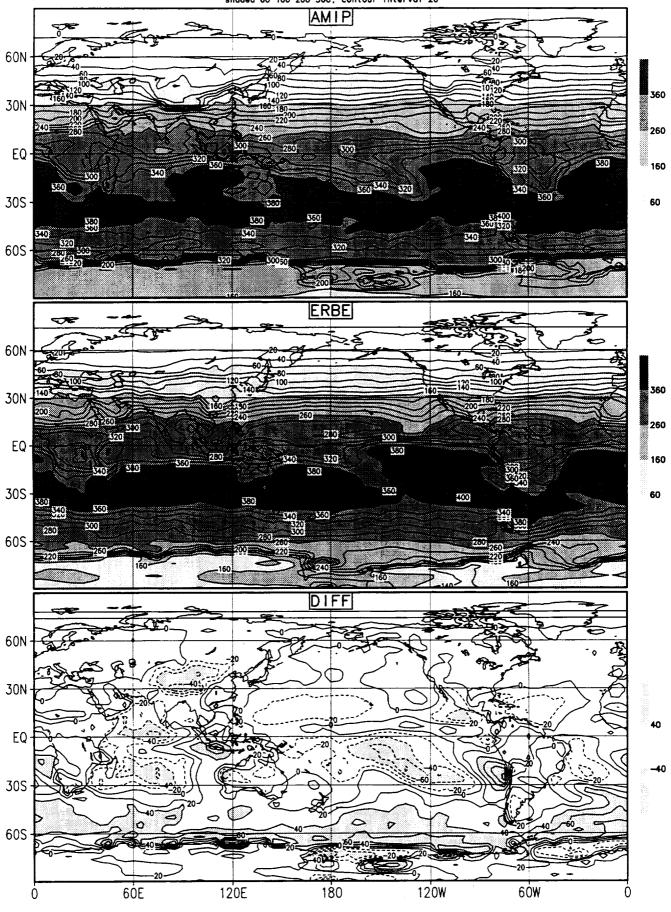


VIII. RADIATION

A. NET SHORTWAVE RADIATION

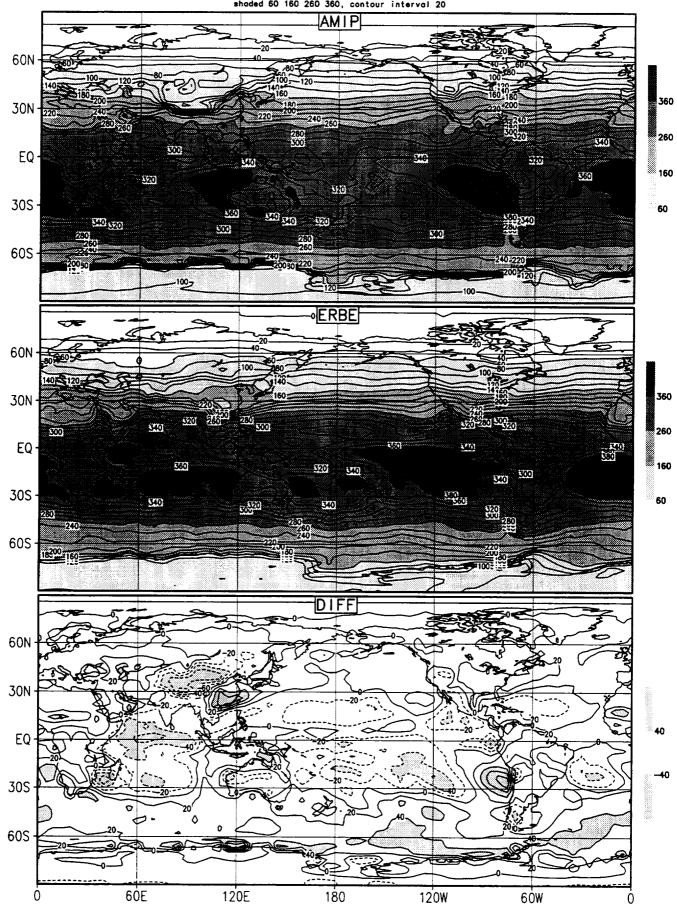
NETSWTOA/JAN(85-88) (W/m**2) 4 Year Mean (1985-88)

shaded 60 160 260 360, contour interval 20

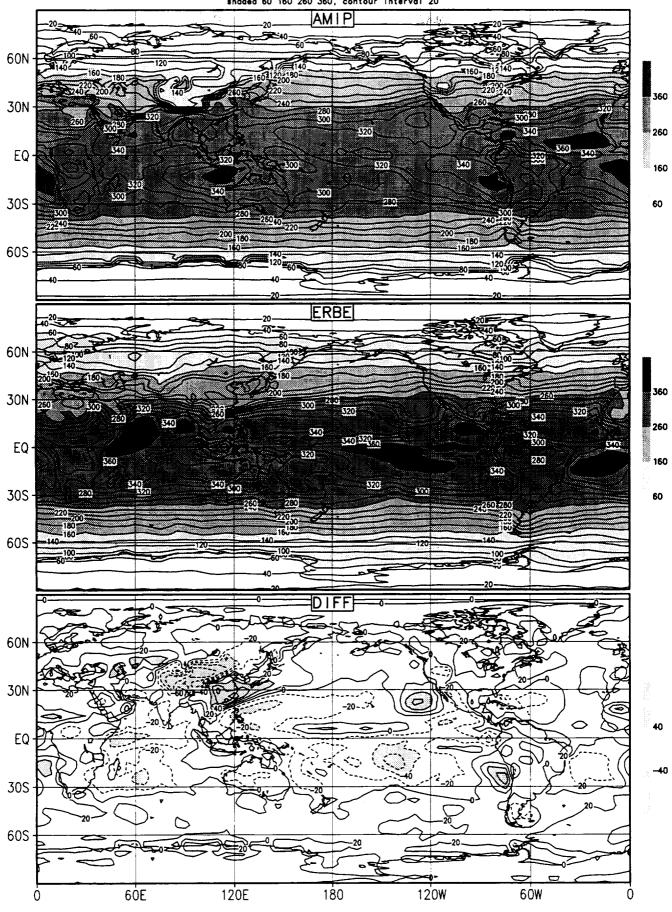


NETSWTOA/FEB(85-88) (W/m**2)

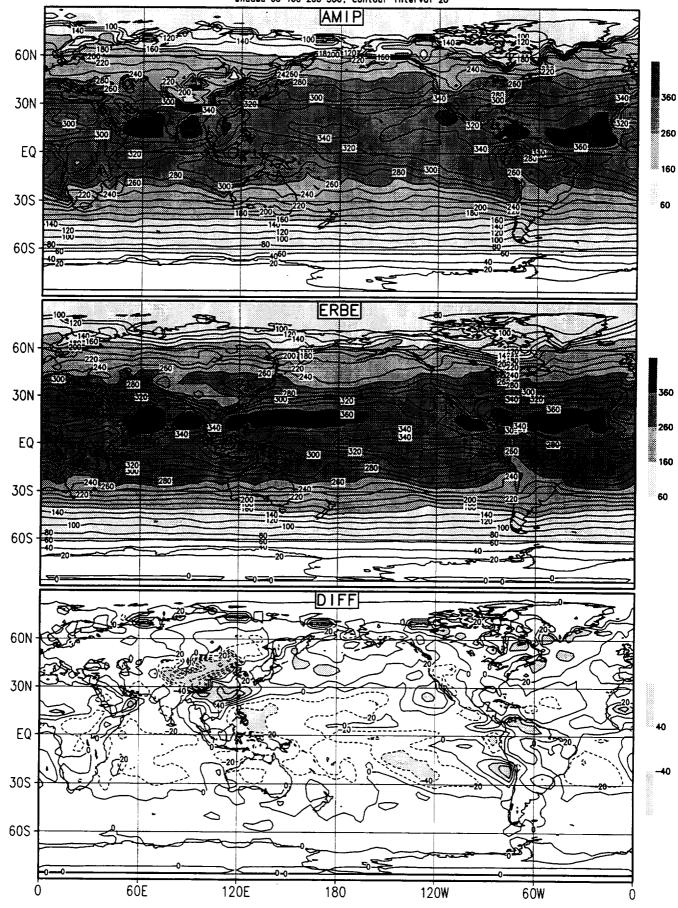
4 Year Mean (1985-88)
shaded 60 160 260 360, contour interval 20



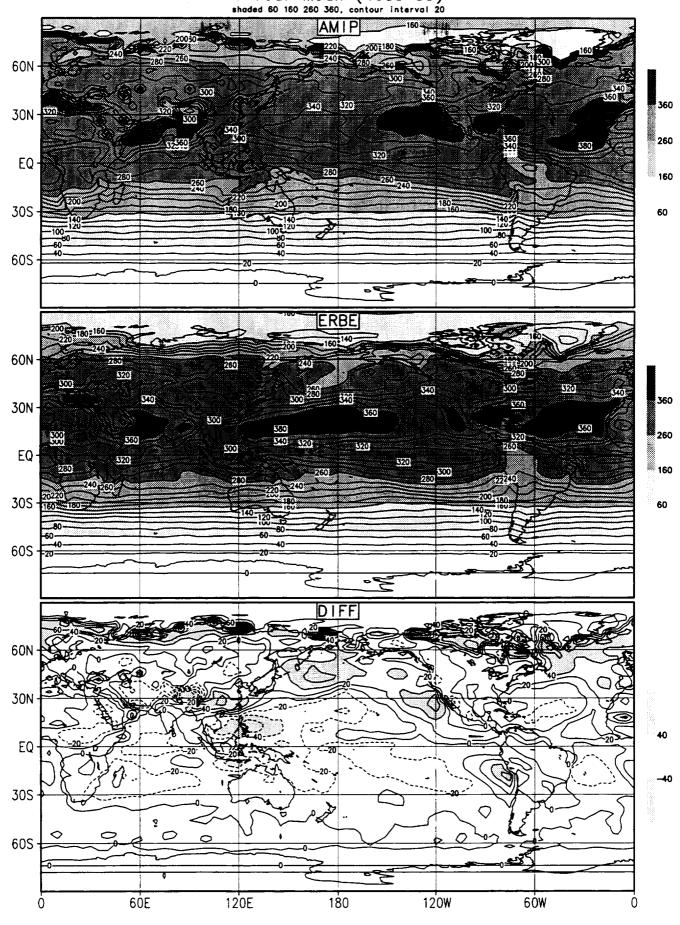
NETSWTOA/MAR(85-88) (W/m**2) 4 Year Mean (1985-88) shaded 60 160 260 360, contour interval 20



NETSWTOA/APR(85-88) (W/m**2) 4 Year Mean (1985-88) shaded 60 160 260 360, contour interval 20

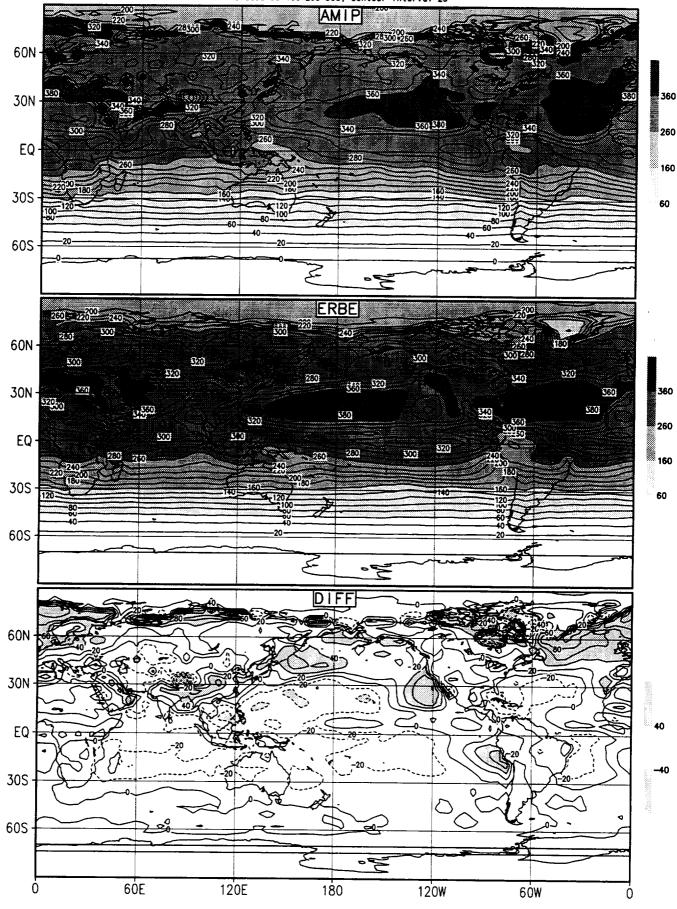


NETSWTOA/MAY(85-88) (W/m**2) 4 Year Mean (1985-88)

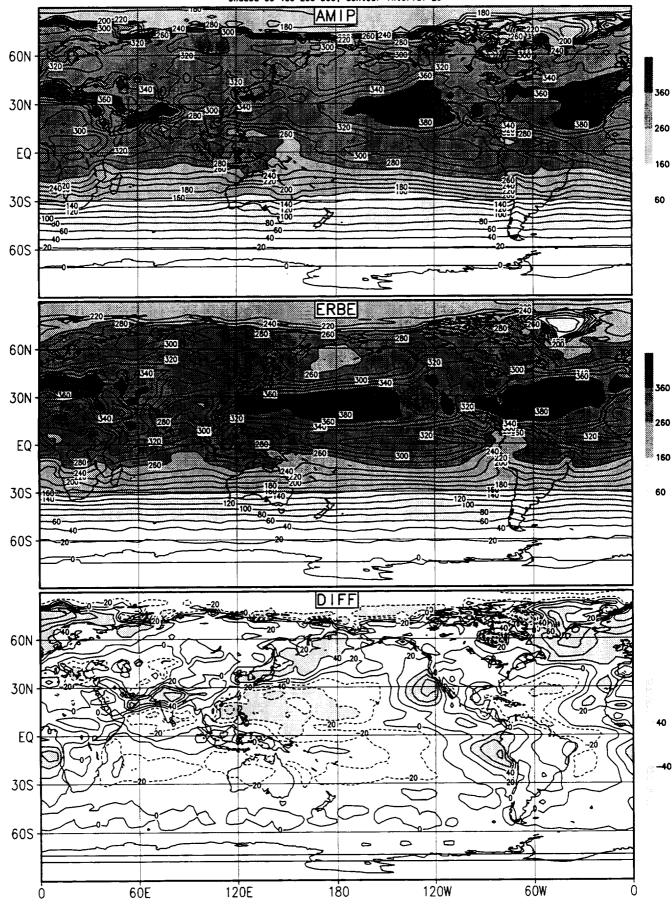


NETSWTOA/JUN(85-88) (W/m**2)

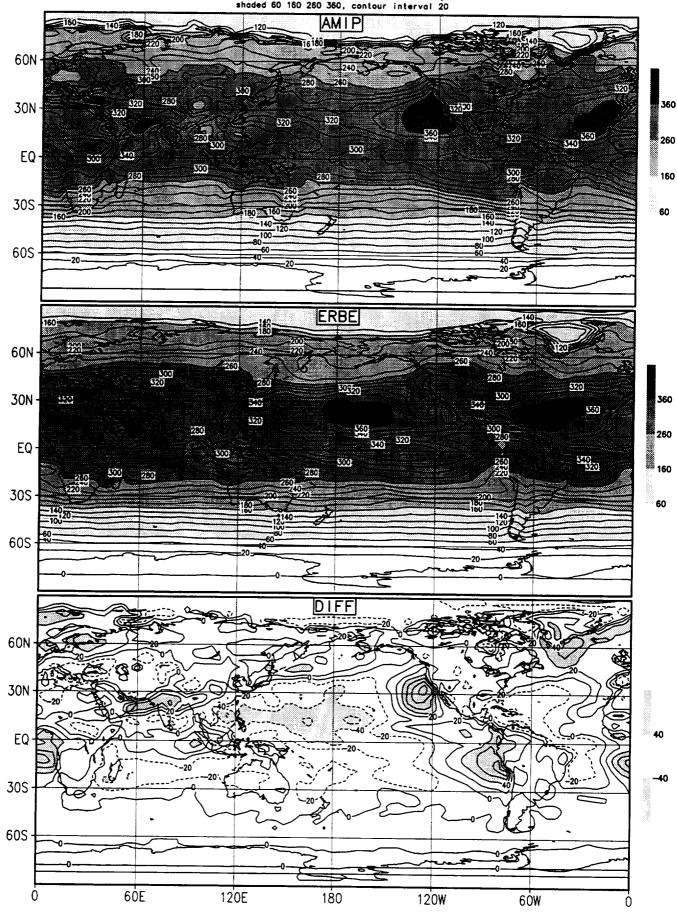
4 Year Mean (1985-88)
shoded 60 160 260 360, contour interval 20



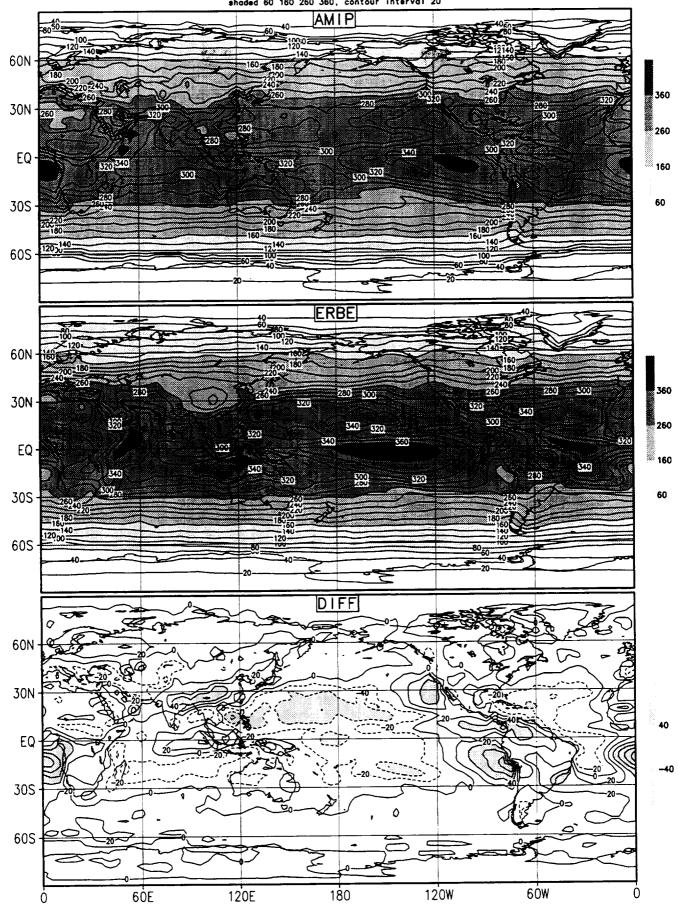
NETSWTOA/JUL(85-88) (W/m**2) 4 Year Mean (1985-88) shaded 60 160 260 360, contour interval 20



NETSWTOA/AUG(85-88) (W/m**2) 4 Year Mean (1985-88) shaded 60 160 260 360, contour interval 20

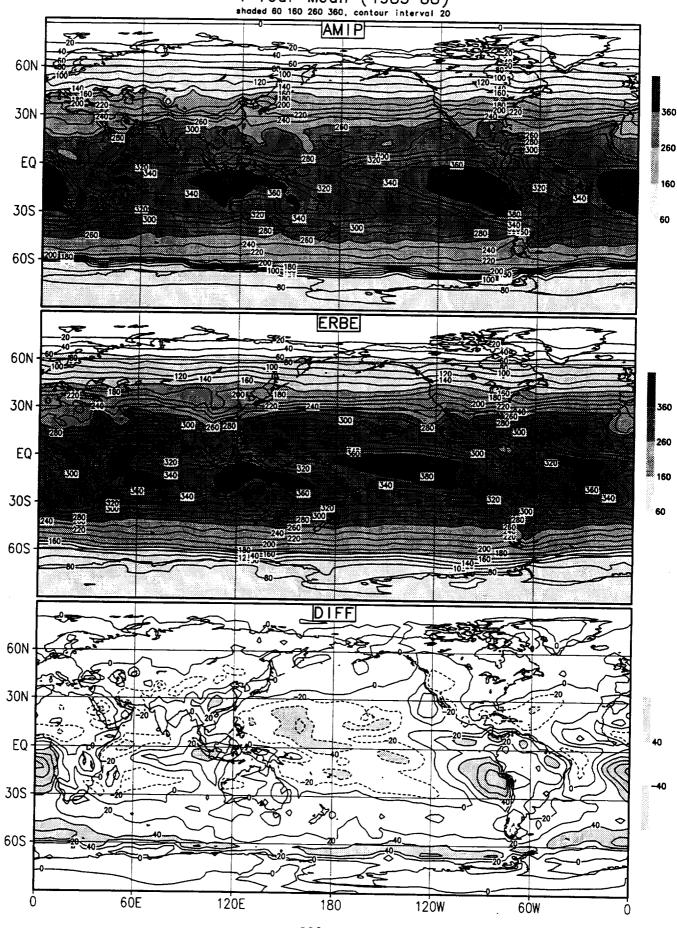


NETSWTOA/SEP(85-88) (W/m**2) 4 Year Mean (1985-88) shoded 60 160 260 360, contour interval 20

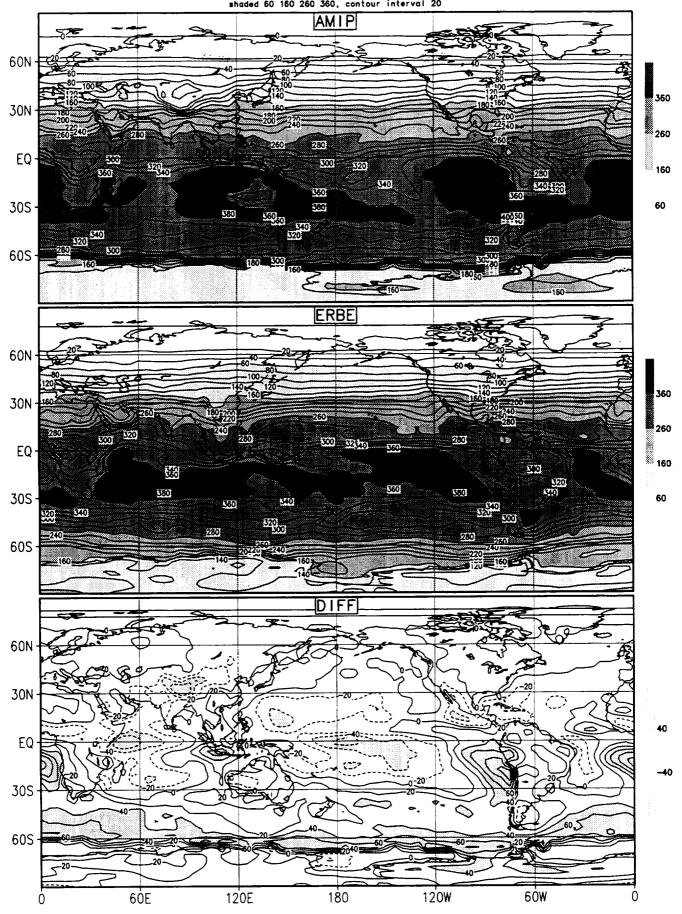


NETSWTOA/OCT(85-88) (W/m**2)

4 Year Mean (1985-88)



NETSWTOA/NOV(85-88) (W/m**2) 4 Year Mean (1985-88) shaded 60 160 260 360, contour interval 20



NETSWTOA/DEC(85-88) (W/m**2) 4 Year Mean (1985-88) shaded 60 160 260 360, contour interval 20 AMIP 60N 360 30N 260 EQ S00 280 320 160 320 30S -460 60 400 400 360 60S · ERBE 60N 30N 260 EQ-380 EM TH 340 30S · 330 60 360 60S DIFF 60N **30N** EQ. 30S 60S

180

120W

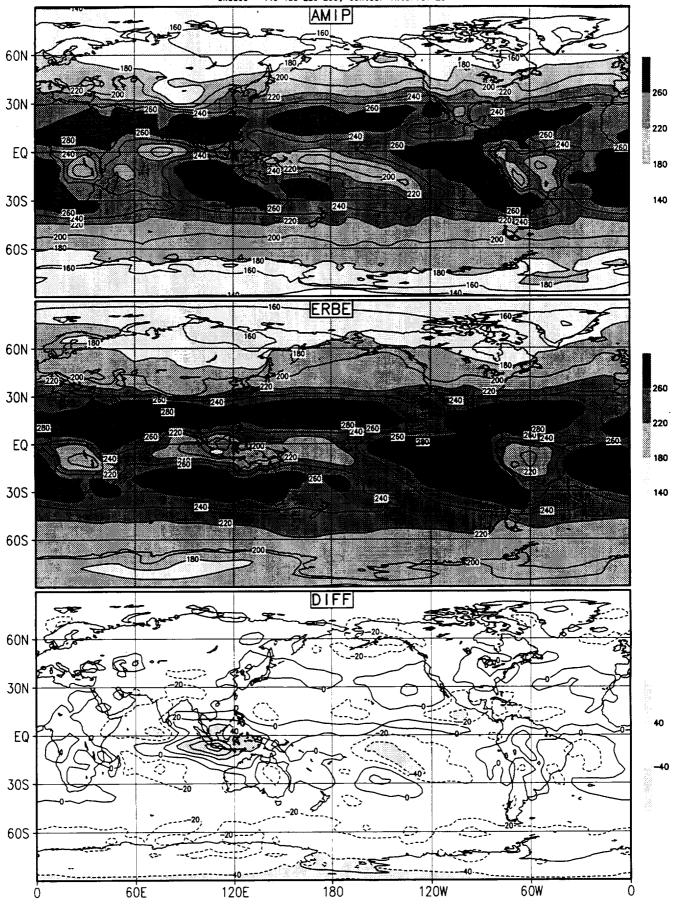
60W

120E

60E

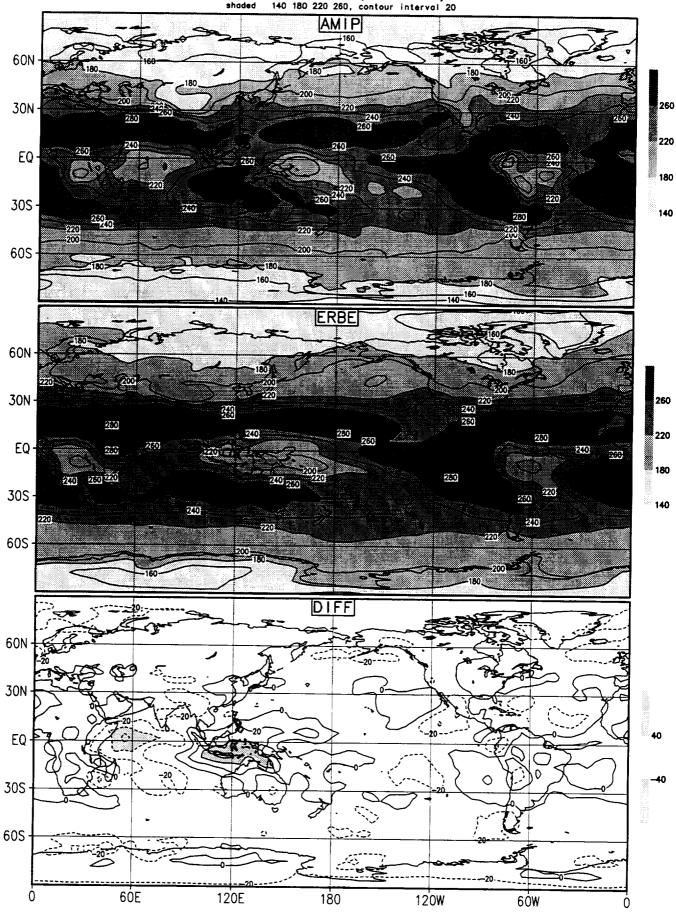
B. OLR

OLR/JAN(85-88) (W/m**2) 4 Year Mean (1985–88) haded 140 180 220 260, contour interval 20



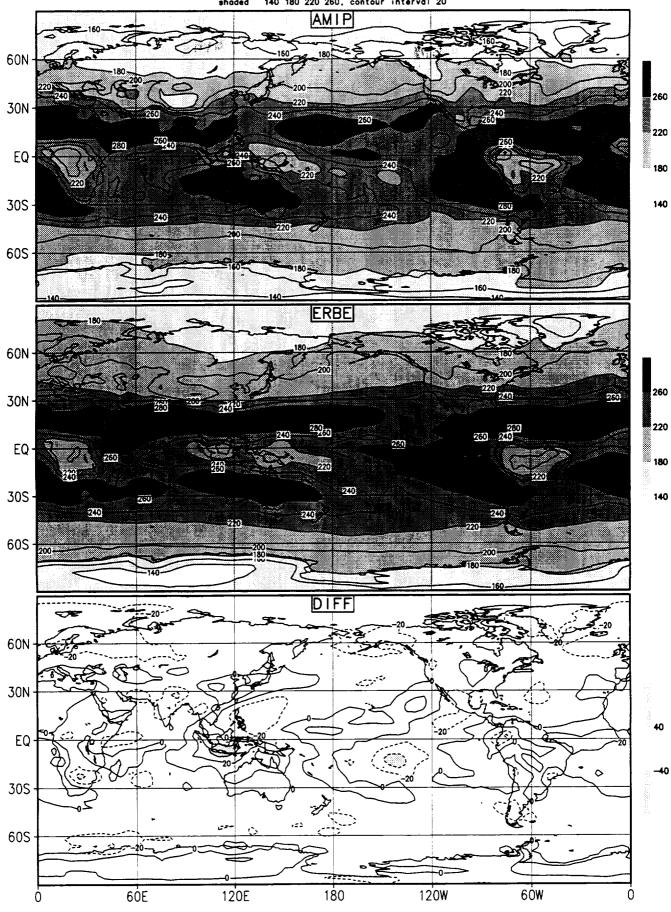
OLR/FEB(85-88) (W/m**2)

4 Year Mean (1985-88)
shaded 140 180 220 260, contour interval 20



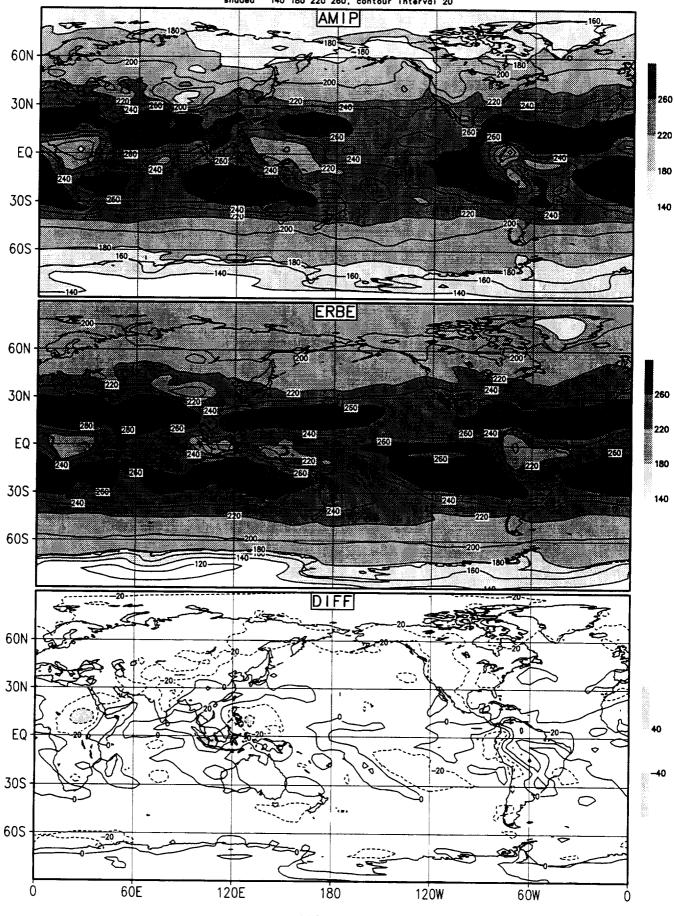
OLR/MAR(85-88) (W/m**2)

4 Year Mean (1985-88)
shaded 140 180 220 280, contour interval 20

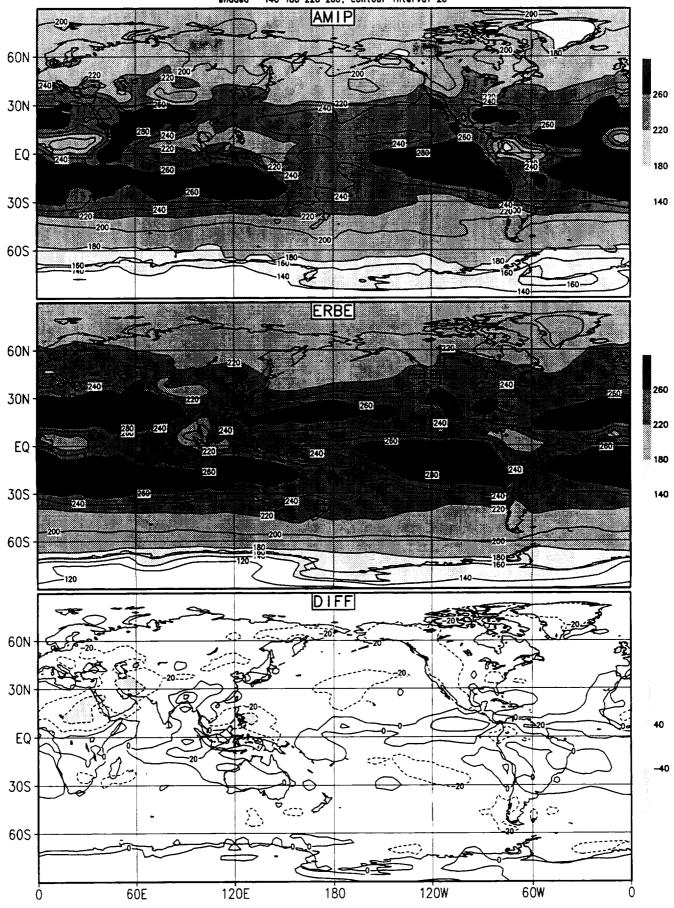


OLR/APR(85-88) (W/m**2)

4 Year Mean (1985-88)
shaded 140 180 220 260, contour interval 20

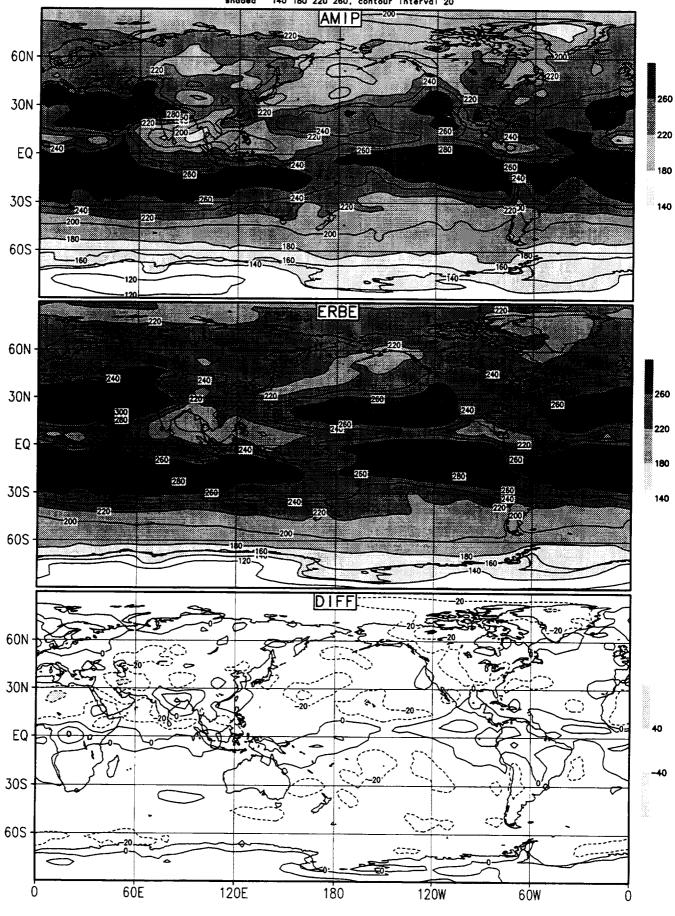


OLR/MAY(85-88) (W/m**2) 4 Year Mean (1985-88) shaded 140 180 220 260, contour interval 20



OLR/JUN(85-88) (W/m**2) 4 Year Mean (1985-88)

shaded 140 180 220 260, contour interval 20



OLR/JUL(85-88) (W/m**2) 4 Year Mean (1985-88) shaded 140 180 220 280, contour interval 20

₂₂₀ **AM** I P 60N 260 30N · 220 EQ-260 180 240 260 30S -140 60S ERBE 270 60N -240 200 210 260 260 Mil 30N -220 260 260 EQ. 180 200 280 260 280 30\$ -140 210 60S 100> DIFF 60N 30N EQ 30S 60S

180

120W

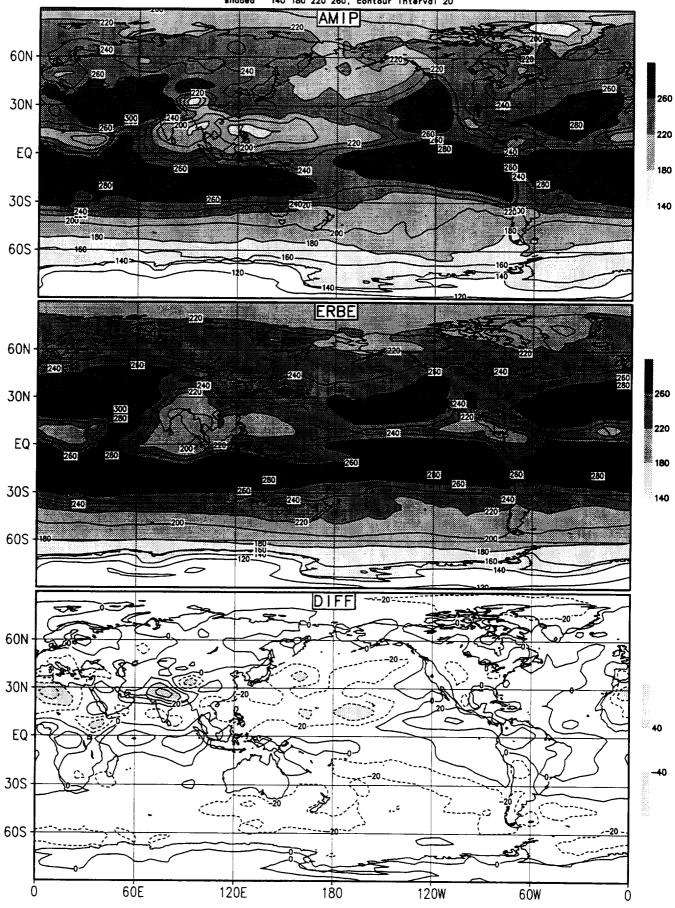
120E

6ÒE

6ÓW

OLR/AUG(85-88) (W/m**2)

4 Year Mean (1985-88)
shaded 140 180 220 260, contour interval 20



OLR/SEP(85-88) (W/m**2)

4 Year Mean (1985-88)
haded 140 180 220 260, contour interval 20 AMIP 200 60N 30N 220 EQ: 180 30S -140 60S ERBE 60N 240 260 200 30N -260 280 300 220 EQ-180 200 280 260 280 280 280 30S -140 200 240 60S DIFF 60N 30N EQ 30S 60S

180

120E

60E

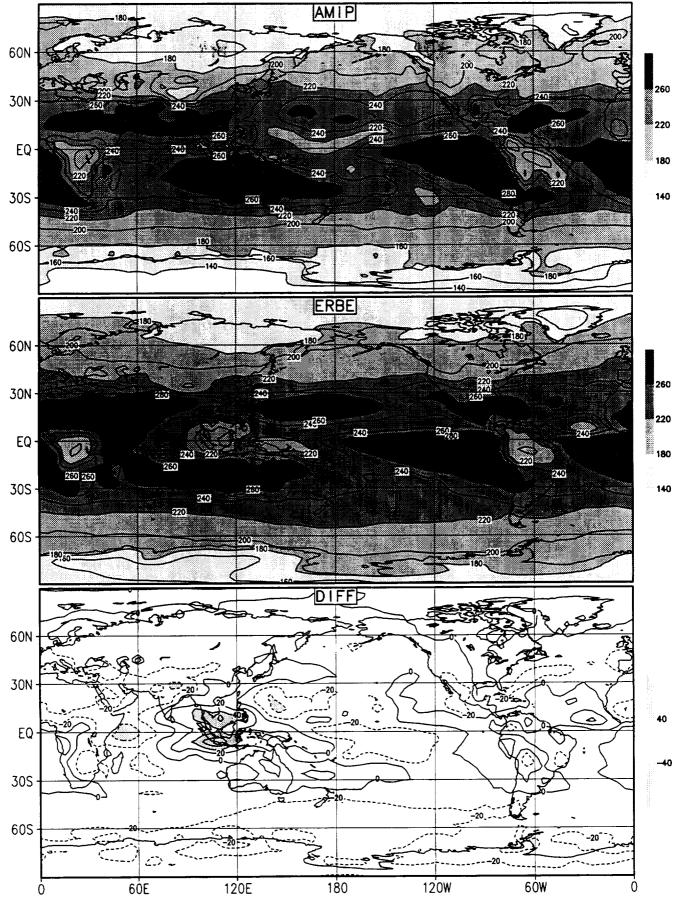
120W

6ÓW

OLR/OCT(85-88) (W/m**2) 4 Year Mean (1985-88)

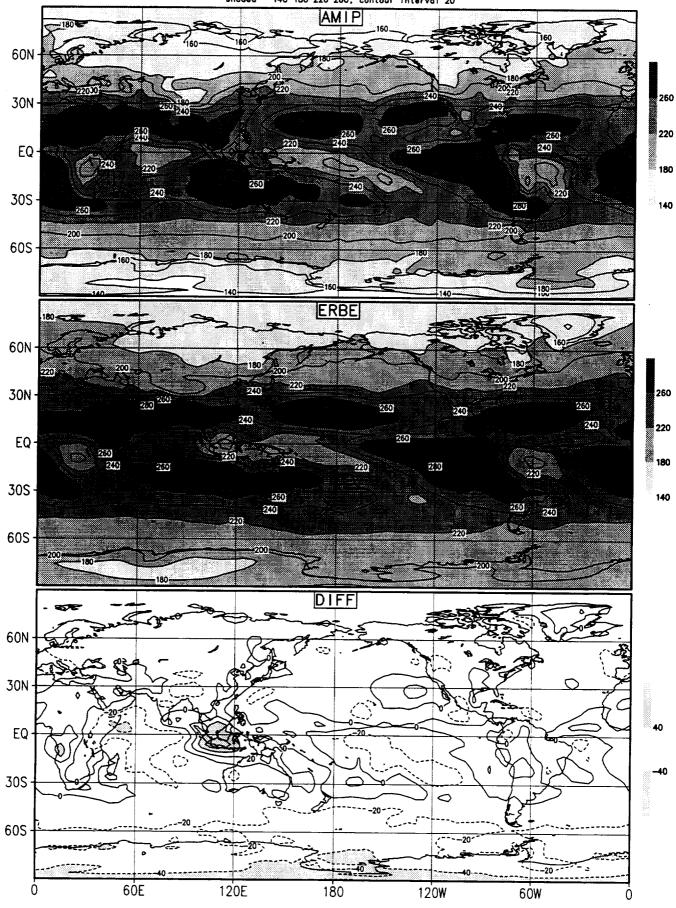
140 180 220 260, contour interval 20 AMIP 60N 260 260 30N 280 240 220 EQ 180 280 220 240 30S 140 240 60S **ERBE** 60N 20 270 30N 260 260 260 220 260 240 230 220 EQ-200 180 330 220 260 280 305-240 140 240 60S DIFF 60N 30N EQ 30S 60S 60E 120E 120W 180 6ÓW 0

OLR/NOV(85-88) (W/m**2) 4 Year Mean (1985-88) shaded 140 180 220 260, contour interval 20



OLR/DEC(85-88) (W/m**2)

4 Year Mean (1985-88)
shoded 140 180 220 260, contour interval 20



REPORT DOCUMENTATION PAGE

Form Approved OMB No. 0704-0188

Public reporting burden for this collection of information is estimated to average 1 hour per response, including the time for reviewing instructions, searching existing data sources,

	ducing this burden, to Washington Head	quarters Services, Directorate fo	or Information Operations and Reports, 1215 Jefferson Project (0704-0188), Washington, DC 20503.	
1. AGENCY USE ONLY (Leave blank)	2. REPORT DATE	3. REPORT TYPE AN	D DATES COVERED	
	September 1993 Technical Me		emorandum	
4. TITLE AND SUBTITLE Circulation and Rainfall Clin Integration With the Goddard			5. FUNDING NUMBERS	
Circulation Model	2 Zacoratory for 7 minosp	meres conerar		
6. AUTHOR(S)	913			
JH. Kim and Y. C. Sud				
7. PERFORMING ORGANIZATION NAME(S) AND ADDRESS (ES)			8. PEFORMING ORGANIZATION REPORT NUMBER	
Goddard Space Flight Center Greenbelt, Maryland 20771			93B00105	
9. SPONSORING / MONITORING ADGEN	CY NAME(S) AND ADDRESS (SG1	10. SPONSORING / MONITORING	
3. 57 511557 MONTONING ADULA	OT MAINE(O) AND ADDITION (I	-0,	ADGENCY REPORT NUMBER	
National Aeronautics and Space Administration				
Washington, DC 20546-0001			NASA TM-104591	
11. SUPPLEMENTARY NOTES Kim: Applied Research Corp Greenbelt, Maryland		yland; Sud: Godda	ard Space Flight Center,	
12a. DISTRIBUTION / AVAILABILITY STA	TMENT		12b. DISTRIBUTION CODE	
Unclassified - Unlimited				
Subject Category 47				
13. ABSTRACT (Maximum 200 words)				

A 10-year (1979-1988) integration of Goddard Laboratory for Atmospheres (GLA) general circulation model (GCM) under Atmospheric Model Intercomparison Project (AMIP) is analyzed and compared with observation. We present the first momentum fields of circulation variables and also hydrological variables including precipitation, evaporation, and soil moisture. Our goals are i) to produce a benchmark documentation of the GLA GCM for future model improvements, ii) to examine systematic errors between the simulated and the observed circulation, precipitation, and hydrologic cycle, iii) to examine the interannual variability of the simulated atmosphere and compaste it with observation, and iv) to examine the ability of the model to capture the major climate anomalies in response to events such as El Niño and La Niña. The 10-year mean seasonal and annual simulated circulation is quite reasonable compared to the analyzed circulation, except the polar regions and area of high orography. Precipitation over tropics are quite well simulated, and the signal of El Niño/La Niña episodes can be easily identified. The time series of evaporation and soil moisture in the 12 biomes of the biosphere also show reasonable patterns compared to the estimated evaporation and soil moisture.

14. SUBJECT TERMS Simulated/Observed Cli Cycle; Seasonal and An	15. NUMBER OF PAGES 247 16. PRICE CODE		
17. SECURITY CLASSIFICATION OF REPORT	18. SECURITY CLASSIFICATION OF THIS PAGE	19. SECURITY CLASSIFICATION OF ABSTRACT	20. LIMITATION OF ABSTRACT
Unclassified	Unclassified	Unclassified	UL